Mechanistic and Kinetic Aspects of Furfural Degradation in Dilute Acidic Media

by

Andrew Charles Dudley Pringle Steiner

Thesis presented in partial fulfilment
of the requirements for the Degree

of

MASTER OF ENGINEERING
(CHEMICAL ENGINEERING)

in the Faculty of Engineering
at Stellenbosch University

The financial assistance of the National Research Foundation (NRF) towards this research is hereby acknowledged. Opinions expressed and conclusions arrived at, are those of the author and are not necessarily to be attributed to the NRF.

Supervisor

Prof JF Görgens

Co-Supervisor

Dr. S Farzad

Dr. B Danon

April 2019

Stellenbosch University https://scholar.sun.ac.za

Declaration

By submitting this thesis electronically, I declare that the entirety of the work contained therein is my own, original work, that I am the sole author thereof (save to the extent explicitly otherwise stated), that reproduction and publication thereof by Stellenbosch University will not infringe any third party rights and that I have not previously in its entirety or in part submitted it for obtaining any qualification.

Date: *April 2019*

Copyright © 2019 Stellenbosch University

All rights reserved

Stellenbosch University https://scholar.sun.ac.za

Plagiarism Declaration

1. Plagiarism is the use of ideas, material and other intellectual property of another's work and to present is as my own.
2. I agree that plagiarism is a punishable offence because it constitutes theft.
3. I also understand that direct translations are plagiarism.
4. Accordingly all quotations and contributions from any source whatsoever (including the internet) have been cited fully. I understand that the reproduction of text without quotation marks (even when the source is cited) is plagiarism.
5. I declare that the work contained in this assignment, except where otherwise stated, is my original work and that I have not previously (in its entirety or in part) submitted it for grading in this module/assignment or another module/assignment.

Student number: 16440439

Initials and surname: ACDP Steiner

Signature:

Date: 28 January 2019

Stellenbosch University https://scholar.sun.ac.za

Abstract

Furfural is a renewable platform chemical produced from lignocellulosic biomass. Many chemicals are derived from furfural including furfuryl alcohol, cosmetic ingredients & fragrances, flavour ingredients, nematocides & other agricultural chemicals, biofuels/fuel additives, solvents, resins, nylon, spandex (PolyTHF), etc.

Furfural is mostly produced by an acid catalysed dehydration of the xylan in the biomass. The same acid catalyst also catalyses furfural degradation reactions which are known to convert furfural into formic acid and solid, insoluble, heterogeneous, carbonaceous, furan-rich macromolecules known as *humins*.

In this study, furfural degradation was investigated, considering reaction temperatures of 140 °C - 200 °C, initial furfural concentrations of 1.5 wt% - 6 wt% and the sulfuric acid catalyst concentration of 0.5 wt% - 2 wt%. The reaction kinetics of degradation were established by fitting experimental data to the Arrhenius equation.

The results showed formic acid as a significant product of furfural degradation. It was found that for each mol of degraded furfural, 0.86 mol formic acid was formed under the conditions of this study.

Humins were primarily composed of bifurylic and trifurylic structures and the humins composition was independent of reaction conditions and was uniform under all reaction conditions in the present study.

Combustion of humins provides a route to valorise humins but generates only 1.3 % of the energy required for furfural production. In a scenario where furfural is produced from biorefinery pre-treatment stages or from pulp mill pre-hydrolysis liquor (not directly from biomass) combustion of humins is a viable application as it facilitates removal of humins which otherwise block up the system.

In this study, it was found that initial furfural concentration was the most influential factor towards furfural degradation. Increasing the initial furfural concentration caused an increase in the rate of degradation, more humins were formed and more formic acid was formed. Increasing reaction temperature caused an increase in the amount of humins formed and an increase in the rate of degradation. Increasing the concentration of sulfuric acid caused an increase in the rate of degradation.

Stellenbosch University https://scholar.sun.ac.za

Opsomming

Furforaal is ’n hernubare platform chemikalie wat vervaardig word uit lignosellulosiese biomassa. Baie chemikalieë word geproduseer uit furforaal insluitend furfurielalkohol, skoonheidsbestanddele en geure, geurbestanddele, nematodedoder en ander landbouchemikalieë, biobrandstowwe of brandstof bymiddels, oplosmiddels, hars, nylon, spandeks (PolyTHF), etc.

Furforaal word meestal vervaardig deur ’n suur gekataliseerde dehidrasie van die xilaan in die biomassa. Dieselfde suurkatalis kataliseer ook furfuraal afbrekingsreaksies wat bekend is om furfuraal na metanoësuur en soliede, onoplosbare, heterogene, koolstofryke, furaanryke makromolekules, genaamd humien, om te sit.

In hierdie studie is furforaal afbreking ondersoek met inagneming van reaksietemperature van 140–200 °C, aanvanklike furfuraalkonsentrasies van 1.5–6wt.% en die swawelsuur kataliskonsentrasie van 0.5–2 wt.%. Die reaksie kinetika van afbreking is bepaal deur eksperimentele data op die Arrhenius vergelyking te pas.

Die resultate het gewys dat metanoësuur ’n beduidende produk van furfuraal afbreking is. Dis gevind dat vir elke mol van afgebreekte furfuraal, 0.86 mol metanoësuur gevorm is onder die toestande van hierdie studie.

Humien het hoofsaaklik bestaan uit bifurkaat en trifurkaat strukture en die humien samestelling was onafhanklik van reaksiekondisies en was uniform onder alle reaksiekondisies in die huidige studie.

Verbranding van humien verskaf ’n roete om humien te valoriseer, maar genereer slegs 1.3% van die energie benodig vir furfuraalproduksie. In ’n scenario waar furfuraal vervaardig word uit bioraffinadery voorbehandelingstadia, of uit pulpmeul voorhidrolise vog (nie direk uit biomassa nie) is verbranding van humien ’n haalbare toepassing as dit verwydering van humien fasiliteer wat andersins die sisteem sou blokkeer.

In hierdie studie is gevind dat reaksietemperatuur die mees beduidende faktor tot furforaal-afbreking was. Verhoging van reaksietemperatuur het ’n verhoging in die kwantiteit van furforaal wat afbreek, ’n verhoging in die hoeveelheid humien gevorm

Stellenbosch University https://scholar.sun.ac.za

en verhoging in die tempo van afbreking, tot gevolg gehad. Verhoging van die aanvanklike furforaal-konsentrasie het ’n verhoging in die tempo van afbreking gehad, meer humien is gevorm en meer mieresuur is gevorm. Verhoging in die konsentrasie van swaelsuur het ’n verhoging in die tempo van afbreking gehad en ’n verhoging in die hoeveelheid furforaal wat gereageer het.

Stellenbosch University https://scholar.sun.ac.za

Acknowledgements

Firstly, I would like to thank my parents Mary-Ann and Philipp Steiner for their extensive support throughout my school and university career building up to this master's. I want to acknowledge my father for inspiring my passion for biorefining and helping me to prepare this thesis by sharing his extensive technical knowledge of furfural processing with me. I would like to thank my mother for checking my grammar before all my submissions and for all her practical ideas and words of encouragement.

To my supervisor Professor Johann Görgens, thank you for sharing your wealth of knowledge with me, keeping me on track and for making this master's a possibility by accepting my late application and sorting out all the admin so that I could start in early 2016.

To my co-supervisor Doctor Bart Danon, who was always available and happy to help and give advice, thank you for your wisdom and patience. I have immense respect for you as a researcher and as a person. To my co-supervisor Doctor Somayeh Farzad, who picked up the reigns for the co-supervision of my master's, thank you for your guidance and the meaningful comments and suggestions in writing my thesis.

Thank you to Nugent Lewis who kindly coordinated the extension of my bursary for 2018 after I had to take medical leave in 2017. Your input made it possible for me to pursue my goal of completing my studies and I am truly grateful for that.

I would like to thank all the personnel of the department of process engineering that assisted me with my laboratory and analytical work.

I'd like to express my gratitude to the National Research Foundation for the funding that they provided for this research.

Finally, I acknowledge that the completion of this work serves as a testament to the bottomless kindness and love of Jesus Christ. It is by His grace that I am alive today and able to write this thesis.

Stellenbosch University https://scholar.sun.ac.za

Nomenclature

Symbol	Description	Unit
FF	furfural	-
HMF	5-hydroxymethylfurfural	-
FOL	furfuryl alcohol	-
PFA	polyfurfuryl alcohol	-
FA	formic acid	-
LA	levulinic acid	-
AA	acetic acid	-
HHV	higher heating value	-
LCV	lower calorific value	-
MIBK	methyl isobutyl ketone	-
DHH	2,5-dioxo-6-hydroxyhexanal	-
DMC	dihydroxy-2-methylchromone	-
BT	1,2,4-benzenetriol	-
TP	1,2,5-tripentanon	-
HCl	hydrochloric acid	-
H_2SO_4	sulfuric acid	-
GVL	γ-valeracetone	-
X_n	mass fraction of component “n”	%
C_{FF}	concentration of FF	wt%
$C_{FF,max}$	maximum FF concentration	wt%
k	rate constant	s^{-1}
A	pre-exponential factor	s^{-1}
Ea	activation energy	$kJ \cdot mol^{-1}$

Stellenbosch University https://scholar.sun.ac.za

R	universal gas constant	$\mathrm{J \cdot mol^{-1} \cdot K^{-1}}$
T	temperature	K
$\mathbf{Ka_{H_2SO_4,1}}$	1st dissociation constant for H_2SO_4	M
$\mathbf{Ka_{H_2SO_4,2}}$	2nd dissociation constant for H_2SO_4	M
$\mathbf{pKa_{HCl}}$	acidity index of HCl	-
$\mathbf{pka_{H_2SO_4,1}}$	acidity index of H_2SO_4 $(-\log(\mathrm{Ka_{H_2SO_4,1}}))$	-
$\mathbf{pKa_{H_2SO_4,2}}$	acidity index of H_2SO_4 $(-\log(\mathrm{Ka_{H_2SO_4,2}}))$	-
$\mathbf{C_{FF_0}}$	initial FF concentration	M
$\mathbf{C_{X_0}}$	initial xylose concentration	M
$[\mathbf{H^+}]$	hydrogen ion concentration	M
$[\mathbf{HSO_4^-}]$	hydrogen sulfate ion concentration	M
$[\mathbf{H_2SO_4}]$	H_2SO_4 concentration	M
$[\mathbf{H_2SO_{4,0}}]$	initial concentration of H_2SO_4	M

Stellenbosch University https://scholar.sun.ac.za

Table of Contents

Declaration ii

Plagiarism Declaration iii

Abstract iv

Opsomming v

Acknowledgements vii

Nomenclature viii

Table of Contents x

List of Figures xiii

List of Tables xvi

1. Introduction 1

2. Literature Review 4

2.1 Furfural degradation 4

2.2. Humins 7

2.2.1 Valorisation 7

2.2.2 Biphasic systems 8

2.2.3 Mechanism & structure 9

2.2.4 Other degradation reactions 21

2.2.5 Catalyst, substrate and humin yields & composition 21

2.3. Formic acid 24

2.3.1 Formic acid as furfural degradation product 24

2.3.2 Furfural to formic acid degradation mechanism 28

2.3.3 Alternate sources of formic acid in furfural production 28

2.4. Kinetics 29

2.4.1 Reaction kinetics for this study 29

Stellenbosch University https://scholar.sun.ac.za

2.4.2 Reaction kinetics for previous kinetic studies 31
2.4.3 Studies where 1st or 2nd order reaction kinetics were detected 34
2.5. Furfural degradation in xylose dehydration reactions 36
2.6 Extent of fragmentation, resinification & condensation reactions 37
3. Objectives 39
3.1 Problem Statement 39
3.2 Goals 39
3.3 Novelty 40
4. Material & methods 42
4.1 Experimental setup 42
4.2 Experimental Procedure 45
4.3 Kinetic Modelling 46
5. Results & discussion 50
5.1. Mass balance 51
5.2 Kinetics 51
5.2.1 Kinetics for specified sulfuric acid and FF concentrations 53
5.2.2 Repeatability 59
5.3. Rate of furfural degradation 62
5.4. Humins 64
5.4.1 Humins composition 64
5.4.2 Humins formation mechanism 65
5.4.3 Humins soxhlet washing 70
5.4.4 Humins concentration 71
5.5. Formic acid 73
5.5.1 Overall quantity of formic acid produced 73
5.5.2 Extent of fragmentation reaction under studied conditions 74
5.5.3 Formic acid yield as a function of acid catalyst type 75

Stellenbosch University https://scholar.sun.ac.za

6. Conclusions & Recommendations 77

6.1 Conclusions 77

6.1.1 Summary of reaction conditions 79

6.2. Recommendations 79

7. References 82

Appendix I 88

Python code 88

Appendix II 93

Sketch of ice bath and sampling system 93

Appendix III 94

Calorific value of humins 94

Stellenbosch University https://scholar.sun.ac.za

List of Figures

Figure 1: Proposed mechanism of xylose reaction to furfural in acid media. X^- indicates halides ions, and M^{3+} indicates metal cations. (sourced from Danon, Marcotulio and de Jong (2013)) 5
Figure 2: Sánchez mechanism for humin formation involving the formation of bifurylic and trifurylic structures. (sourced from Hoang *et al.* 2015; Hu & Ragauskas, 2014; Sanchez, Hernandez & Keresztury, 1994) 10
Figure 3: FF is transformed into acyclic species (IV & V) and structure VI is the humin network (more conjugated than in Figure 2) (sourced from Sánchez, Hernández and Keresztury, (1994)) 11
Figure 4: Radical intermediate for the thermal resinification of FF. Tertiary hydrogen atoms in the polyfurylic structures generate radicals, which are stabilised as the structures become more conjugated (sourced from Gandini and Belgacem (1997)) 12
Figure 5: Humin growth mechanism: Polycondensation occurs via electrophilic substitution with the formation of carbon-carbon bonds between rings 13
Figure 6: Ring opened furfural binds with cyclic furfural to form a short chain oligomer with many double bonds 13
Figure 7: Diels-Alder reaction between 2 FF molecules (sourced from Danon, van der Aa and de Jong (2013)) 14
Figure 8: Hydrolytic ring opening of HMF and possible aldol addition reactions (adapted from Patil, Heltzel and Lund (2012)) 15
Figure 9: 3,8-dihydroxy-2-methylchromone, potential intermediate in humins formation mechanism. 16
Figure 10: Possible furfural ring opening, and aldol reactions as suggested by Lamminpaa, Ahola & Tanskanen (2014) 16
Figure 11: Model representing the molecular structure of a xylose derived humin fragment, including the most important linkages (sourced from van Zandvoort *et al.* (2013)) 17
Figure 12: One molecule of FF reacts with the first pentose dehydration intermediate to give “furfural xylose”, Two FF molecules react with an intermediate to give “difurfural xylose” (sourced from Zeitsch (2000)) 18
Figure 13: Reductic acid: a potential furfural degradation product 21
Figure 14: Hydrolytic fission of the aldehyde group on furfural to form formic acid .. 28

Stellenbosch University https://scholar.sun.ac.za

Figure 15: Reaction scheme for FF formation in acidic conditions excluding condensation reaction. (Sourced from Lamminpää (2015)) 33
Figure 16: Reaction scheme for FF formation in acidic conditions including condensation reaction. (Sourced from Lamminpää (2012)) 33
Figure 17: Reaction scheme for FF formation in acidic conditions including condensation reaction and xylose decomposition reaction. (Sourced from Lamminpää (2012)) 33
Figure 18: Schematic diagram of experimental setup for the polyclave reactor, labelled according to the legend. 43
Figure 19: Photo of experimental setup, labelled according to the legend in the schematic diagram. 43
Figure 20: Kinetics for all runs 52
Figure 21: FF degradation experimental data and fitted model values with 1.5 wt% FF and 0.5 wt% H_2SO_4 54
Figure 22: FF degradation experimental data and fitted model values with 1.5 wt% FF and 1 wt% H_2SO_4 54
Figure 23: FF degradation experimental data and fitted model values with 1.5 wt% FF and 2 wt% H_2SO_4 55
Figure 24: FF degradation experimental data and fitted model values with 3.0 wt% FF and 0.5 wt% H_2SO_4 55
Figure 25: FF degradation experimental data and fitted model values with 3.0 wt% FF and 1 wt% H_2SO_4 56
Figure 26: FF degradation experimental data and fitted model values with 3.0 wt% FF and 2 wt% H_2SO_4 56
Figure 27: FF degradation experimental data and fitted model values with 6.0 wt% FF and 0.5 wt% H_2SO_4 57
Figure 28: FF degradation experimental data and fitted model values with 6.0 wt% FF and 1 wt% H_2SO_4 57
Figure 29: FF degradation experimental data and fitted model values with 6.0 wt% FF and 2 wt% H_2SO_4 58
Figure 30: Experimental data from duplicate runs at 170 °C, 1.5 wt% FF & 2 % sulfuric acid 59
Figure 31: Experimental data from duplicate runs at 200 °C, 1.5 wt% FF & 1 % sulfuric acid 60

Stellenbosch University https://scholar.sun.ac.za

Figure 32: Experimental data from duplicate runs at 200 °C, 3 wt% FF & 1 % sulfuric acid 60
Figure 33: Experimental data from duplicate runs at 200 °C, 6 wt% FF & 3 % sulfuric acid 61
Figure 34: 3D Surface Plot of FF Degradation Rate ($g \cdot L\text{-}1 \cdot min\text{-}1$) against Temperature (°C) and Initial FF Concentration (wt%) 62
Figure 35: 3D Surface Plot of FF Degradation Rate ($g \cdot L\text{-}1 \cdot min\text{-}1$) against Initial FF Concentration (wt%) and Sulfuric acid concentration (wt%) 64
Figure 36: Van Krevelen diagram for humins formed during FF degradation 69
Figure 37: C:H:O data for soxhlet washes 71
Figure 38: 3D Surface Plot of Humins Concentration (g/L) against Sulfuric Acid Concentration (wt%) and Initial FF Concentration (wt%) 72
Figure 39: 3D Surface Plot of Humins Concentration (g/L) against Temperature (°C) and Initial FF Concentration (wt%) 73
Figure 41: 3D Surface Plot of Formic Acid Concentration (g/L) against Initial FF Concentration (wt%) and Temperature (°C) 74

Stellenbosch University https://scholar.sun.ac.za

List of Tables

Table 1: Summary of proposed mechanisms for FF degradation 19
Table 2: Summary of humins studies 23
Table 3: Formic acid as direct degradation product of furfural 26
Table 4: Furfural degradation kinetics studies. 32
Table 5: Studies which report 1st/2nd order reaction kinetics for the FF degradation reaction 35
Table 6: FF degradation studies from pure FF 41
Table 7: Factors of factorial design & naming convention 44
Table 8: Experimental factors for FF degradation 50
Table 9: Asymptotic significance of experimental factors with respect to FF degradation rate 62
Table 10: Standard deviation, variance and mean for C, H & O elemental composition of humins formed in this study 65
Table 11: Summary of possible FF degradation mechanisms which produce humins 66
Table 12: Mass loss due to soxhlet washing of humins for 24 hours 70
Table 13: Asymptotic significance of experimental factors with respect to humins concentration 72
Table 14: Asymptotic significance of experimental factors with respect to the mass of formic acid produced through fragmentation 74
Table 15: Summary of influential factors in this study 79

Stellenbosch University https://scholar.sun.ac.za

1. Introduction

Currently, fossil fuel refineries are still our main source for energy and materials. Due to their future availability and mainly because of environmental concerns, the feasibility and desirability of oil-based products is on the decline. Alternative, renewable solutions are necessary to mitigate climate change. Replacing oil with biomass for fuels and chemicals requires new production technology. Lignocellulosic biomass, which is abundantly available, is a potential and sustainable feedstock for production of green fuels and chemicals such as furfural (FF).

Green chemistry is also known as sustainable chemistry and it is the design of chemical products and processes that reduce or eliminate the use or generation of substances hazardous to humans, animals, plants and the environment. The integration of green chemistry into biorefineries and the use of technologies with a low environmental impact has made it possible to use sustainable production chains for biofuels and high value chemicals from biomass (Cherubini, 2010). The transformation of FF to different products is an excellent example of an environmentally friendly methodology that fulfil the principles of green chemistry (Mariscal et al., 2016).

Furfural is a diverse, useful platform chemical with reportedly, more than 80 chemicals being derived from it directly or indirectly (Mariscal *et al.*, 2016). Due to FF's conjugated double bonds, FF hooks on to molecules containing double bonds while ignoring molecules without double bonds. It is therefore used in the following applications: to remove aromatics from lubricating oils to improve the viscosity/temperature relationship, to remove aromatics from diesel fuels to improve the ignition characteristics and to obtain unsaturated compounds from vegetable oils such as soybean oil to make "drying oils" suitable for paints and varnishes (Zeitsch, 2000). Industrial FF production started in 1922. As early as 1923, it was found that FF is a very effective fungicide. FF inhibits the growth of wheat smut and it is much more effective than formaldehyde (which is a cheaper way to treat wheat smut through seed treatment) (Kiesselbach & Lyness, 1993).Formaldehyde is, however, known to be a human carcinogen(Council, 2014) and soaking seed in 0.5 % aqueous formaldehyde, completely destroyed the germination power (Zeitsch, 2000). In recent years the global annual FF production has grown to about 300-

Stellenbosch University https://scholar.sun.ac.za

700 kton (Cai et al., 2014; de Jong & Marcotullio, 2010). Worldwide, plant-parasitic nematodes cause an estimated agricultural loss of 60 billion U.S. dollars per annum and FF has been found to be a very effective nematode control agent (Zeitsch, 2000). FF is cheaper for equal effect than other nematocides, nontoxic for humans, safely and easily applicable and it is not taken up by the plant to be protected, so that it can be applied until harvest (Zeitsch, 2000). Interest in using FF as a feedstock for biofuels and bio-based chemicals is currently increasing, as proved by the number of publications on catalytic technologies for FF production and/or transformation, particularly in the past eight years (± 65 publications in 2010 compared with 245 publications in 2014) (Mariscal *et al.*, 2016).

Furfuryl alcohol (FOL), currently the main product of FF which is generated from 65 % of the overall FF produced, can be produced via the catalytic hydrogenation of FF, either in gas or liquid phase process. The gas-phase Cu-catalysed hydrogenation of FF is the preferred industrial route for FOL production (Mariscal *et al.*, 2016). FOL is the precursor to the following: resins, biofuels, fragrances, solvents, tetrahydrofurfuryl alcohol (organic solvent in the production of resin, paint and lipid.), ethyl furfuryl ether (food additive), ranitidine (medication which decreases stomach acid production), levulinic acid and γ-valerolactone (potential fuel and green solvent).

A typical FF production process includes the following steps:

1. Pentosan containing biomass (such as corn stover, sugarcane bagasse, oat hulls, flax shives and other agricultural residues or wood) and dilute acid are charged to a reactor.
2. Steam is fed to the reactor to heat the reactants to the desired conversion temperature and simultaneously strip the FF into the vapour phase, which then continues to a recovery system (Dunlop, 1948) and
3. Whilst this is a simple production process, used since 1922, its disadvantage is that FF degrades to form humins via condensation and resinification and formic acid (FA) via fragmentation (Mariscal *et al.*, 2016). These degradation reactions are mainly responsible for the low yields in FF production reactions and they begin to occur as soon as FF is formed.

Furfural has been produced from biomass for nearly a century. However, for most of this time, its production could be considered as niche because of the economically competitive alternatives that are not renewable. At present, industrial processes rely on inefficient production processes with around 50 % FF yields, compared to the

Stellenbosch University https://scholar.sun.ac.za

theoretical maximum, which reduces the capacity of the FF industry. Other challenges include high energy consumption, expensive downstream processing, corrosion and lack of co-products (Peleteiro *et al.* 2015) .

To improve the industrial potential of FF as a product, a better understanding of the aforementioned degradation and the kinetics of this reactions is required. The degradation reaction kinetics have a substantial influence over the final yields and that is why it is necessary to consider them. Degradation reactions contribute to yield losses. Therefore, it is important to study how they occur and what the products of these reactions are. This requires identification of the reaction conditions that result in higher yield loss, in order to control the loss reactions or to establish operating conditions to maximise FF production.

The experimental work of this study is conducted with pure FF, subjecting it to acidic conditions and temperatures that are similar to the conditions of FF production, in order to study their influence on FF degradation.

Degradation of FF occurs via 3 mechanisms which occur simultaneously.

1. Condensation is the reaction that occurs between FF and intermediates of the xylose to FF dehydration reaction (Root *et al.* 1959).
2. Resinification is the reaction between two FF molecules (Zeitsch, 2000) and in this study, it is the only possible degradation mechanism which produces humins, since experiments were only done with pure FF. In actual FF-from-biomass processes, both condensation and resinification are responsible for the formation of humins which are solid insoluble, heterogeneous, carbonaceous, furan rich macromolecules that form during degradation.
3. Fragmentation is the first-order conversion of FF to FA. It is known that FA is a degradation product of FF, as a product of the hydrolytic fission of the aldehyde group of FF (Dunlop, 1948; Williams & Dunlop, 1948). Fragmentation receives less attention in literature; however, it is significant under the conditions of this study.

The goal of this study is to explore the kinetic aspects of FF degradation reactions in the absence of xylose and intermediates in the xylose-to-FF reaction, to generate an industrially relevant understanding of the contribution of resinification and fragmentation to FF degradation. In previous studies, condensation was not excluded (by excluding xylose from the reaction mixture) and so there is novelty in its exclusion because the reaction kinetics discovered in this study reflect only fragmentation and resinification. This is practical and feasible because in

Stellenbosch University https://scholar.sun.ac.za

conventional biomass-based FF production, the humins are an integral part of the lignocellulosic residue that is used as boiler fuel. However, if hydolysate from biorefinery pre-treatment stages or from pulp mill pre-hydrolysis liquor is used to make FF, humins will be available for valorisation and it will be necessary to remove them so that they don't block up the system. By combusting humins, the issue of their presence as waste is resolved and they are turned into a bio-based fuel.

Humins (also referred to by the industry as "polymers") are the other product of the degradation reaction. They have the potential to block up pipes (AVA Biochem AG, 2018) and stick to reactor walls (Buzzard, 2003). The reaction by which humins are formed and their composition isn't clearly understood. It is therefore important that the mechanism of their formation is researched and that humins are either valorised (as a co-product) or their formation is reduced.

First-order kinetics have generally been applied successfully to the FF degradation reaction. A few studies have indicated that the reaction may not be exactly first-order, so there is room to explore the reaction kinetics of the reaction. The factors that affect degradation are mentioned by a few authors but a single concise interpretation of the various factors and their impact on the FF degradation reaction is missing.

Using pure FF as feedstock, this study will elucidate the reaction kinetics for FF degradation (without condensation or the interference of other sugars from the biomass). This allows us to determine whether the reaction is indeed first-order or whether there is a slight variation from unity. In addition, the factors which contribute to the rate of FF disappearance will be clarified. The factors which affect humin formation (temperature, initial FF concentration and sulfuric acid concentration) are discussed.

2. Literature Review

2.1 Furfural degradation

FF degradation reactions have been investigated by previous researchers because there is no clear understanding about which reactions occur and to what extent they occur. The reaction kinetics are also not clearly understood and a first order approximation is the best representation of the kinetics at present.

Stellenbosch University https://scholar.sun.ac.za

Danon, Marcotulio and de Jong (2013) conducted a detailed review of the mechanistic and kinetic aspects of FF formation in aqueous acidic media. Their review considers a reaction mechanism for FF formation that consists of a few reaction routes from acyclic xylose. The key steps involved are 1,2-enolization, β-elimination or isomerization via 1,2-hydride shift (See Figure 1).

Zeitsch (2000) identified 2 types of FF degradation reactions, namely resinification (See Equation 5) and condensation (See Equation 4) (Zeitsch, 2000). The products of these reactions are solids referred to as humins. An example of condensation is illustrated in Figure 1 where pentoses may be degraded to low molecular weight products, generated from the fragmentation of intermediate **3e** and **4**. These side products are mainly organic acids and aldehydes and they may react with FF to form humins. This degradation route entails the loss of already formed FF and reduced FF yield from xylose.

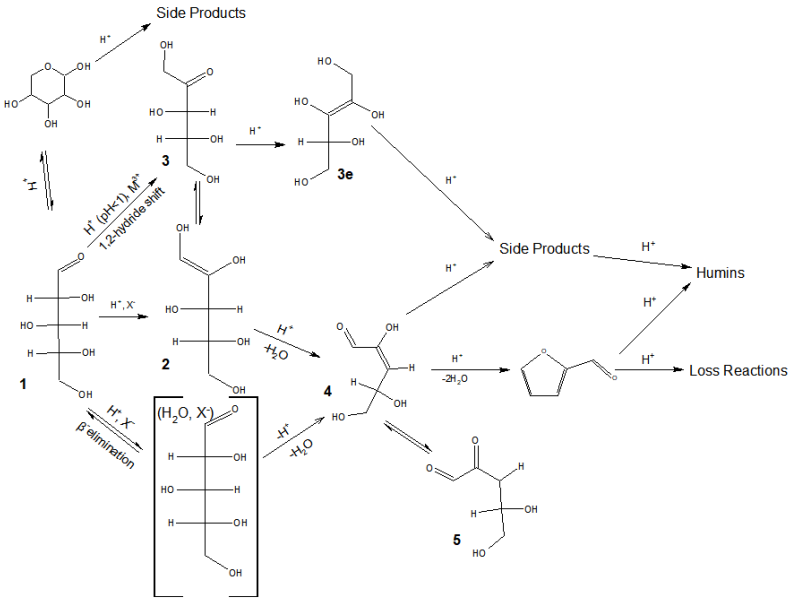

Figure 1: Proposed mechanism of xylose reaction to furfural in acid media. X^- indicates halides ions, and M^{3+} indicates metal cations. (sourced from Danon, Marcotulio and de Jong (2013))

Choudhary et al. (2011) found that in order to produce FF from xylose, an Sn-beta zeolite as well as a Brønsted acid are required in an organic solvent to catalyse the reaction. Under these conditions, the reaction proceeds at much lower temperatures than the typical temperature of this reaction. (100°C) Unfortunately the cost of

Stellenbosch University https://scholar.sun.ac.za

separating the FF from the solvent is too high and makes the process uneconomical (Choudhary *et al.*, 2011)

O'neil *et al.* (2009) proposes a variation of the condensation mechanism. The reaction proceeds as follows: isomerization of xylose to lyxose, dehydration of both pentoses to FF, rehydration of FF to organic acids, oligomerization of FF to two- and tridimensional Furilic oligomers and complete dehydration of organic acids to carbonaceous deposits (humins). It should be noted that the catalyst used in the study was a solid ZSM-5 zeolite and the reaction mechanism might be specific to this catalyst.

It is important to note that FF degrades under the same conditions of pH and temperature at which it is usually formed, yielding other products such as reductic acid and FA. It was postulated that FA is formed via hydrolytic fission of the aldehyde group on FF (Williams & Dunlop, 1948).

In general, there are consistent trends amongst degradation mechanisms, but certain attributes of each mechanism differ. In Figure 1, the "Loss reactions" arrow from FF consists of resinification and fragmentation reactions. The mechanisms of FF degradation will be discussed with the goal of expanding on the "Loss reactions" and "Humins" pathways in Figure 1. In summary 3 types of degradation reaction are assumed for FF degradation:

1. Resinification: FF and FF react to form humins (Equation 5)
2. Condensation (Equation 4): FF and xylose dehydration intermediates react to form humins
3. Fragmentation (Equation 6): FF is broken down into FA via hydrolytic fission of the aldehyde group on FF

Lamminpaa, Ahola & Tanskanen (2014) found that when FF was studied without the presence of xylose, FF reacted with itself, forming polymeric resins (resinification). FF can also undergo destruction reactions to smaller molecules (fragmentation) (Lamminpaa, Ahola & Tanskanen, 2012). Zeitsch (2000) classifies FF degradation as a reaction of FF with itself, commonly called "FF resinification" and a reaction of FF with an intermediate of the pentose-to-FF conversion, this reaction being commonly called "FF condensation" (Zeitsch, 2000). O'Neil *et al.* (2009) note that FF reacts with the fragmentation of FF to organic acids (O'Neil *et al.* 2009).

Stellenbosch University https://scholar.sun.ac.za

The following sections on humins and fragmentation will deal with the reaction mechanisms that have been proposed for these degradation reactions. The corresponding kinetics representations are subsequently discussed.

2.2. Humins

Humins and “polymers”, are the names given to the solid, insoluble, heterogeneous, carbonaceous, furan rich macromolecules that precipitate as a by-product of acid-catalysed conversion of biomass containing C_6 and C_5 sugars, hereinafter referred to as humins (Hoang *et al.* 2015; Hu & Ragauskas, 2014; Sanchez, Hernandez & Keresztury, 1994). The pathway to humin formation has not been established unequivocally. The structure of humins has also not been established but it is known that the structure depends strongly on the feedstock. The yield of humins is dependent on the feedstock and processing parameters such as temperature, glucose and acid concentration (Van Zandvoort *et al.* 2013).

Humins are by-products of FF formation and in order to deal with this issue, two strategies have arisen; humins are valorised or their formation is avoided under certain (usually expensive) biphasic processing conditions. At present, the valorisation of humins is not established and biphasic reactors are not yet economical or practical.

2.2.1 Valorisation

Recent literature has focussed on the valorisation of these insoluble by-products. The following are some of the valorisation options:

1. Humins can be combined with Polyfurfuryl Alcohol (PFA) to give a lower cost resin composite with decreased brittleness and higher tensile strength compared to pure PFA resins (Pin *et al.* 2014).
2. Hydrogen and synthesis gas can be produced through catalytic dry reforming of humins (Hoang *et al.*, 2015).
3. Humins can be functionalized and used as solid acid catalysts (Patil, Heltzel & Lund, 2012; van Zandvoort, 2015).
4. Humins can be converted to biochar which reduces the pH of saline soil and increases the available phosphorous in the soil (Wu, Xu & Shao, 2014).

None of these applications, however, have reached the level of industrial implementation. Another valorisation option, that is currently practiced on conventional FF plants, is to combust the humins formed during degradation and to

Stellenbosch University https://scholar.sun.ac.za

contribute to the energy for the operation of the FF plant. Combustion of humins (as part of the FF residue) formed amongst biomass fibres in conventional FF reactors is currently the only method of valorisation that is practiced. Based on the equation to calculate the higher heating value (HHV) of humins (Equation 1), knowing their elemental make up, it was determined that humins have an average HHV of 23.9 MJ/kg which is just less than half of the HHV of butane. (Sokhansanj, 2011) This value is calculated on a dry basis, so it is an overestimation of the energy that will be available from combusting humins.

$$\mathrm{HHV} = 0.35\mathrm{X_C} + 1.18\mathrm{X_H} + 0.10\mathrm{X_S} - 0.02\mathrm{X_N} - 0.10\mathrm{X_O} - 0.02\mathrm{X_{ash}} \qquad 1$$

$$\mathrm{HHV} = 0.35(63.75) + 1.18(4.07) - 0.10(32.17) = 23{,}898\ \mathrm{MJ \cdot kg^{-1}}$$

where X is the mass fraction (dry basis) for Carbon (C), Hydrogen (H), Sulfur (S), Nitrogen (N), Oxygen (O), and ash content (ash). The unit of HHV is MJ/kg dry mass.

The calculated calorific value of humins is shown in Appendix III. It was determined that combusting humins would generate 1.3 % of the energy required to produce FF. When producing FF from biomass, the humins are trapped in the processed biomass fibres (known as FF residue), which are used as boiler fuel. In the scenario where FF is produced from biorefinery pre-treatment stages or from pulp mill pre-hydrolysis liquor, the water-insoluble humins would have to be removed by filtration for use as boiler fuel.

2.2.2 Biphasic systems

To prevent the formation of humins, FF can be extracted continuously (in situ extraction) from the severe (aqueous acidic) environment where it is formed. This can be achieved by increasing stripping or by using a biphasic reaction system, where formed FF is rapidly extracted from the aqueous reaction mixture into a separate organic layer, such as water-methyl isobutyl ketone (MIBK) (Weingarten *et al.*, 2010). The organic layer thus serves as “storage” for the extracted FF where no further decomposition occurs and in their model, it was assumed that the FF decomposition occurred only in the aqueous phase (Weingarten *et al.*, 2010). Mandalika and Runge (2012) described a process of reactive batch distillation where a portion of the vapour is continuously removed from the reactor headspace

Stellenbosch University https://scholar.sun.ac.za

(Mandalika & Runge, 2012). This method results in high FF yields (85 %) and recovery of a highly porous cellulose stream during fractionation that can be further processed for production of pulp or cellulosic ethanol. Sener *et al.* (2018) conducted xylose dehydration in a sustainable solvent system composed of GVL and water and observed FF yields up to 93 % (Sener *et al.* 2018)

Cai *et al.* (2014) state that FF production is not economically viable without a low-cost feedstock and coproduction of other higher-value chemicals, such as bio-ethanol or carboxylic acids from the remaining lignin and cellulosic residues (Cai *et al.*, 2014). This further supports the incentive for an extractive reaction system. However, they also note that these biphasic systems require costly recovery operations to recycle the solvent and the solids loading must be reduced (to uneconomical levels) in order to maintain a distinct organic phase (Cai *et al.*, 2014). These are the disadvantages of a biphasic system.

Steam stripping, the status quo for conventional FF production from biomass, involves stripping with large quantities of steam (Lange *et al.*, 2012) resulting in a dilute aqueous FF stream. Zeitsch (2000) observed that the FF output increases with increasing stripping steam input, but this effect levels out (Zeitsch, 2000). The goal of stripping is to remove FF into the vapour phase and halt degradation reactions. Industrial FF processes, operating at temperatures below 220 °C and featuring a continuous removal of FF by steam stripping, have typical yields below 60 % (Zeitsch, 2000).

2.2.3 Mechanism & structure

To characterise humins, the different proposed mechanisms for their formation are discussed along with the general “structure” of the resulting macromolecules. It is not possible to definitively identify a structure for humins, because they are highly complex, cross-linked structures.

Sánchez, Hernández and Keresztury (1994) found that FF can take part in condensation reactions typical of aldehydes and that the furan ring can participate in addition, substitution, condensation and ring cleavage reactions (Sánchez, Hernández and Keresztury, 1994). The authors proposed that the formation of humins begins with (1) Brønsted acid catalysed protonation of the carbonyl oxygen in the FF molecule. (2) This molecule then attacks the (highly activated) 5-position of the furan ring of another FF and (3) the resulting (bifurylic) molecule then participates

Stellenbosch University https://scholar.sun.ac.za

in an aldol condensation with a third FF producing a trifurylic structure (Hoang *et al.* 2015; Hu & Ragauskas, 2014; Sanchez, Hernandez & Keresztury, 1994; Sumerskii, Krutov & Zarubin, 2010). The FF resinification mechanism, as described to this point, is used by several authors and will be referred to hereinafter as the Sánchez mechanism (demonstrated in Figure 2). Various authors have, departing from the Sánchez mechanism, proposed various growth/propagation mechanisms.

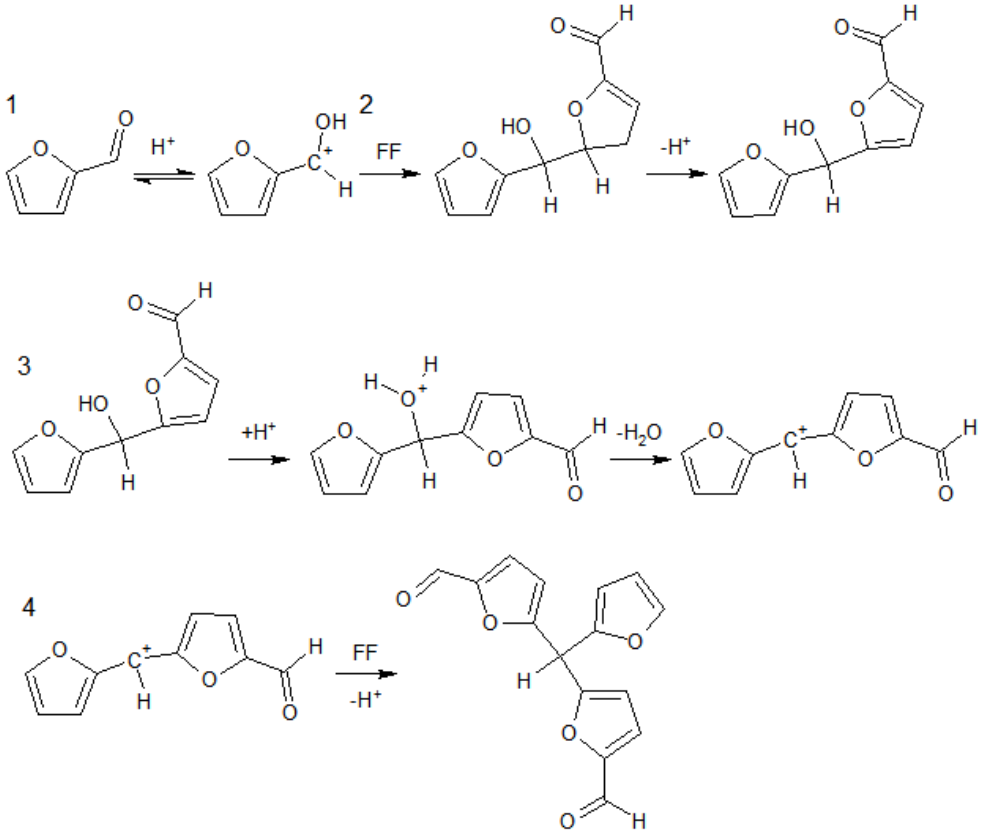

Figure 2: Sánchez mechanism for humin formation involving the formation of bifurylic and trifurylic structures. (sourced from Hoang *et al.* 2015; Hu & Ragauskas, 2014; Sanchez, Hernandez & Keresztury, 1994)

Sánchez, Hernández and Keresztury proposed that the bifurylic, trifurylic and acyclic molecules react to give the network structure of a humin (Sánchez, Hernández and Keresztury, 1994). Structure VI (the humin network) in Figure 3 is a result of reactions between the bifurylic and trifurylic molecules formed in reactions 3 and 4 (Figure 2) with acyclic species IV and V (Figure 3).

Stellenbosch University https://scholar.sun.ac.za

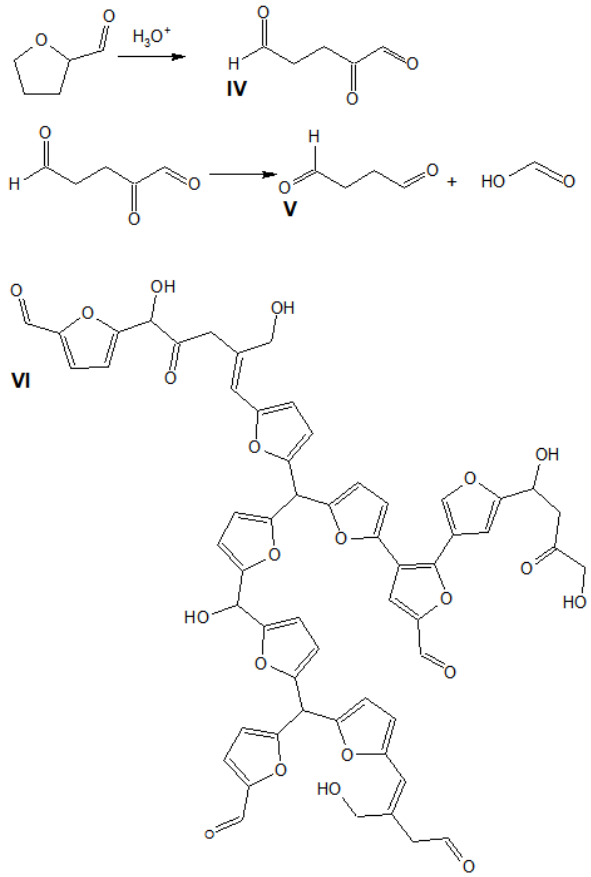

Figure 3: FF is transformed into acyclic species (IV & V) and structure VI is the humin network (more conjugated than in Figure 2) (sourced from Sánchez, Hernández and Keresztury, (1994))

Sanchez, Hernandez, Jalsovszky & Czira (1994) conducted a study to elucidate the structural units present in acid catalysed FF humins. The humins were obtained from fresh vacuum distilled FF. They used a strong mineral acid as catalyst and dried the humins under high vacuum. The humins were subjected to pyrolysis at 400 °C and FT-i.r. (Fourier transform infrared) was used to detect products of pyrolisis. They found that FF can behave as a cyclic ether, a diene or an aromatic compound (Danon et al (2013) also observed this behaviour),so many products are possible. There was an abundance of AA and 2-furylmethyl ketone in the pyrolysis of humins at 400 °C; these compounds can only be formed through structures with linear segments originating from species IV and V (See Figure 3) which form part of the postulated humin structure in the Sanchez mechanism. They detected O-H groups and normal vibration modes of C-H at positions 3 and 4 of a disubstituted furan ring. They also detected carbonyl groups present in the groups -CH_2CHO and -CH_2COCHR- and they detected 2-substituted and 2,5-disubstituted furan rings.

Stellenbosch University https://scholar.sun.ac.za

These are all characteristic of the postulated humin structure in the Sanchez mechanism (see Figure 2).

Gandini and Belgacem (1997) proposed that tertiary hydrogen atoms in the polyfurylic structures are particularly mobile and can leave the structures, generating radicals, which are stabilised as the structures become more conjugated (Gandini & Belgacem, 1997). Mariscal *et al.* (2016) found the same intermediate molecule and that the mechanism consists of hydrolytic ring opening, which generates aliphatic open-chain products. (Mariscal *et al.*, 2016) The difference between the Sanchez mechanism and the Gandini mechanism is that the hydrogen atoms of the Gandini mechanism can leave the structure and generate radicals, whereas the Sanchez mechanism does not include these mobile hydrogen atoms. The Gandini intermediate is shown in Figure 4.

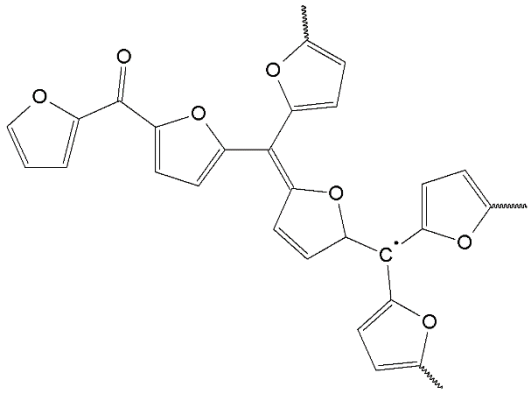

Figure 4: Radical intermediate for the thermal resinification of FF. Tertiary hydrogen atoms in the polyfurylic structures generate radicals, which are stabilised as the structures become more conjugated (sourced from Gandini and Belgacem (1997))

Sumerskii, Krutov and Zarubin (2010) proposed that further resinification occurs via a mechanism similar to aromatic electrophilic substitution with the formation of carbon-carbon bonds between rings (Sumerskii *et al.*, 2010). This growth mechanism is depicted in Figure 5.

Stellenbosch University https://scholar.sun.ac.za

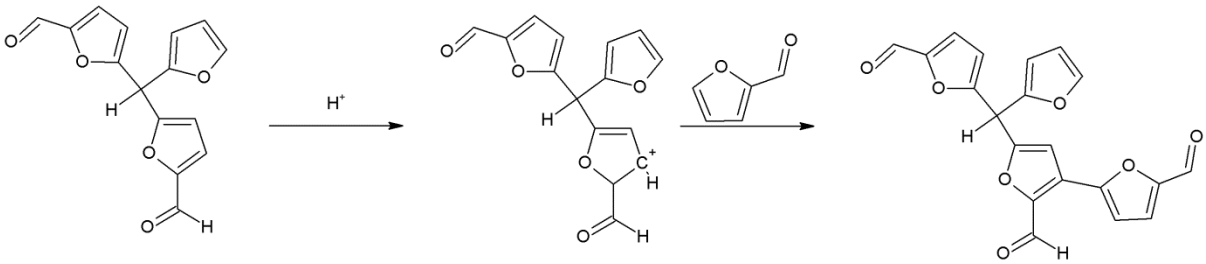

Figure 5: Humin growth mechanism: Polycondensation occurs via electrophilic substitution with the formation of carbon-carbon bonds between rings

O'Neil *et al.* (2009) initially believed that humins were formed through a reaction between FA and FF. This mechanism was then experimentally disproven in favour of the following: FF molecules react with each other to form oligomers. The oligomerization of FF has been demonstrated to occur via the aldolic condensation of FF which forms two- and three-dimensional furylic species The reactions occur either via ring opening or via addition reactions with the formyl group. The open ring binds with cyclic FF to form a short chain oligomer with many double bonds, which are very reactive and undergo further addition reactions. The oligomer structure can be seen in Figure 6.

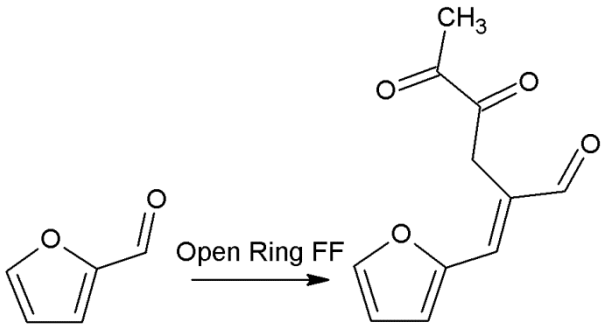

Figure 6: Ring opened furfural binds with cyclic furfural to form a short chain oligomer with many double bonds

Danon, van der Aa and de Jong (2013) studied FF degradation with and without glucose present in the reaction mixture and found that an additional (second-order) reaction had to be added to the kinetics of the degradation reaction to satisfactorily predict the experimental data. They suggested that the second order humin formation reaction could be accounted for by a Diels-Alder reaction,(Danon, Van Der Aa & De Jong, 2013) i.e. a second order reaction between 2 FF molecules or a reaction between glucose or one of its degradation products: 5-hydroxymethylfurfural (HMF) or Levulinic Acid (LA) and FF. The proposed Diels-Alder reaction between FF

Stellenbosch University https://scholar.sun.ac.za

molecules is illustrated in Figure 7. For the Diels-Alder reaction, it is suggested that a second order formation reaction occurs between 2 FF molecules, followed by first order propagation. Mariscal *et al.* (2016) found that due to the electron-withdrawing effect of the carbonyl group, the furan ring of FF is less susceptible to hydrolytic ring cleavage and Diels–Alder cycloaddition reactions (Mariscal *et al.*, 2016). This suggests that a Diels-Alder reaction is unlikely.

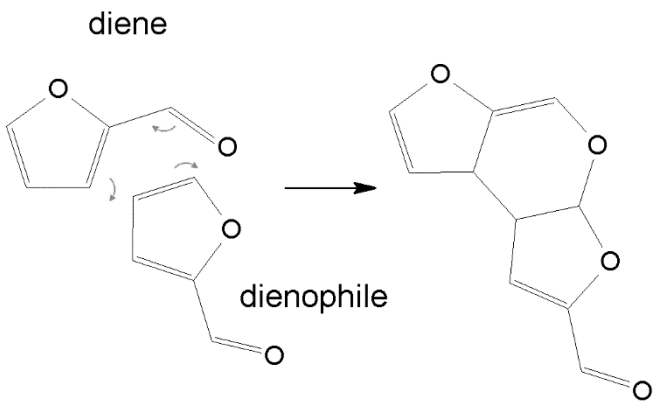

Figure 7: Diels-Alder reaction between 2 FF molecules (sourced from Danon, van der Aa and de Jong (2013))

Literature has focused on C_6-derived humins more than C_5-derived humins and although it is not of direct relevance to FF degradation, it is potentially interesting to discuss these C_6-derived humin formation mechanisms due to the similar nature in which C_5 and C_6 sugars react under dilute acidic conditions.

HMF is an important, highly functionalized, bio-based chemical building block, produced from the dehydration of hexose sugars. It has been designated as the sister molecule of FF and it, like FF, can be converted to other valuable chemicals such as carboxylic acids and p-xylene (Tsilomelekis *et al.* 2016). Like the acid catalysed hydrolysis of hemicellulose, acid catalysed hydrolysis of cellulosic biomass is afflicted with the co-production of humins. The discussion hereinafter will involve comparisons between HMF- and FF-derived humins.

Patil, Heltzel and Lund (2012) compared humins formed from glucose, fructose and HMF and found that these species must first be converted to HMF and then to the highly reactive intermediate 2,5-dioxo-6-hydroxyhexanal (DHH) via ring opening, before humins can form via subsequent aldol addition and condensation reactions (See Figure 8),(Patil *et al.*, 2012) i.e. direct conversion of hexoses to humins is

Stellenbosch University https://scholar.sun.ac.za

insignificant. Hu and Ragauskas (2014) as well as Wang *et al.* (2016) reinforced the fact that FF and HMF are the key intermediates for humin formation (Hu & Ragauskas, 2014; Wang, Lin, Zhao, Chen & Zhou, 2016).

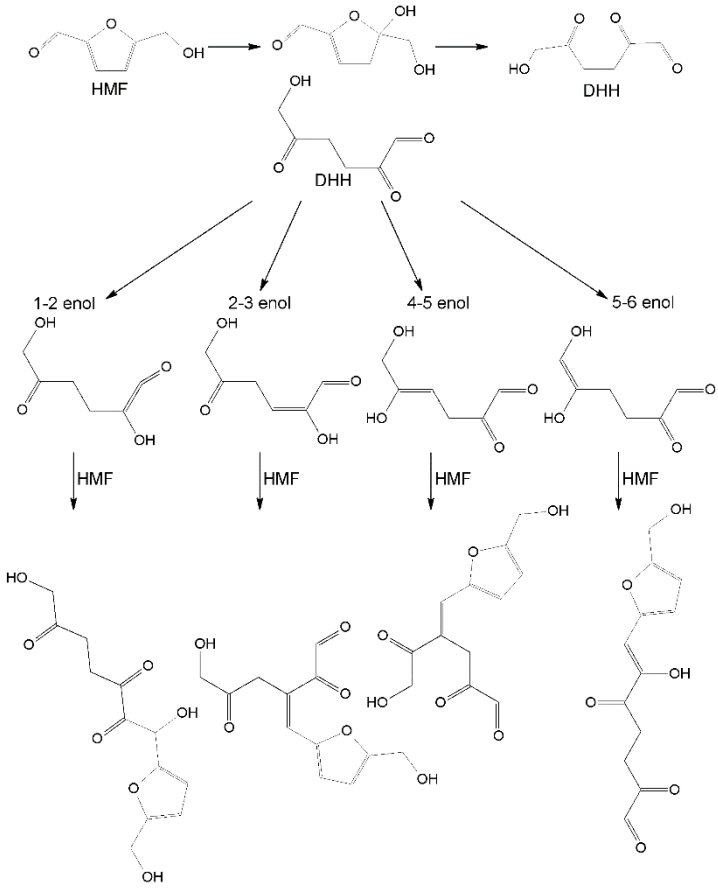

Figure 8: Hydrolytic ring opening of HMF and possible aldol addition reactions (adapted from Patil, Heltzel and Lund (2012))

Rasmussen *et al.* (2014) proposed that humins form via polymerisation reactions from the key intermediate 3,8-dihydroxy-2-methylchromone (DMC) derived from FF (See Figure 9) (Rasmussen, Sørensen & Meyer, 2014).

Shinde *et al.* (2018) supported this claim. DMC, a benzenoid derivative, was found to be a major aromatic product in the acid degradation of xylose (Shinde *et al.* 2018). Popoff & Theander (1970) found that DMC, isolated in small amounts after heating alginic acid and other polyuronides at 160 °C, was the only benzenoid compound that has been reported from acidic degradation of sugars (Popoff & Theander, 1970). In this study, no sugars are present, so it is unlikely that DMC is an intermediate for the humin formation reaction.

Stellenbosch University https://scholar.sun.ac.za

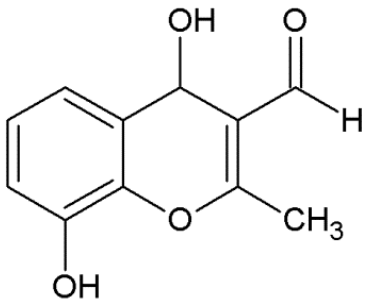

Figure 9: 3,8-dihydroxy-2-methylchromone, potential intermediate in humins formation mechanism.

Lamminpaa, Ahola & Tanskanen (2014) suggested that hydrolytic ring opening of FF produced 1,2,5-tripentanon (TP), which has eno and keto forms. Thus, it is plausible that FF can undergo the same kind of reaction scheme as HMF through aldol addition/condensation. This is notable and a potential reaction mechanism has been illustrated in Figure 10, which mimics the mechanism of Figure 8.

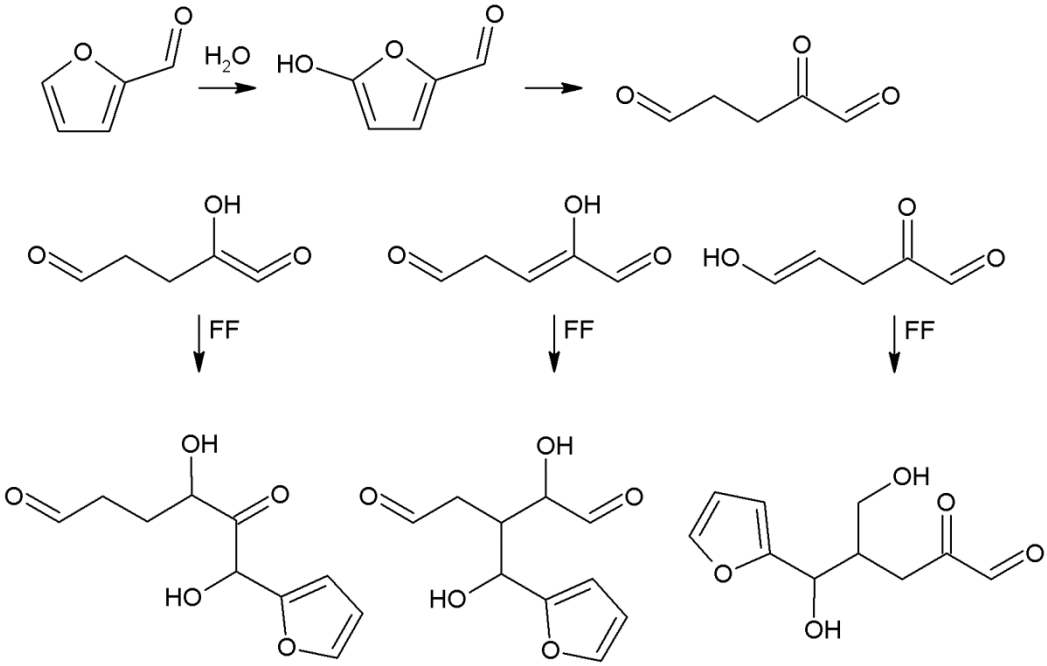

Figure 10: Possible furfural ring opening, and aldol reactions as suggested by Lamminpaa, Ahola & Tanskanen (2014)

Van Zandvoort *et al* (2015) found that xylose-derived humins differ in molecular structure from glucose-derived humins because of the free 5-position of FF which allows for resinification. The xylose-derived humin structure is a network of furanic units, linked by aliphatic CH_2 and CH groups. Van Zandvoort *et al.* (2013) included a model representation of a C_5 humin fragment (See Figure 11), which is similar to the

Stellenbosch University https://scholar.sun.ac.za

structure first proposed by Gandini and Belgacem (1997) (Gandini & Belgacem, 1997; Van Zandvoort *et al.*, 2013) .

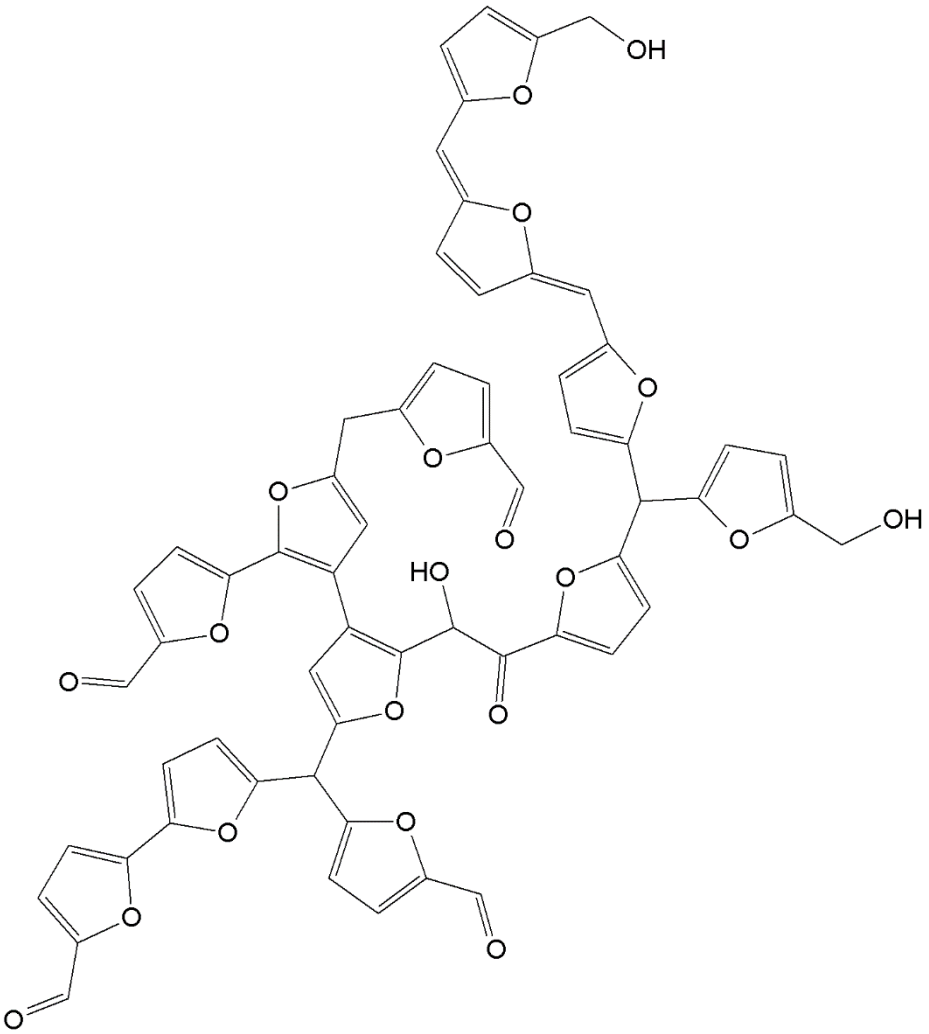

Figure 11: Model representing the molecular structure of a xylose derived humin fragment, including the most important linkages (sourced from van Zandvoort *et al.* (2013))

Zeitsch only described the mechanism for FF condensation and proposed that resinification plays a much lesser role in humins formation. In condensation reactions, FF condenses with one of the pentose dehydration intermediates in either of the following ways: one molecule of FF reacts with the first intermediate to give “furfural xylose” or two FF molecules react with an intermediate to give “difurfural xylose”. The mechanism is illustrated in Figure 12; A summary of the proposed mechanisms discussed in this section is presented in Table 1.

Stellenbosch University https://scholar.sun.ac.za

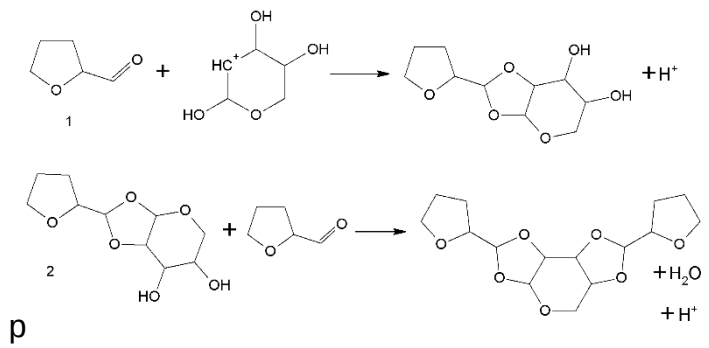

Figure 12: One molecule of FF reacts with the first pentose dehydration intermediate to give “furfural xylose”, Two FF molecules react with an intermediate to give “difurfural xylose” (sourced from Zeitsch (2000))

Table 1: Summary of proposed mechanisms for FF degradation

Description	Reagents	Resinification/ Condensation	Key Intermediates	Ref.
FF condenses with itself to form difuryl ketonic aldehyde and trifurylic dialdehyde These structures are susceptible to hydrolytic ring cleavage to acyclic species and growth occurs through reactions between the acyclic and cyclic forms of these structures.	FF+FF	Resinification		(Sánchez, Hernández and Keresztury , 1994)
FF condenses with itself to form difuryl ketonic aldehyde and trifurylic dialdehyde, tertiary hydrogen atoms in the molecule leave the structures and generate radicals, which are stabilised as the structures become more conjugated	FF+FF	Resinification	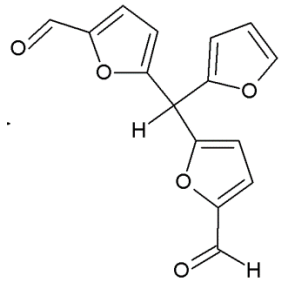	(Gandini & Belgacem, 1997), (Mariscal *et al.*, 2016)
FF condenses with itself to form difuryl ketonic aldehyde and trifurylic dialdehyde, growth occurs via electrophilic substitution	FF+FF	Resinification		(Sumerskii *et al.*, 2010)
The free 5-position of FF allows for resinification. The humin structure is a network of furanic units, linked by aliphatic CH2 and CH groups.	FF+FF	Resinification		(Van Zandvoort *et al.*, 2013)
FF molecules react with each other to form oligomers. The reactions occur either via ring opening or via addition reactions with the formyl group. The open ring binds with cyclic FF to form a short chain oligomer with many double bonds	FF+FF	Resinification	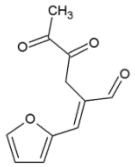	(O'Neil *et al.*, 2009)
Diels-alder reaction between two FF molecules	FF, FF	Resinification	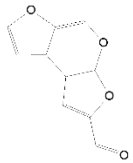	(Danon *et al.*, 2013)

Stellenbosch University https://scholar.sun.ac.za

Polymerisation reactions involving FF and DMC	FF, DMC	Resinification	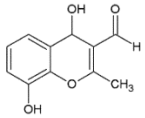	(Rasmussen *et al.*, 2014)
FF undergoes hydrolytic ring opening to form TP and then aldol addition occurs between TP and FF	FF, TP	Resinification	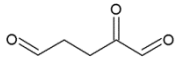	(Lamminpaa, Ahola & Tanskanen, 2014)
Either 1 or 2 FF molecules react with a pentose-to-FF intermediate to give “furfural xylose” or “difurfural xylose”	FF, Xylose dehydration Intermediate	Condensation	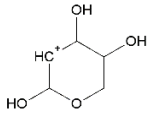	(Zeitsch, 2000)

Stellenbosch University https://scholar.sun.ac.za

2.2.4 Other degradation reactions

Another possible degradation product from FF is reductic acid, which is ultimately formed with the α-C atom of FF at C_2 of reductic acid (Feather, 1969). Reductic acid was formed from FF at 150 °C in 5 % sulfuric acid as demonstrated in Figure 13.

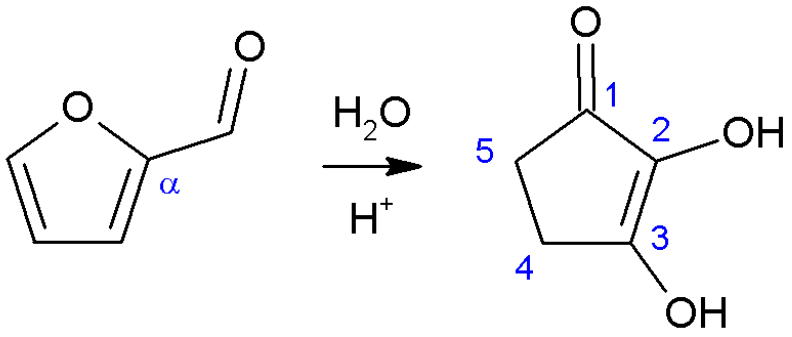

Figure 13: Reductic acid: a potential furfural degradation product

Reductic acid was mentioned as a possible decomposition product by Feather (1968) but the reaction remains seemingly unexplored (Danon, Marcotullio & De Jong, 2013; Marcotullio, 2011; Marcotullio *et al.*, 2009). It could be a humin precursor or intermediate.

2.2.5 Catalyst, substrate and humin yields & composition

Previous studies dealing with humins considering different conditions i.e. temperature, reaction time, catalyst and substrate as well as the resulting humins yield and the C:H:O elemental ratio of these humins, are listed in Table 2. Since characterisation of C_5-derived humins has not received much attention in literature, most of these studies are based on humins derived from hexoses or HMF.

In general, experiments with a higher severity (higher temperature (180 °C+), higher acid concentration (0.1 M+) and longer reaction time (1 h+)) lead to a higher yield of humins (Sannigrahi *et al.* 2011). The “yield” of humins varies between 0.4 wt% and 30 wt% (see Table 2) based on total FF degraded and the yield is dependent on the severity and the substrate used.

Weingarten *et al.* (2011) compared the yield of humins from xylose, FF and a combination thereof (Weingarten *et al.*, 2011). They conducted dehydration experiments with heterogeneous acid catalysts HCl (Brønsted acid) and $Yb(OTf)_3$ (Lewis acid) at 88 °C. The temperature was very low, but the acids catalysed 5 % to 30 % humins yields in 90 min reactions. In FF production, Brønsted acids are

Stellenbosch University https://scholar.sun.ac.za

generally used as a catalyst (HCl, and sulfuric acid(H_2SO_4)). They found that xylose dehydration did not occur at the low reaction temperature due to its high activation energy (Ea), relative to that of the condensation and resinification reactions. The condensation reactions were suppressed because of the negligible amounts of FF and xylose dehydration intermediates. However, even at relatively low severity, resinification humins formed (10.4 %) when FF only was reacted. This is the only study where FF was used as the sole precursor in humins formation reactions. There is a gap in literature in this regard.

H_2SO_4 with a concentration of 1 wt% or $\pm$0.1 M is common amongst humins studies and 180 °C is a common temperature. In all studies with these parameters, some humins are formed (See Table 2). Therefore, it is for this reason that these conditions were included in the range of the present study.

Table 2: Summary of humins studies

Reference	Temperature (°C)	Catalyst	Substrate	C:H:O	Humins Yield
(Wang *et al.*, 2016)	180 (3 h)	H_2SO_4 (0.01 M)	Glucose	66.3:4.8:28.9	-
			Xylose	66.9:4.4:28.7	
(Wang et al., 2015)	150 (45 min)	AlCl3.6H2O (0.025 M)	Glucose	52.4:5.3:42.4 (insoluble)	0.67 wt%
				58.1:5.4:36.5 (soluble)	4.17 wt%
(Hoang *et al.*, 2015)	180 (6h)	H_2SO_4 (0.01 M)	Glucose	66.3:4.4:29.3	35 ± 1 wt%
(Hu & Ragauskas, 2014)	180 (40 min)	H_2SO_4 (0.1 M)	Control[c]	-	7.94%[a]
			O_2[c]		16.15% [a]
			N_2[c]		9.30% [a]
			DMSO[c]		5.56% [a]
			Tween[c]		6.93% [a]
(Pin *et al.*, 2014)	-	-	Fructose in methanol solvent	60.0:5.0:32.0	-
(Van Zandvoort *et al.*, 2013)	180 (6 h)	H_2SO_4 (0.01 M)	D-glucose	64.7:4.3:31.1	30 wt%
	180 (6 h)		D-fructose	64.8:4.1:31.1	39 wt%
	180 (6 h)		D-xylose	66.8:3.8:29.4	32 wt% (26 wt% FF)
	180 (6 h)		D-glucose, D-fructose (1:1)	65.3:4.2:30.5	36 wt%
	180 (6 h)		D-glucose, D-fructose, D-xylose (1:1:1)	66.0:4.1:29.9	30 wt% (2 wt% FF)
	180 (6 h)		D-glucose, HMF (1:0.2)	65.9:4.2:29.9	30 wt%
(Patil *et al.*, 2012)	125 (5 h)	H_2SO_4 (0.1 M)	Glucose	-	29%
	125 (2 h)		Fructose		24%
	125 (2 h)		HMF		18%
(Sannigrahi *et al.*, 2011)	160 (5 min)	H_2SO_4 (0.1 M)	Pretreated holocellulose	-	0.4 wt%[b]
	170 (20 min)	H_2SO_4 (0.1 M)			0.8 wt% [b]
	170 (40 min)	H_2SO_4 (0.1 M)			8.8 wt% [b]
	180 (40 min)	H_2SO_4 (0.1 M)			9.3 wt% [b]
	170 (60 min)	H_2SO_4 (0.2 M)			11.7 wt% [b]
	180 (60 min)	H_2SO_4 (0.2 M)			19.3 wt% [b]
(Weingarten *et al.*, 2011)	88 (1.5 h)	HCl (0.01 M)	Xylose (3 wt%)	-	5.3%
			Furfural (2 wt%)		10.4%
			1:1 Mixture FF:X		5.3%
		$Yb(OTf)_3$ (0.01 M)	Xylose (3 wt%)		27.5%
			Furfural (2 wt%)		7.4%
			1:1 Mixture FF:X		17.4%
(Sumerskii *et al.*, 2010)	175-180 (2 h)	H_2SO_4 (0.5 %)	D-Glucose	66.4:4.7:28.9	21%
			D-Mannose	65.7:4.7:29.6	24%
			D-Galactose	66.1:4.7:29.2	26%
			D-Arabinose	68.3:4.9:26.8	29%
			D-Cellobiose	65.1:5.1:29.8	25%
			Methyl-α-D-glucopyranoside	66.1:4.9:28.9	23%
			5-hydroxymethylfurfural	-	7.4%

[a]wt% based on K-Lignin (acid insoluble) found in solids recovered [b]wt% based on mass of K-lignin per mass pretreated holocellulose [c]Dilute Acid Pretreatment hydrolysis monosaccharides

Stellenbosch University https://scholar.sun.ac.za

2.3. Formic acid

2.3.1 Formic acid as furfural degradation product

Williams and Dunlop (1948) first mentioned the formation of FA during the course of FF destruction via hydrolytic fission of the aldehyde group on FF. They noted that it is formed in a small quantity and that it did not significantly alter the initial hydrogen ion concentration as a consequence of its low degree of dissociation (Williams & Dunlop, 1948). It is possible that FF fragmentation to smaller molecules can occur in acid catalysed dehydration conditions where only FF is present (Lamminpaa *et al.*, 2012). These smaller molecules may include formaldehyde, acetaldehyde, crotonaldehyde, lactic acid, dihydroxyacetone, glyceraldehyde, pyruvaldehyde, acetol, and glycolaldehyde (Antal et al., 1991; Rice & Fishbein, 1956). O'Neil *et al.* (2009), who studied the aqueous phase dehydration of xylose into FF, identified FA formation from decomposition of open chain xylose as well as rehydration of FF (O'Neil *et al.*, 2009). Marcotullio *et al.* (2009) found that FA couldn't be clearly identified and quantified for FF destruction in a coiled tube reactor at 150-200 °C and H_2SO_4 concentration between 36 and 145 mM. Quantitative analysis of HPLC-UV chromatograms deemed the presence of FA to be marginal (Marcotullio *et al.*, 2009). Weingarten *et al.* (2010) mentioned that quantifiable amounts of FA were detected after 8 hours of FF dehydration (Weingarten *et al.*, 2010). Sumerskii, Krutov and Zarubin (2010) found that FF decomposes with the formation of FA only upon prolonged heating in the presence of dilute acids(Sumerskii *et al.*, 2010). However, Hongsiri et al. (2014) observed almost 20 % degradation of FF to FA when imposing conditions of 200 °C and 0.05 M HCl for 1 hr. They also found that at 180 °C, the concentrations of FA were very low and at 160 °C they were so low that they became immeasurable(Hongsiri, Danon & De Jong, 2014). Lamminpaa, Ahola & Tanskanen found that the decomposition reactions of FF impact more on the yield than reactions between xylose intermediate and FF, i.e. condensation played a lesser role than fragmentation and resinification (Lamminpaa *et al.*, 2012). Antal et al. (1991) found that although FA had been stated to be a co-product of humin formation, it is produced in significant yield under relatively mild conditions in the absence of detectable resin

formation (Antal *et al.*, 1991), i.e. fragmentation is separate from condensation/resinification. FA formation, as a direct FF destruction product, is not

Stellenbosch University https://scholar.sun.ac.za

clearly understood and different sources have reported its presence or absence under similar reaction conditions. A summary of the works where FA is detected is presented in Table 3.

Stellenbosch University https://scholar.sun.ac.za

Table 3: Formic acid as direct degradation product of furfural

Precursor	Relative FF Concentration (M)	Conditions	Formic Acid Detected	Ref
FF	0.104 & 0.208	150-210 °C, 25 mM & 50 mM H_2SO_4, 50 mM & 100 mM HCl, up to 270 min	Small quantity	(Williams & Dunlop, 1948)
Xylose	-	Relatively long exposure at elevated temperatures is required to bring about extensive destruction by dilute aqueous acids	Yes	(Dunlop, 1948)
Xylose	0.057	250 °C, 20mM formic acid catalyst	Yes	(Antal *et al.*, 1991)
Xylose	0.076	220 °C, plain water (no acid), 50 min	7 %	(Oefner *et al.* 1992)
Biomass	-	FF waste water is known to contain formic acid at roughly 10 % of the acetic acid load (5 %)	±0.5 wt%	(Zeitsch, 2000)
FF	0.060-0.073	150-200 °C, 36-145 mM H_2SO_4	Marginal	(Marcotullio *et al.*, 2009)
Xylose	0.784	200 °C, 3 wt% ZSM-5 zeolite	Yes	(O'Neil *et al.*, 2009)

Stellenbosch University https://scholar.sun.ac.za

Individual monosaccharides, disaccharides, and furan compounds	-	0.5 % H_2SO_4, 2 h, 175–180 °C	Yes	(Sumerskii *et al.*, 2010)
xylose, arabinose, and FF	0.05	200 °C, 50 mM HCl for 1 hr	±18.4 % of FF	(Hongsiri *et al.*, 2014)
Xylose	0.417	180 °C, 0.17 M acetic acid for 24 hrs	Yes	(Chen et al., 2015)

Stellenbosch University https://scholar.sun.ac.za

2.3.2 Furfural to formic acid degradation mechanism

The mechanism by which FA is formed from FF was first suggested by Williams and Dunlop (Williams & Dunlop, 1948). The mechanism is hydrolytic fission of the aldehyde group (See Figure 14) (Dunlop, 1948). This mechanism is similar to the mechanism by which HMF is rehydrated. Yang *et al.* (2012) support the hydrolytic fission of the aldehyde group of FF towards FA, because FF waste water at Wuji Furfural Co. of China contained a lot of FA (7.8 g/L) (Yang *et al.* 2012). No other works have attempted to reconcile this mechanism since.

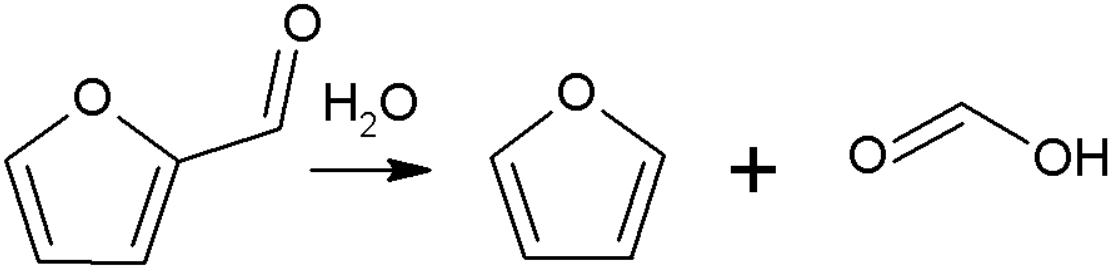

Figure 14: Hydrolytic fission of the aldehyde group on furfural to form formic acid

2.3.3 Alternate sources of formic acid in furfural production

As mentioned in the FF degradation section, FA is a degradation product of xylose under dilute acidic conditions (Danon, Marcotullio & De Jong, 2013; Liu *et al.*, 2013). Aldehydes, ketones, pyruvic acid, glycolic acid, FA, LA, and acetic acid (AA)are all products of xylose decomposition. These products are formed by “fragmentation” of xylose or its isomers (Liu *et al.*, 2013). Oefner *et al.* (1992) & Antal *et al.* (1991) found that FA is a degradation product of xylose degradation (Antal *et al.*, 1991; Oefner *et al.*, 1992), so it is possible that the FA quantity found after a FF degradation reaction, where xylose is the starting material, is not exclusively generated by FF degradation but also by xylose degradation.

In a genuine FF production plant, the Escher Wyss process, for example, is operated without a mineral acid by relying on the “innate” carboxylic acids that are liberated from the raw material (Zeitsch, 2000). This phenomenon of autohydrolysis occurs in the Illovo FF plant reactors in Sezela, KZN (Rushin, 1992). The only acids formed in large enough quantities to make a significant contribution to the hydrogen ion concentration are AA and FA. The two acids contribute evenly to the acidity because there is 10 times as much AA present as FA and FA is approximately 10 times as strong as AA (Rushin, 1992; Zeitsch, 2000). This autohydrolysis is only possible for

Stellenbosch University https://scholar.sun.ac.za

processes where the feedstock is biomass. As explained by Zeitsch (2000), the pentosan chains of different biomass materials contain acetyl and formyl groups (in a ratio of 10:1) to various extents. The hydrolysis of these lead to the liberation of AA and FA (Zeitsch, 2000). Xing, Qi and Huber (2011) found that FA and AA were mainly produced via the hydrolysis of formylated and acetylated xylose oligomers (Xing, Qi & Huber, 2011). Rivas *et al.* (2014) noted that FA was present in the autohydrolysis liquors of pine wood, due to hydrolysis of formyl groups present in the raw material (Rivas *et al.*2014). In a study of acid catalysed hydrolysis of sugar cane bagasse, insignificant amounts of AA were detected in the hydrolysates but FA is formed (Girisuta *et al.* 2013).

In summary, FA can form during the production of FF in the following ways:

1. Fragmentation of xylose and its isomers
2. During dilute acid pretreatment of biomass, formyl and acetyl groups on the pentosan polymer are hydrolysed to their respective carboxylic acids
3. Glucose (from the cellulose fraction of biomass) is converted to LA and FA via HMF under hydrolysis conditions
4. FF decomposes to FA under the conditions of acid hydrolysis

It is possible that the presence of FA can be attributed to the formylated xylose oligomers and polymers in the raw materials that are present in FF production reactors (Zeitsch, 2000). However, in the present study, the focus is on the direct degradation of FF to FA and no raw materials (biomass) is present so only one route to FA production is possible: fragmentation of FF.

2.4. Kinetics

2.4.1 Reaction kinetics for this study

In general, kinetic studies suggest a reaction mechanism including a single degradation reaction, with respect to FF that follows first order kinetics because the degradation of FF is referred to as pseudo-unimolecular (Jing & Lü, 2007; Rose *et al.*, 2000; Weingarten *et al.*, 2010; Williams & Dunlop, 1948). The rate of the FF degradation reaction is generally given by Equation 2 or some derivation thereof.

$$\frac{dC_{FF}}{dt} = -kC_{FF}^{n} \times [H^{+}]^{m} \qquad 2$$

Stellenbosch University https://scholar.sun.ac.za

where C_{FF} is FF molar concentration (M), k is the rate constant (min^{-1}), n is the degradation reaction order and m is the index factor of the hydrogen ion concentration: a unitless hydrogen ion concentration exponent.

The rate constant (k) is a function of temperature and the Arrhenius expression is used to define this relationship (See Equation 3).

$$k = A' e^{-\frac{Ea}{R}(\frac{1}{T}-\frac{1}{T_0})} \quad 3$$

where k is the rate constant (min^{-1}), A' is the pre-exponential factor (min^{-1}), Ea is the activation energy ($kJ \cdot mol^{-1}$), R is the universal gas constant ($kJ \cdot mol^{-1} \cdot K^{-1}$), T is the temperature (K) and T_0 is the reference temperature (453.15 K)

and T_0

Table 4 is an overview of the various degradation studies to date and their Arrhenius parameters. Equations 4, 5 & 6 describe the condensation, resinification and fragmentation reactions as covered in section 2.1.

$$\mathrm{FF + Intermediate \rightarrow Condensation\ Product} \quad 4$$

$$\mathrm{FF + FF \rightarrow Resinification\ Product} \quad 5$$

$$\mathrm{FF \rightarrow FA} \quad 6$$

The dehydration of xylose and FF degradation are acid catalysed reactions. For these reasons, the hydrogen ion concentration should be included in the rate expression (See Equation 2). Zeitsch (2000) noted that the temperature dependence of acidity differs from acid to acid and that to formulate an accurate kinetic model, the temperature must be accounted for both in the exponential factor (See Equation 3) as well as in the acidity. These two effects oppose each other because increasing temperature causes a decrease of acidity, but an increase in the energy of the reacting molecules (Zeitsch, 2000). The temperature dependency of acid dissociation can be taken into account either by using activity-based models(Hongsiri, Danon & de Jong, 2015; Marcotullio *et al.*, 2009) or by empirical equations (Lamminpää, 2015) . For sulfuric acid, there are 2 protons (H atoms) per sulfuric acid molecule that can be donated and it is termed a “diprotic” acid. The 2 H

Stellenbosch University https://scholar.sun.ac.za

atoms can be removed and made available to react with water to produce H_3O^+ which is what reacts with the contents of the solution. The first dissociation constant for sulfuric acid is high, meaning that the first proton dissociates almost completely in water, but the second proton dissociates less readily and the extent of the dissociation is very temperature dependent. The overall acidity of a sulfuric acid/water solution is equal to the sum of the acidity contributed by both dissociation constants. The temperature dependence of acid dissociation in the present study is accounted for by empirical equations (Zeitsch, 2000).

2.4.2 Reaction kinetics for previous kinetic studies

In Table 4, the activation energies (Ea) for the first order kinetic approximation of FF loss reactions are presented and the values range from 50 to 135 kJ/mol. The pre-exponential factor for these studies (A) varies between 3 s^{-1} and 27 s^{-1}. It should be noted that the acid catalyst, catalyst concentration and temperature ranges differ between studies. Some studies have included the hydrogen ion concentration in the rate expression (Lamminpaa *et al.*, 2014; Root *et al.*, 1959; Rose *et al.*, 2000; Williams & Dunlop, 1948). The reaction temperatures selected for the present study cover the range 140 °C-200 °C which is similar to the temperature ranges used in previous studies (See Table 4). The reaction temperature for the dehydration of pentose to form FF is ± 175 °C (Dalinyebo, 2018) so the present study covers this temperature as well as temperatures above and below it. There is no apparent trend in terms of acid catalyst and activation energy/pre-exponential factor.

Stellenbosch University https://scholar.sun.ac.za

Table 4: Furfural degradation kinetics studies.
A = pre-exponential factor (s^{-1}); Ea = activation energy (kJ·mol^{-1}); $[H^+]$ = hydrogen ion concentration (M); a_{H^+} = hydrogen ion activity (−)

Temperature Range (°C)	Precursor	Acid Catalyst (N)	$\ln(A)\ (s^{-1})$	$Ea(kJ \cdot mol^{-1})$	Ref
120 - 200	birchwood xylan	H_2SO_4 (0, 0.038 & 0.38 N)	4.26· $[H^+]^{0.09}$	49.6	(Lau *et al.*, 2015)
150 - 210	FF	H_2SO_4 (0.05 & 0.1 N) HCl (0.05 & 0.1 N)	12.36	83.7	(Williams & Dunlop, 1948)
150 - 200	FF	H_2SO_4 (0.073-0.291 N)	a_{H^+} ·26.64	125.1	(Marcotullio *et al.*, 2009)
160 - 240	xylose	H_2SO_4 (0.006, 0.025, 0.05, 0.1, 0.2, 0.4 & 0.8 N)	17.15· $[H^+]$	92.3	(Root *et al.*, 1959)
130 - 200	FF & xylose	FA (1.536-6.875 N)	9.72 27.34· $[H^+]$	75.5 (Uncatalysed) 135.0 (Catalysed)	(Lamminpaa *et al.*, 2012)
160 - 200	FF	FA (0.435, 2.206 & 6.906 N)	-13 24.22· $[H^+]$	0 (Uncatalysed) 113.6 (Catalysed)	(Lamminpaa *et al.*, 2014)
160 - 200	FF	HCl (0.05 N) & NaCl (0.5 N)	16.84	102.1	(Danon *et al.*, 2013)
130 - 170	xylose	HCl (0.1 N)	8.43 (Resinification) 13.5 (Condensation)	67.6 (Resinification) 72.5 (Condensation)	(Weingarten *et al.*, 2010)
180 - 220	FF/xylose	High Temperature Liquid Water (Uncatalysed)	7.59	58.8	(Jing & Lü, 2007)
130 - 170	FF	HCl (0.1 N)	3.07	48.1	(Rose *et al.*, 2000)
170 - 210	xylose	AA (0.17 N)	22.08	64.4	(Chen *et al.*, 2015)

Lamminpää (2015) presented results which show that the pH has a greater effect on the reaction rate when the temperature rises. Therefore, independent activation energies for uncatalysed and acid catalysed terms were used in kinetic modelling (See Equation 7) (Lamminpää, 2015). This technique was also used in an earlier study by the same author (See Table 4). The H^+ concentration was calculated via an empirical equation for pKa (a measure of acid strength).

$$\frac{dC_{FF}}{dt} = -k_0 C_{FF}^n - k_H C_{H+} C_{FF}^p \qquad 7$$

where k_0 is the rate constant for an uncatalysed reaction(s^{-1}) in the solvent, k_H is the rate constant for an acid catalysed reaction (s^{-1}), C_{H+} is the concentration of the H+ molecule and n and p are the order of uncatalysed and acid catalysed reactions, respectively.

Stellenbosch University https://scholar.sun.ac.za

The overall reaction order varied around one, indicating that multiple reactions with different reaction orders may exist but first order reactions are dominant. It is likely that resinification occurs because of the formation of humins. Lamminpää (2015) proposes that a polymerisation reaction is initiated with FF resinification and polymer growth occurs one FF molecule at a time (Lamminpää, 2015). If growth is dominant, the reaction order will be closer to unity (as it is). Danon, van der Aa and de Jong (2013) proposed a Diels-Alder reaction, which could be the second order initiation step for the described polymerisation (Danon *et al.*, 2013). The main mechanisms proposed for the reaction of FF, including formation and degradation are illustrated in Figure 15, Figure 16 & Figure 17.

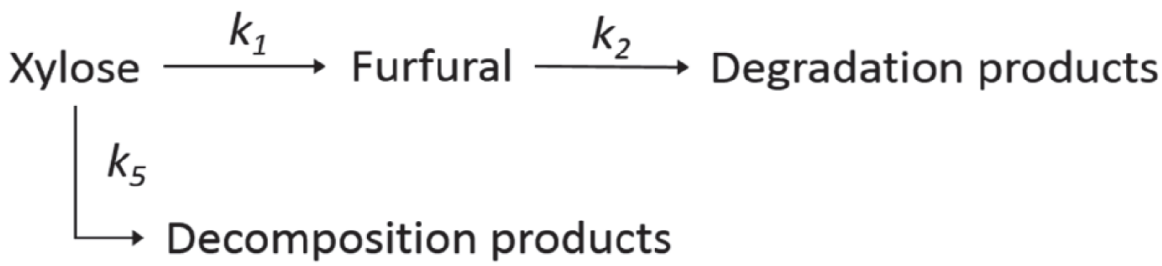

Figure 15: Reaction scheme for FF formation in acidic conditions excluding condensation reaction. (Sourced from Lamminpää (2015))

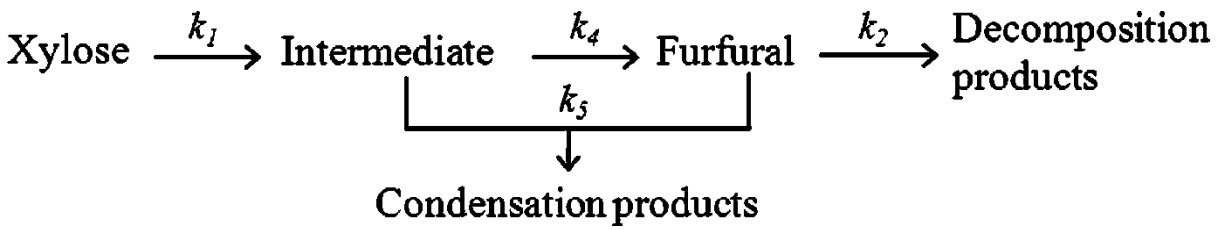

Figure 16: Reaction scheme for FF formation in acidic conditions including condensation reaction. (Sourced from Lamminpää (2012))

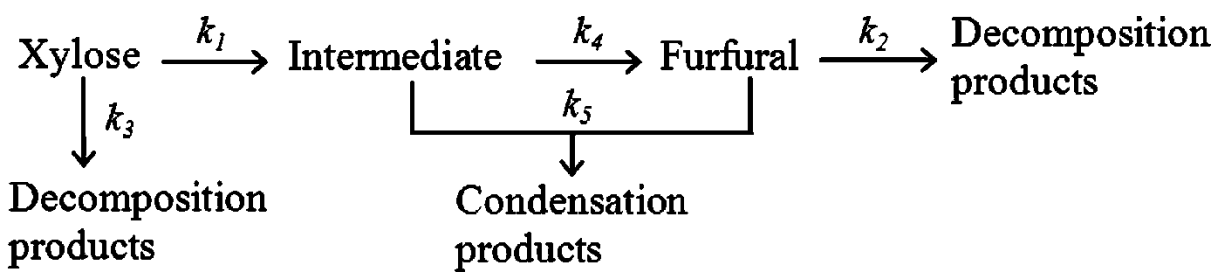

Figure 17: Reaction scheme for FF formation in acidic conditions including condensation reaction and xylose decomposition reaction. (Sourced from Lamminpää (2012))

Stellenbosch University https://scholar.sun.ac.za

Considering these reaction mechanisms, the mechanism of Figure 17 is most probable because it is known that xylose forms decomposition products in acidic conditions (Chen *et al.*, 2015). Condensation and resinification are also known reactions (Root *et al.*, 1959). In the present study, Figure 17 is supported with the understanding that the reaction of FF to decomposition products includes both resinification (Equation 5) and fragmentation (Equation 6).

2.4.3 Studies where 1st or 2nd order reaction kinetics were detected

So far, the discussion has centred on xylose and FF, but the reality is that the cellulose and hemicellulose constituents of lignocellulosic biomass are both hydrolysed under acidic conditions in a FF production plant. This means that FF degradation could involve intermediates from the cellulose. Danon, van der Aa and de Jong (2013) noticed second order FF degradation kinetics when glucose was included in the reaction mixture (Danon *et al.*, 2013). Essentially it is not fully clarified whether condensation involves xylose, xylose dehydration intermediates towards FF, other xylose dehydration intermediates or even glucose. Due to this uncertainty, a few degradation studies have been tabulated (See Table 5) to determine what the general understanding is with regard to the order of the FF degradation reaction. One can observe that the order of the degradation reaction is not affected by the initial xylose/FF concentration (See Table 5).

Stellenbosch University https://scholar.sun.ac.za

Table 5: Studies which report 1st/2nd order reaction kinetics for the FF degradation reaction

C_{FF_0} or C_{X_0} (M)	1st/2nd order	Resinification/ Condensation	Reference
0.05 xylose	1st order	Condensation	(Antal *et al.*, 1991)
0.688 xylose	1st order	Condensation	(O'Neil *et al.*, 2009)
0.0478 FF	1st order	Both	(Root *et al.*, 1959)
0-0.08 FF 0-0.2 xylose	1st order resinification	Both	(Lamminpaa *et al.*, 2012)
0.05, 0.1 & 0.16 FF	1st order / slightly above 1st order (high acid concentration)	Both	(Lamminpää, 2015)
0.104 FF	1st order	Resinification	(Rose *et al.*, 2000)
0.688 xylose	1st order	Both	(Weingarten *et al.*, 2010)
0.01-0.02 FF	1st order (suggested 2nd order)	Resinification	(Williams & Dunlop, 1948)
0.533 xylose 0.208 FF	1st order	Both	(Chen *et al.*, 2015)
0.034 FF	1st order	Condensation	(Jing & Lü, 2007)
0.05 FF	1st order resinification & 2nd order condensation	Both	(Danon *et al.*, 2013)
0.05, 0.10 and 0.16 FF	Order varies around unity depending on the FA concentration	Both	(Lamminpaa *et al.*, 2014)
0.0604 & 0.0725 FF	1st order	Both	(Marcotullio *et al.*, 2009)

Stellenbosch University https://scholar.sun.ac.za

0.05 xylose, 0.05 L-arabinose & 0.05 FF	1st order	Resinification	(Hongsiri *et al.*, 2014)
0.1 FF	1st order	Resinification	(Xu *et al.* 2017)

2.5. Furfural degradation in xylose dehydration reactions

Dussan et al. (2015) conducted kinetic experiments at temperatures between 130 and 170 °C in various FA solutions (10-64 wt%) with hemicellulose-based sugars from the Formosolv pulping process. The goal was to elucidate the reaction kinetics of major components in the hemicelluloses fraction of biomass. Dussan et al. (2015) acknowledge that FF undergoes resinification and decomposition through hydrolytic cleavage of its saturated ring. The kinetics of FF degradation were modelled following a first-order reaction rate and the temperature dependence was represented by the Arrhenius equation. It was found that the best fitting reaction mechanism for dehydration of xylose to FF was the mechanism where xylose is converted to an intermediate, followed by dehydration to FF and then conversion of FF to resinification products. (Dussan *et al.* 2015)

Sener et al. (2018) conducted xylose dehydration reactions in γ-valeracetone (GVL) and water (80:20) at temperatures of 200 -250°C in 1-10 mM HCl and found that a 93 % FF yield was obtained in this GVL water solvent system. In this monophasic, environmentally benign solvent system, degradation is minimised, leading to maximum FF yields. Reaction orders with respect to FF and xylose were found to follow apparent first-order kinetics. The rates of xylose and FF disappearance are proportional to the hydrogen ion concentration in aqueous media using mineral acids as catalysts. It was found that reaction temperature has the greatest influence on FF yield. (Sener *et al.*, 2018)

Chen et al. (2015) found that the FF degradation rate only depends on the reaction time and is not affected by the FF concentration. This characteristic conforms to a first order reaction. Due to the very low ionization constant, the AA used in their study has little effect on the hydrogen ion concentration. It was found that increasing temperature could accelerate the transformation rate of xylose into FF but the FF yield was unaffected. (Chen *et al.*, 2015)

Stellenbosch University https://scholar.sun.ac.za

Degradation of D-xylose in either plain water or aqueous sulfuric acid at temperatures ranging from 180–220 °C resulted in the production of up to 50 mol% of FF. During the reaction, pyruvic acid, glycolic acid, lactic acid, FA and AA were formed (Oefner *et al.*, 1992). Oefner *et al.* (1992) also found that there was no significant difference between the activation energy of the hydrolysis of D-xylose in plain water or sulfuric acid which is strange because Dussan et al. (2015) found that there were different ranges of activation energies for different acid catalysts.

Wang et al. (2018) found that chromium (III) enhanced the reaction rate of xylose conversion to FF in sulfuric acid solution. Chromium (III) addition favoured the main reaction to FF without significantly increasing the rate of the consecutive side reaction. Xylose conversion in sulfuric acid solution in a stainless-steel reactor was higher than xylose conversion in pure sulfuric acid (non-steel reactor). Wang et al. (2018) chose first order reaction kinetics for this analysis and the experimental data was shown to fit well. Wang et al. (2018) conducted the conversion of xylose to FF in 50 mM sulfuric acid in both 316 stainless-steel and a reactor lined with glass and coated with Teflon. It was found that the reaction in 316SS has an apparent rate constant of almost three times that of the glass lined reactor. When using only chromium (III) sulfate, the reaction from FF to FF degradation products is greatly reduced and can be reduced to 0 when more chromium is used (Wang *et al.* 2018) .

In summary of these FF degradation reactions in xylose dehydration reactions, the FF yield in biphasic reactors doesn't exceed 50 % irrespective of temperature, mineral acid catalyst concentration and xylose concentration. FF degradation follows first-order reaction kinetics. FF is formed from xylose via an intermediate. Increased temperature increased the rate of xylose transformation but did not increase FF yield. Chromium (III) enhances the reaction rate of xylose conversion to FF but does not enhance the rate of degradation reactions and in fact reduces the FF degradation reactions. 316 stainless-steel also enhances the xylose conversion to FF.

2.6 Extent of fragmentation, resinification & condensation reactions

Based on the lack of a trend amongst the studies in Table 3 for the quantity of FA detected,it can be said that the fragmentation reaction is not affected by acid catalyst concentration, initial FF concentration or reaction temperature. The studies in Table

Stellenbosch University https://scholar.sun.ac.za

3 make use of various different acid catalysts but in the present study, the factors affecting fragmentation will be elucidated for sulfuric acid.

Zeitsch (2000) believed that the propensity for resinification decreases with increasing temperature and that at higher temperatures, FF is more easily consumed in condensation reactions than in resinification reactions (Zeitsch, 2000). Sener *et al.* (2018) found the opposite, that condensation was negligible in their xylose dehydration reactions in GVL at 200 – 250 °C, 0.001 – 0.01 M H_2SO_4/HCl and 0.066 - 0.66 M xylose concentration (7.2 – 72 g/L maximum FF yield) (Sener *et al.*, 2018). The present study covers initial FF concentrations of 15-60 g/L and sulfuric acid concentrations of 0.05 - 0.2 M, i.e. the acid concentration that Sener *et al.*(2018) used is ± 5 % of the acid concentration used in this study and the reaction temperature that they used is ± 50℃ higher. Sener *et al.*(2018) studied xylose dehydration (not pure FF degradation) in a biphasic reactor (GVL-water) and concluded that FF loss due to condensation of xylose and FF is minimized at elevated temperature. This conclusion was not tested in this study because a) pure FF was used and no xylose was present to facilitate condensation and b) a biphasic reactor was not used. If their postulation is correct, that FF loss due to condensation of xylose and FF is minimized at elevated temperature, then an interesting optimization problem exists. Elevated temperature causes more resinification but condensation is minimised. Karinen, Vilonen & Niemelä (2011) found that the selectivity of FF in xylose dehydration gradually increases with time, and at 140 °C, for example, a maximum selectivity is obtained after 9 h. Thereafter the selectivity starts to decrease because of degradation reactions of FF, such as the condensation (Karinen, Vilonen & Niemelä, 2011). The implication of this finding is that the reaction duration is also a factor that should be considered when optimizing degradation.

Stellenbosch University https://scholar.sun.ac.za

3. Objectives

3.1 Problem Statement

FF degrades in the same dilute acidic reaction medium in which it is formed. Degradation products (humins & FA) are formed in this study as a result of resinification and fragmentation reactions. A clear reaction order for FF degradation has not been established. The reaction conditions under which FA & humins form and the relationship between these conditions (temperature, catalyst concentration & FF concentration) and the amount of degradation products formed is unknown. Once humins are formed, there is no strategy to deal with them and no valorisation plan exists.

3.2 Goals

The following objectives have been identified for this study:

To investigate FF degradation at industrially relevant conditions. To conduct mass balances which accounts for the products of pure FF degradation i.e. for the given reaction system. To establish the possible reaction mechanism, responsible for humins production based on elemental data of the humins. To determine how each degradation product is affected by the experimental factors. To select the appropriate kinetic scheme for pure FF degradation from literature. To establish what the reaction order of pure FF degradation is with respect to FF. To establish a valorisation method for humins. To determine whether a relationship exists between processing conditions and humins elemental composition. To determine whether functional groups are trapped in the humins structure by conducting a soxhlet wash and elemental analysis of the wash fluid.

Stellenbosch University https://scholar.sun.ac.za

3.3 Novelty

Most literature which attempts to deal with yield loss has focussed on (expensive) extractive methods instead of attempting to bring clarity to the nature of the degradation reactions. Literature which has focused on understanding FF degradation has not been in harmonious agreement. By performing degradation experiments with FF alone (without xylose), it is possible to more accurately determine the kinetics of resinification and fragmentation of FF independently. This study involves the clarification of the extent to which degradation products are formed under various reaction conditions. Although degradation studies have been conducted before (See Table 6), using pure FF as precursor, this study makes use of industrially relevant operating conditions. Actual industrial operating conditions are Temperature:165−180°C, FF Concentration:3.0−5.0% & Acid concentration:0.3−1.0% (H_2SO_4)

Stellenbosch University https://scholar.sun.ac.za

Table 6: FF degradation studies from pure FF

Reference	Acid	Acid Conc. (wt%)	Furfural Conc. (wt%)	Temp (°C)
(Williams & Dunlop, 1948)	H_2SO_4 & HCl	0.48 (H_2SO_4) & 0.36 (HCl)	0.10-0.21	150 - 210
(Marcotullio *et al.*, 2009)	H_2SO_4	0.36-1.43	0.58-0.70	150 - 200
(Lamminpaa *et al.*, 2014)	HCOOH	2.00-30.00	0.48-1.54	160 - 200
(Danon, Van Der Aa, *et al.*, 2013)	HCl	0,18	0,48	160 - 200
(Rose *et al.*, 2000)	HCl	0.36	1.00	130 - 170
Present work	H_2SO_4	0.50-2.00	1.50-6.00	140-200

Stellenbosch University https://scholar.sun.ac.za

4. Material & methods

4.1 Experimental setup

A Büchiglasuster Hastelloy C-22 polyclave reactor (6), as shown in Figure 18 and Figure 19, was used for this research. The volume of the reactor was 2.1 L. The C-22 alloy is highly corrosion and wear resistant compared to common iron alloys and for a boiling aqueous solution of 2 % sulfuric acid, the corrosion on Hastelloy C-22 is only 125 µm/y. Maximum allowable pressure and temperature were 60 bar and 250 °C, respectively. The reactor was surrounded with a jacket which was used for heating/cooling the reactor. The jacket was heated electrically and the reactor was cooled with cooling water which runs through the jacket. At the bottom of the reactor there was a flush valve (7) used to empty the reactor and at the top of the reactor there were 3 needle valves (4, 5 & 9). One of the needle valves was for the sampling system and the other two were for the dosing system. The sampling system was made up of a 1/8” stainless steel button filter to keep humins out of the samples (8), a 3 mm pipe running from the filter inside the reactor to the needle valve outside the reactor (9). After the needle valve, the 3 mm tubing was coiled (10) and placed in a small ice bath (11).

The dosing system was made up of a nitrogen bottle (1), followed by a 3-way valve (2) which was open to the atmosphere on one side (which could be used to release excess nitrogen) and on the other side it was connected to a bomb (3). After the bomb there are two needle valves (4 & 5); one below the bomb (so that the bomb can be filled while it is closed) and one that opens to the reactor once the bomb has been prepared.

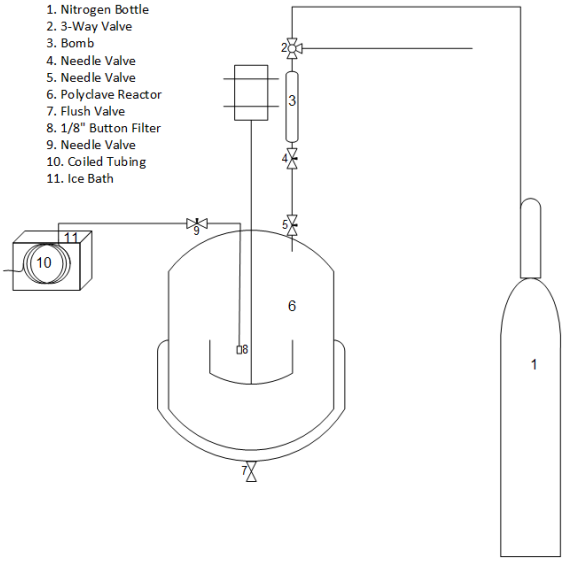

Figure 18: Schematic diagram of experimental setup for the polyclave reactor, labelled according to the legend.

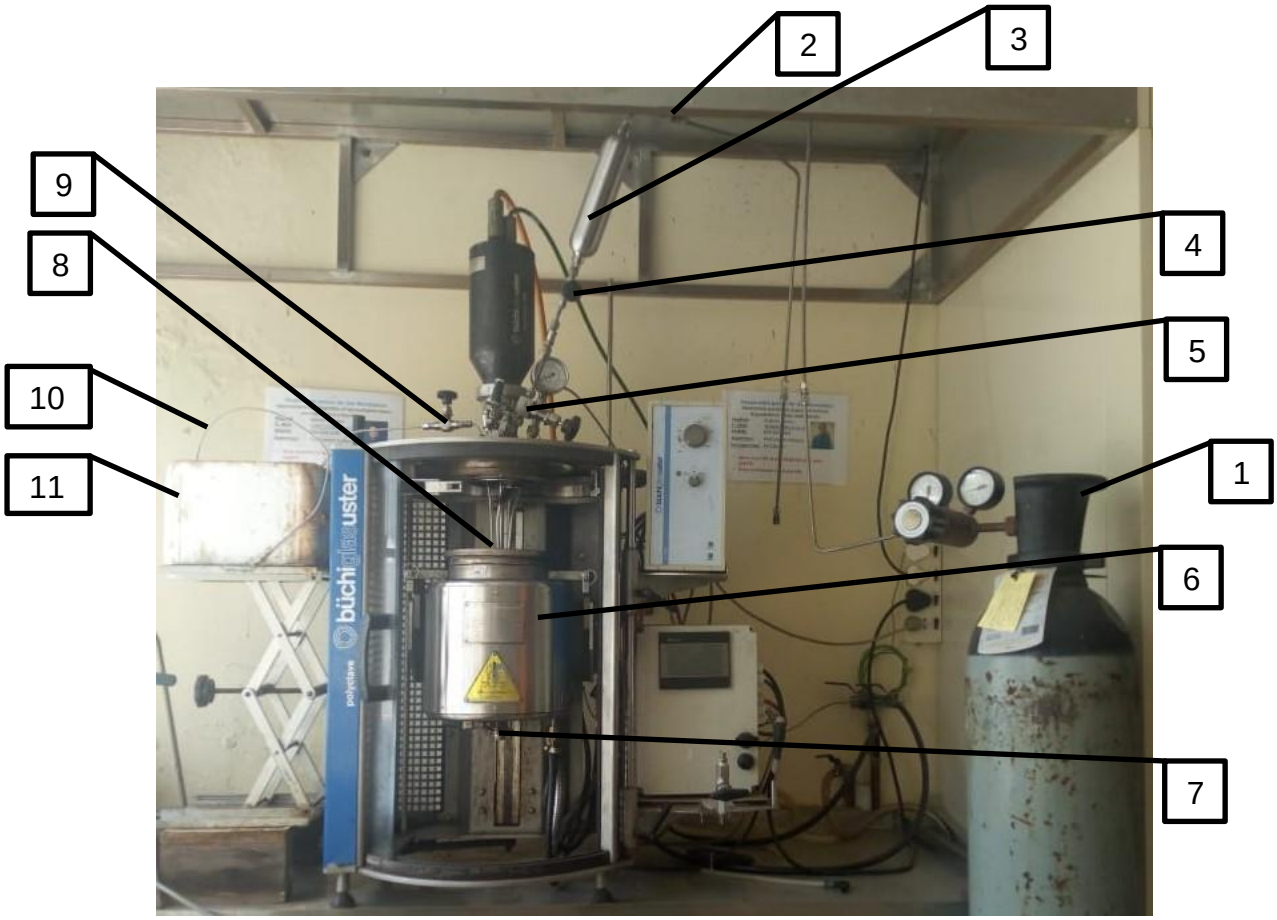

Figure 19: Photo of experimental setup, labelled according to the legend in the schematic diagram.

Stellenbosch University https://scholar.sun.ac.za

The bomb could be disconnected from the system and loaded with 100 mL fluid at 5, 10 and 20 wt% H_2SO_4. For each run, the reactor was loaded with the required amount of FF and reverse osmosis water to give a total of 900 mL, thus bringing the total volume to 1 L. Once the FF water mixture had been prepared and loaded, it was mixed at 500 RPM for a few minutes before the first sample was taken manually. 500 RPM was chosen because it was a value that appeared in other literature and O'neil *et al.* (2009) found that for xylose degradation at 1200 RPM and at 800 RPM there was no difference in xylose concentration profile, therefore the reaction is not affected by increased stirring speed and so 500 RPM should suffice (O'Neil *et al.*, 2009). After the first sample had been taken, heating began. The heating rate was not the same for the three reaction temperatures but acid was only added once the reactor was at the desired reaction temperature so the heating rate/duration had no effect on the reaction kinetics.

The FF used in this work was from Illovo Sezela (KZN) and was 99.2 wt% FF. The H_2SO_4 used in this work was from Fluka Analytical (Sigma-Aldrich) with 95 – 97 % purity.

The experiments were designed based on full factorial design with 3 parameters at 3 levels, as shown in Table 7.

Table 7: Factors of factorial design & naming convention

Temperature	140 °C: A	170 °C: B	200 °C: C
FF Concentration	1.5 wt%: X	3.0 wt%: Y	6.0 wt%: Z
Sulfuric acid Concentration	0.5 wt%: α	1.0 wt%: β	2.0 wt%: γ

The investigated parameters include initial FF concentration (at the start of degradation), sulfuric acid concentration and temperature. The aim was to select an upper and lower level of (initial) FF concentration from previous studies that represents the current industrial operations. The solubility limit of FF is 83 g/L (8.23 wt%) and the average low FF concentration (of previous studies) is 3.3 g/L (0.33 wt%), so the three chosen concentrations were 1.5 wt% (±15.07 g/L), 3.0 wt% (±30.19 g/L) and 6.0 wt % (60.64 g/L). In this study, sulfuric acid was used as mineral acid catalyst because it is the most widely used homogeneous acid catalyst

Stellenbosch University https://scholar.sun.ac.za

commercially and academically. The sulfuric acid concentrations for experiments in the present study were 0.5 wt%, 1 wt% and 2 wt% (±0.1 N, 0.2 N & 0.4 N). The previous studies investigated catalyst concentrations of 0.04 - 8 N (See Table 4). Higher normality of acid was only used for the weaker acids (FA), most acid catalysts were used at concentrations of 0.04 - 0.8 N (H_2SO_4 & HCl). Since most industrial reactors operate between 140 °C and 200 °C and academic studies also fall into this range, 140 °C, 170 °C and 200 °C were selected for this research.

4.2 Experimental Procedure

The reactor was heated with electrical elements in the jacket which were controlled by a Programmable Logic Controller (PLC) which made use of proportional–integral–derivative (PID) values that were determined for each of the reaction temperatures. As the temperature increased, the pressure in the reactor also rose due to the vapour pressure of the solution at increased temperature and due to the pressure increase from bombing in the acid catalyst with nitrogen from the nitrogen bottle (1). At reaction temperature, 10 samples were taken (one every 10 minutes) while the degradation reaction proceeded. The ice used to cool the samples was replenished for each run and it was necessary to cool each sample from the reactor temperature (140/170/200 °C) down to ambient temperature. The needle valve (8) was only opened to draw a sample and there was a pressure difference to push the sample out. Before the second sample was taken, the acid water mixture was bombed in with nitrogen gas so all the degradation that occurred during the heat-up process was uncatalyzed because the acid had not been added yet.

After 10 samples had been taken, the cool-down process began. Once the reactor had cooled down significantly (60 °C), it was emptied through the flush valve and while this was happening the last sample was taken. It is noted that this final sample was not filtered and so it was darker than the other samples. The humins were collected at the end through the flush valve and then that solution was filtered using grade 1289 filter paper (8-12µm retention rate).

The reactor was then rinsed with water until the water coming out after a rinse was clear. All the “dirty” water was collected and filtered through the same grade 1289 filter paper. The first rinse with water was conducted at 60 °C and the reactor was stirred at 500 RPM. Once the rinse water ran clear (after 2 or 3 rinses with water),

Stellenbosch University https://scholar.sun.ac.za

sodium hydroxide was used to clean the reactor. A solution of approximately 0.1 M NaOH was used and after this NaOH wash, the reactor was rinsed again with water to remove residual NaOH so that the reactor was ready for the next experiment. The 1289 filter paper was placed in a Büchner funnel and after all the rinse water had passed through it and only humins remained, the filter paper was removed (with humins) and dried overnight in a kiln at 70 °C. The dry humins were then weighed and stored for Elemental Analysis.

Following this procedure, after each run 12 samples were prepared for High-Performance Liquid Chromatography (HPLC). Each sample was diluted with water in the ratio of 1:20 into a 2 mL Eppendorf tube and filtered through a 0.22 micron syringe filter into the HPLC vial. The pH of this solution was between 0.674 and 1.278. The HPLC apparatus made use of an RI detector which was calibrated to detect FA and FF.

Before starting experimentation, each run was named according to Table 7 so the run named Ayβ, for instance, shows that the reactor is heated to 140 °C, contains 3.0 wt% FF initially and is catalysed by 1 wt% H_2SO_4. All the runs were then randomized on Excel and a list of the 27 runs was produced in random order to remove bias. Once a fair number of runs had been completed for the first time, duplicate runs were performed to ensure repeatability of the experiments.

4.3 Kinetic Modelling

The study aimed to select a standard kinetic model of the acid catalysed FF degradation reaction from literature which best fits experimental data. The kinetic model allows for comparisons with previous work in this topic area and leads to understanding of the effects of the process conditions. Previous studies have generally focussed on the FF formation reaction and dealt with FF degradation simultaneously (Antal *et al.*, 1991; Dunlop, 1948) but in this study, FF degradation is modelled separately.

For the kinetic model (see Equation 2), A, Ea, m and n were directly estimated using a maximum-likelihood approach, based on the minimisation of the sum of squared normalized errors (SSNE) between the ensemble of all the experimental and predicted concentrations at the different temperatures, initial FF concentrations and acid catalyst concentrations. The SSNE equation is given by Danon, Van Der Aa &

Stellenbosch University https://scholar.sun.ac.za

De Jong, 2013 (Equation 10). The minimisation was implemented in Python 3.5 and the “odeint” module was used to calculate all integrations.

The concentration data was entered as text in a text file and input into Python using the “NumPy” “genfromtxt” function which generates an array from a text file. Each integration used 100 points for the “odeint” integration. A function, outputting the hydrogen ion concentration was developed for sulfuric acid. The function considered the sulfuric acid concentration as well as the temperature to calculate the hydrogen ion concentration under the investigated conditions.

The model accounts for the sulfuric acid concentration and the dissociation of sulfuric acid with respect to temperature and this relationship is given by Zeitsch (2000). Sulfuric acid has 2 available hydrogen ions to release per sulfuric acid molecule in an aqueous solution during dissociation, therefore it is referred to as diprotic. The first stage of dissociation produces a hydronium ion and a hydrogen sulfate ion. The second stage involves the reaction of the hydrogen sulphate ion with a second water molecule to produce a second hydronium ion and a sulfate ion. Since sulfuric acid is a strong acid, the first dissociation reaction goes almost to completion and has a high Ka value (Ka expresses how easily the acid releases a proton, in other words, its strength as an acid). The second dissociation reaction has a much lower Ka value ($\mathrm{Ka}_{\mathrm{H_2SO_4},1} = 1 \times 10^3$ M and $\mathrm{Ka}_{\mathrm{H_2SO_4},2} \approx 6 \times 10^{-5}$ M) and is influenced by temperature, i.e. as temperature increases, the dissociation constant for the second dissociation step decreases. At 50 °C, $\mathrm{Ka}_{\mathrm{H_2SO_4},2} \approx 5.6 \times 10^{-2}$ M and at 200 °C $\mathrm{Ka}_{\mathrm{H_2SO_4},2} \approx 6 \times 10^{-5}$ M (Zeitsch, 2000).

To calculate the hydrogen ion concentration, the following equations were used:

$$\mathrm{Ka}_{\mathrm{H_2}SO_4,1} \geq 1$$

$$\mathrm{Ka}_{\mathrm{H_2}SO_4,2} = \mathrm{f(T)} \approx= \pm 6 \times 10^{-5}$$

$$[\mathrm{H^+}][\mathrm{HSO_4^-}] - [\mathrm{H_2SO_4}] \times \mathrm{Ka}_{\mathrm{H_2}SO_4} = 0$$

$$[\mathrm{H^+}] - [\mathrm{HSO_4^-}] = 0 \qquad 8$$

$$\mathrm{Ka}_{\mathrm{H_2}SO_4} = \frac{[\mathrm{H^+}][\mathrm{H^+}]}{[\mathrm{H_2SO_4}]}$$

$$[\mathrm{H_2SO_4}] = [\mathrm{H_2SO_{4,0}}] - [\mathrm{H^+}]$$

Stellenbosch University https://scholar.sun.ac.za

$$\therefore [H^+]^2 = \left(\left([H_2SO_{4,0}] - [H^+]\right) \times Ka_{H_2SO_4,1}\right) + \left(\left([H_2SO_{4,0}] - [H^+]\right) \times Ka_{H_2SO_4,2}\right)$$

where $Ka_{H_2SO_4,1}$ is the first dissociation constant for sulfuric acid, $Ka_{H_2SO_4,2}$ is the second dissociation constant and $Ka_{H_2SO_4}$ is a general term for H_2SO_4 dissociation that applies to both steps of dissociation. $[H^+]$, $[HSO_4^-]$ and $[H_2SO_4]$ are the molar concentrations of each component and $[H_2SO_{4,0}]$ is the initial concentration of H_2SO_4. The solution for $[H^+]$ is found by solving the quadratic equation.

The differential equation which was integrated for each run was as follows:

$$\frac{dC_{FF}}{dt} = -A'e^{-\frac{Ea}{R}\times\left(\frac{1}{T}-\frac{1}{T_0}\right)} \times C_{FF}^n \times [H^+]^m \qquad 9$$

where C_{FF} is FF concentration, A' is the pre-exponential factor (min^{-1}), Ea is the activation energy ($kJ{\cdot}mol^{-1}$), R is the universal gas constant ($kJ{\cdot}mol^{-1}{\cdot}K^{-1}$), T is the temperature (K) and T_0 is the reference temperature (453.15 K). The reaction order is given by n, the hydrogen ion concentration is given by $[H^+]$ (M) and m is the index factor of the hydrogen ion concentration: a unitless hydrogen ion concentration exponent.

The sum of squared normalized errors (SSNE) was then calculated by first passing the model FF concentrations (calculated by integrating Equation 9) through the "NumPy" "interp" function which gave the same FF concentrations but at discrete data-points, i.e. the 10 time values input via the "genfromtxt" function. Now comparing the 10 model FF concentrations and the 10 FF concentrations from experimental data, the SSNE could be calculated. For each set of FF concentrations, a SSNE value was calculated as follows:

$$SSNE = \sum_{i=1}^{N}\left(\frac{C_{FF_n}}{C_{FF_0}} - \frac{C_{FF_i}}{C_{FF_0}}\right)^2 \qquad 10$$

where C_{FF_n} is a FF concentration (data point), C_{FF_0} is the initial FF concentration, C_{FF_i} is a model FF concentration that comes from the "interp" function and N is the total number of values in that run.

As the model fits the data more accurately, the SSNE for that run will be smaller. To find the best fit for all the runs, a minimisation was run with the goal of producing the lowest SSNE values for all runs. A', Ea, m and n were the variables available to the

Stellenbosch University https://scholar.sun.ac.za

minimisation function to produce the lowest SSNE values. This method of estimating kinetic parameters was used by Danon *et al.* (2013) who estimated kinetic parameters using a maximum-likelihood approach, based on the minimization of the SSNE between all of the experimental and predicted concentrations for their work (Danon *et al.*, 2013).

For the minimisation process, the Nelder-Mead method was applied which is a commonly applied numerical method used to find the minimum or maximum of an objective function in a multidimensional space. It is applied to nonlinear optimisation problems for which derivatives may not be known. The “minimise” function is part of the “SciPy.optimize” package in Python and was limited to 1000 iterations. Coefficients of determination were calculated for each run to assess the accuracy of the fits. The coefficients of determination/ R^2 were calculated as follows:

$$R^2 = 100 \times \left(\frac{\sum xy}{\sqrt{(\sum x^2 \times \sum y^2)}}\right)^2 \qquad 11$$

where $\sum x^2 = \sum(C_i - mn)^2$, C_i stands for each value within the experimental data set and mn shows the mean value for that data set. $\sum y^2 = \sum(CFinterp_i - CFmn)^2$, $CFinterp_i$ is each value within the model data set which has been passed through the “interp” function to give 10 discrete FF concentrations and $CFmn$ is the mean value of those 10 data points. $\sum xy = (C_i - mn) \times (CFinterp_i - CFmn)$.

The 2 variables A and Ea, which were manipulated in the minimisation were used to calculate a value for $\ln A$, the pre-exponential factor which can now be compared to literature values:

$$\ln A = \ln\left(\frac{A'}{60} \cdot \frac{Ea}{RT_0}\right) \qquad 12$$

where A and Ea are the pre-exponential factor (s^{-1}) and activation energy ($kJ \cdot mol^{-1}$) respectively and T_0 is the reference temperature (453.15 K)

Finally, the fitted data is plotted against the experimental data with the coefficients of determination for each run displayed on the plot legend.

Stellenbosch University https://scholar.sun.ac.za

5. Results & discussion

The aim of this study was to investigate the kinetics of FF degradation and evaluate the significance of different operating condition affecting the reaction. Therefore, a set of 27 runs was designed considering three different levels for temperature, initial FF concentration and sulfuric acid concentration. FF degradation was measured in terms of humins concentration, FA concentration and FF degradation rate. The products of degradation and the degradation rate are listed in Table 8 for each level of each experimental factor.

Table 8: Experimental factors for FF degradation

Temperature (°C)	Initial Furfural concentration (wt%)	Sulfuric acid concentration (wt%)	Formic acid concentration (g/L)	Humins (g/L)	Furfural degradation rate (g/L/min)
140	1.5	0.5	0.38	0.04	0.01
140	1.5	1	3.29	0.56	0.01
140	1.5	2	4.3	0.38	0.02
140	3	0.5	4.86	0.55	0.02
140	3	1	0.24	1.44	0.02
140	3	2	9.92	1.42	0.04
140	6	0.5	10.53	0.99	0.02
140	6	1	11.78	2.39	0.02
140	6	2	11.75	2.42	0.09
170	1.5	0.5	3.57	0.61	0.01
170	1.5	1	2.1	2	0.04
170	1.5	2	3.95	1.91	0.07
170	3	0.5	5.68	0.82	0.03
170	3	1	6.33	4	0.09

Stellenbosch University https://scholar.sun.ac.za

170	3	2	7.29	5.04	0.17
170	6	0.5	6.9	3	0.14
170	6	1	13.69	6.32	0.19
170	6	2	11.8	21.32	0.33
200	1.5	0.5	1.13	1.75	0.07
200	1.5	1	1.82	5	0.12
200	1.5	2	2.8	6.55	0.1
200	3	0.5	5.54	7.67	0.1
200	3	1	6.94	11.86	0.21
200	3	2	3.3	10.02	0.21
200	6	0.5	12.04	17.36	0.36
200	6	1	6.48	16.31	0.51
200	6	2	12.36	33.77	0.54

5.1. Mass balance

A range of 3-30 % of mass was unaccounted for (due to analytical error or smaller components that were not detected by the HPLC). FA mass percentage varied in the range of 1.7-56%. Humins mass percentage varied in the range of 2.6-33%. Unreacted FF varied in the range of 14-88%. The most significant aspect of the mass balances was the fact that the portion of FF that reacted in degradation reactions to form FA (fragmentation) was much higher than what was reported in literature.

5.2 Kinetics

The solid lines in Figure 20 represent the model fit and the dots represent experimental data points. The coefficients of determination (R^2 values) for all the

Stellenbosch University https://scholar.sun.ac.za

experiments are given in Figure 20, which indicates that the chosen model agrees well with the experimental data since the R^2 values range from 69.33%−99.93%.

It should be mentioned that the pre-exponential factor, activation energy and order (See Figure 20) are determined via minimisation of all the runs. Based on the results, FF degradation under the reaction conditions of this study showed an average reaction order of 1.15 with respect to FF and 0.926 with respect to the hydrogen ion. The natural log of the pre-exponential factor (lnA) detected for this study was 20.221 s^{-1} and the activation energy was 93 630 $J \cdot mol^{-1}$. These values are similar to those found in previous studies (See Table 4). Williams & Dunlop (1948) found that the destruction of furfural was first order with respect to hydrogen ion concentration as well as to FF concentration (Williams & Dunlop, 1948). They conducted experiments at 150 - 210 °C and acid catalyst concentrations of 0.025 & 0.05 M (H_2SO_4) and 0.05 & 0.1 M (HCl) (Williams & Dunlop, 1948). Rose, Epstein & Watkinson (2000) conducted FF degradation reactions at 130 - 170°C and acid catalyst concentration of 0.1 M (HCl) and observed that first-order reaction kinetics best described their experimental results (Rose et al., 2000). First-order kinetics for FF degradation have been detected by other studies (Jing & Lü, 2007; Marcotullio *et al.*, 2009; Weingarten *et al.*, 2010) (See Table 5), both for pure FF degradation and for systems where xylose is present and degradation via condensation occurs.

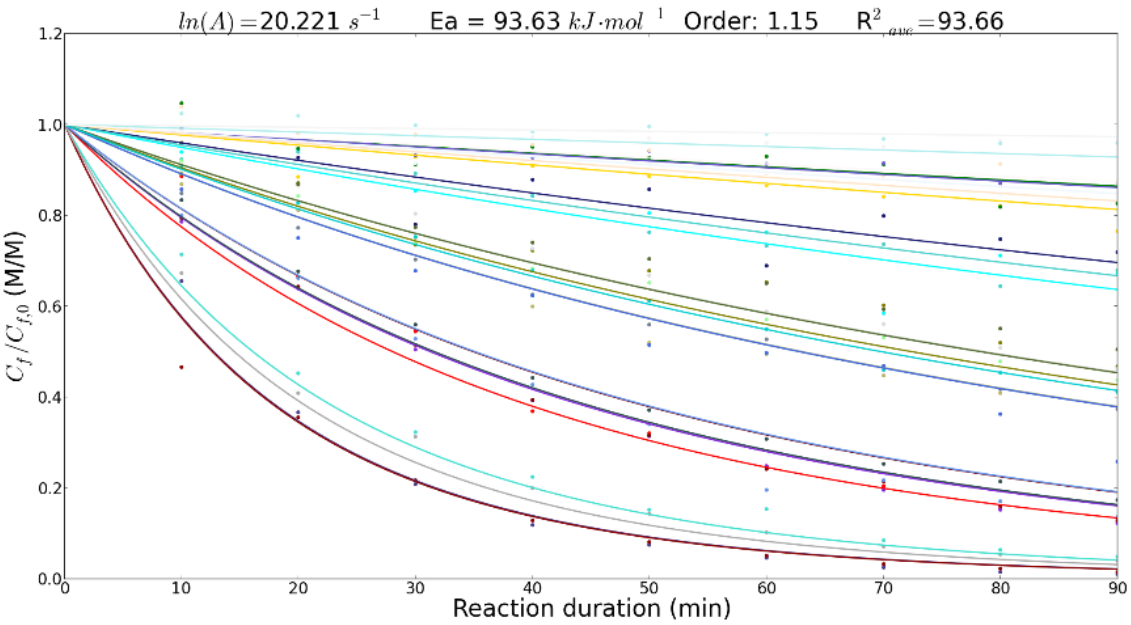

Figure 20: Kinetics for all runs

Stellenbosch University https://scholar.sun.ac.za

5.2.1 Kinetics for specified sulfuric acid and FF concentrations

Figure 21-Figure 29 demonstrate the kinetics of the FF degradation at different initial FF and sulfuric acid concentrations. As can be seen from the results, considering reaction order of 1 for FF degradation is a reasonable assumption since the real value from the kinetic model is found to be 1.15 overall (See Figure 20). The results agree well with literature. Root *et al.* (1959)observed that when acidified aqueous FF was reacted for various lengths of time, FF degradation followed a first-order reaction (Root *et al.*, 1959).

However, Danon, Van Der Aa & De Jong (2013) reported uncertainty about a second-order or first-order model for their experimental data on FF degradation. (Danon *et al.*, 2013). Danon, Marcotullio & De Jong (2013) found that the degradation reaction showed dependency on the FF concentration (which indicates a higher reaction order) at the following conditions: 36.4-145.5 mM sulfuric acid, 150-200 °C, 60.4-72.5 mM FF (Danon, Marcotullio & De Jong, 2013). The present study was conducted using pure FF as precursor for degradation and high concentrations of FF were used (to mimic industrial operating conditions). (Close to) First order kinetics were discovered for rate of FF degradation with respect to FF concentration. The kinetic variables discovered in this work, compared to previous studies (See Table 4) which were conducted in the presence and in the absence of xylose showed similar results, indicating that resinification perhaps occurs to a greater extent than condensation as the occurrence of condensation doesn’t seem to greatly influence reaction kinetics.

Stellenbosch University https://scholar.sun.ac.za

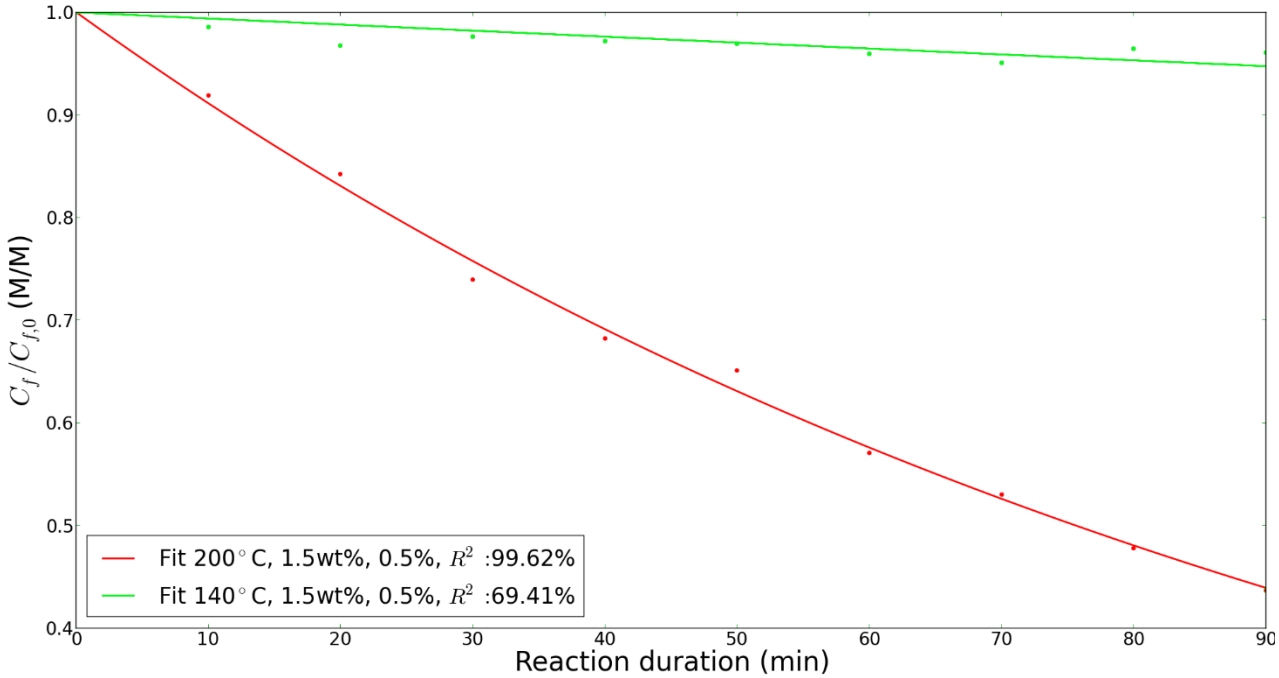

Figure 21: FF degradation experimental data and fitted model values with 1.5 wt% FF and 0.5 wt% H_2SO_4

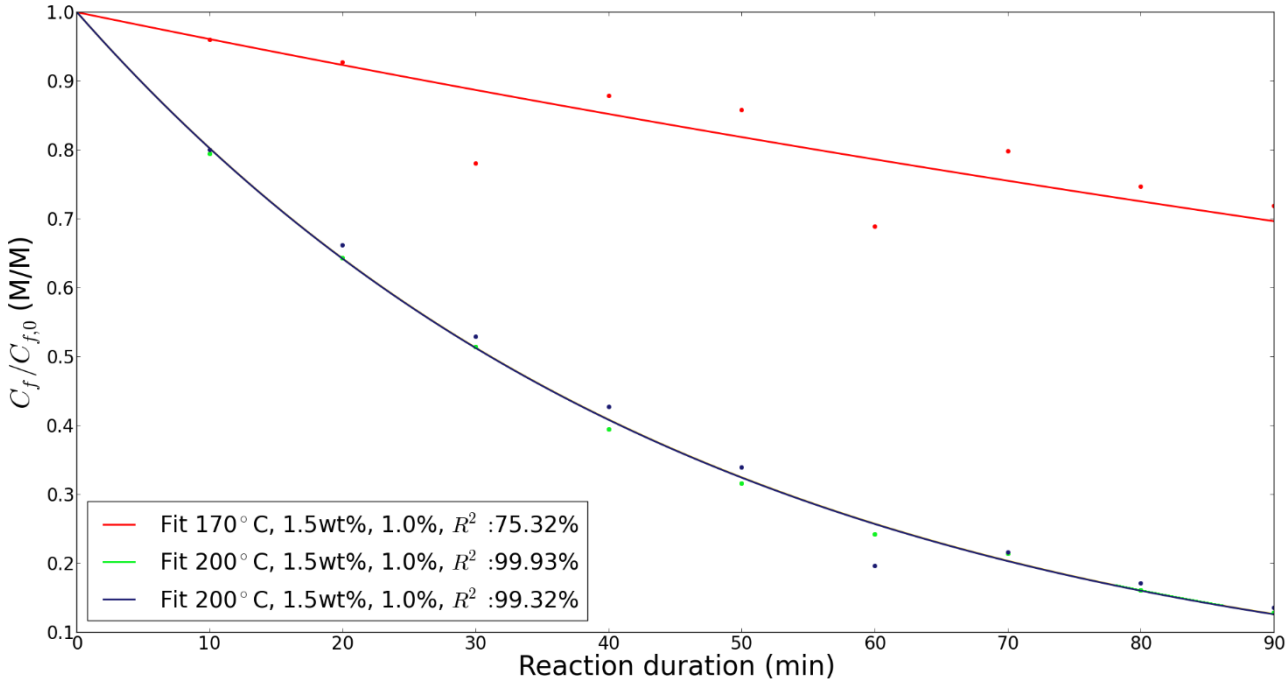

Figure 22: FF degradation experimental data and fitted model values with 1.5 wt% FF and 1 wt% H_2SO_4

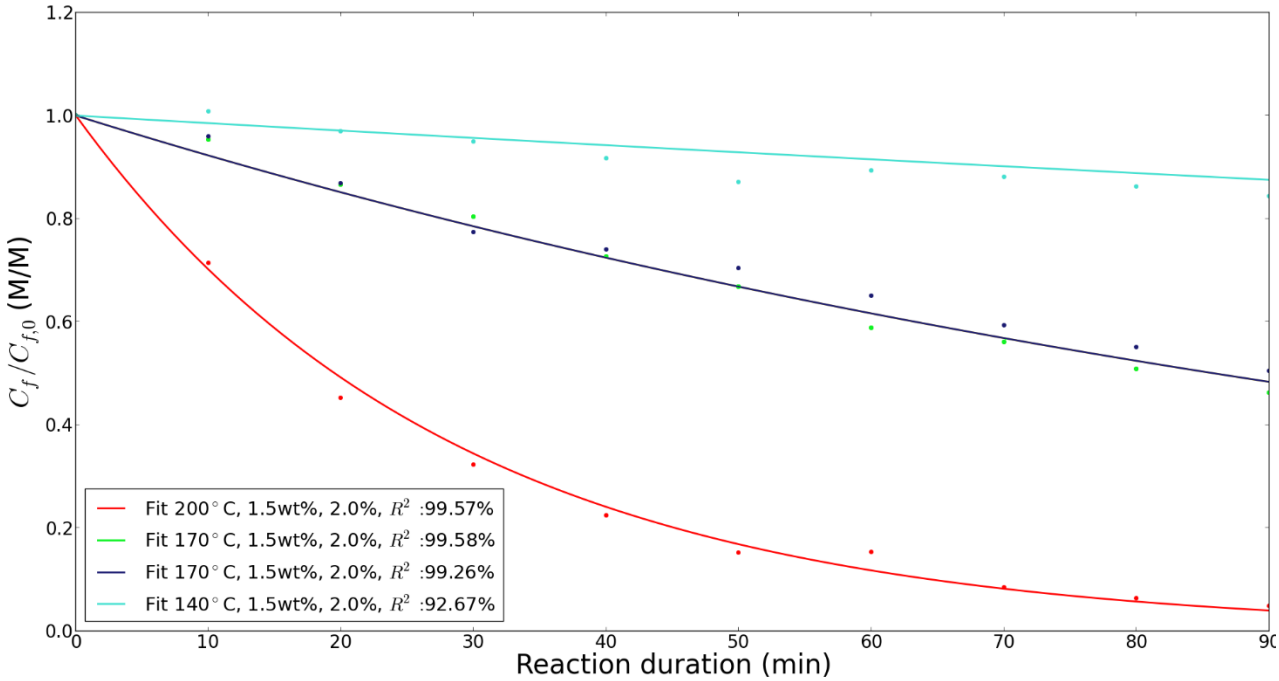

Figure 23: FF degradation experimental data and fitted model values with 1.5 wt% FF and 2 wt% H_2SO_4

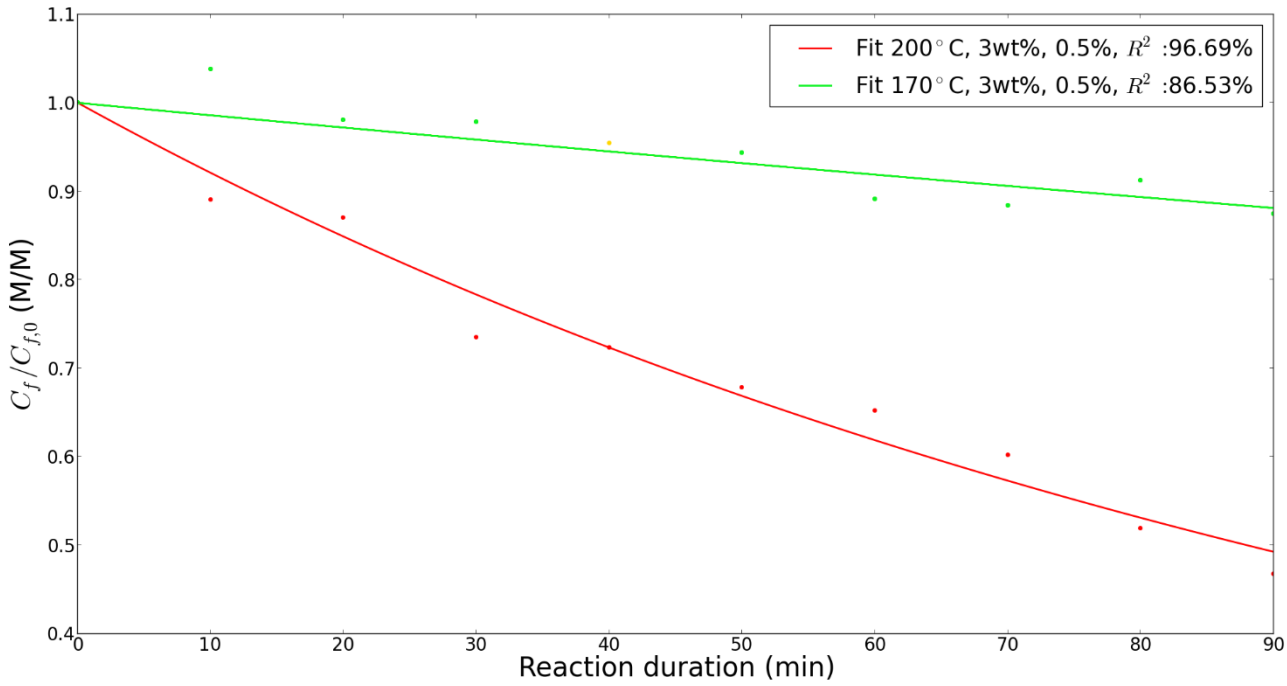

Figure 24: FF degradation experimental data and fitted model values with 3.0 wt% FF and 0.5 wt% H_2SO_4

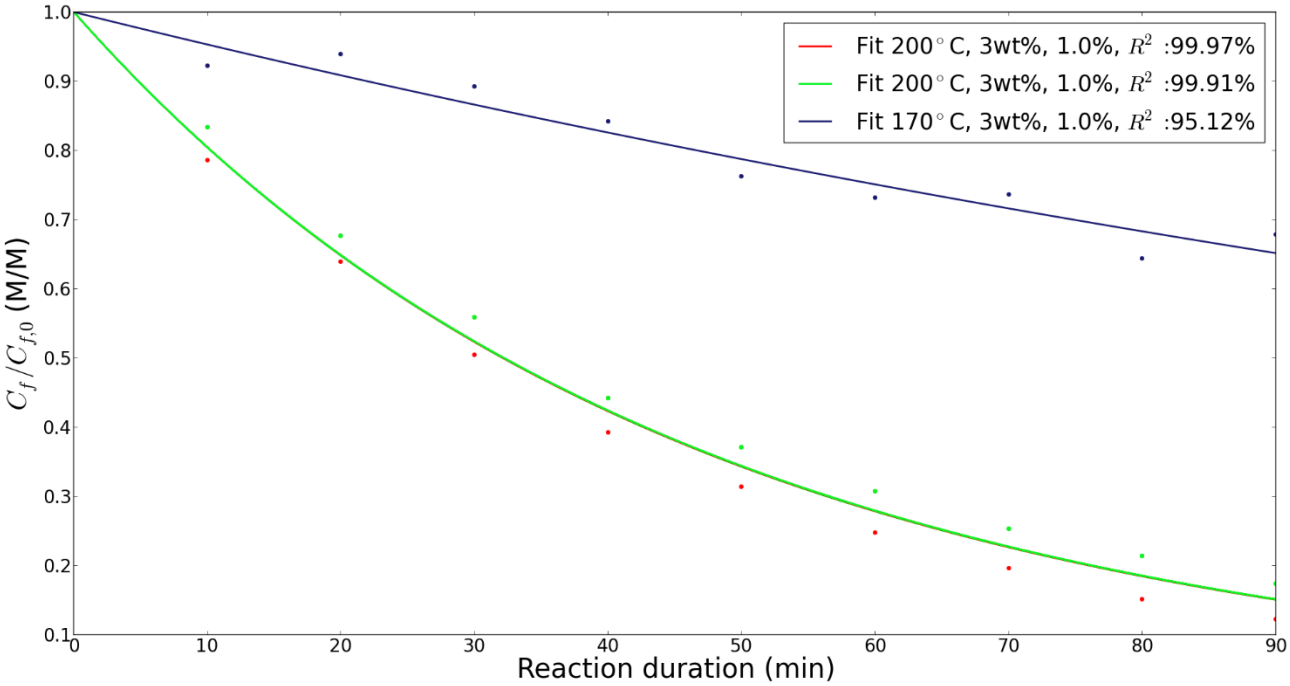

Figure 25: FF degradation experimental data and fitted model values with 3.0 wt% FF and 1 wt% H_2SO_4

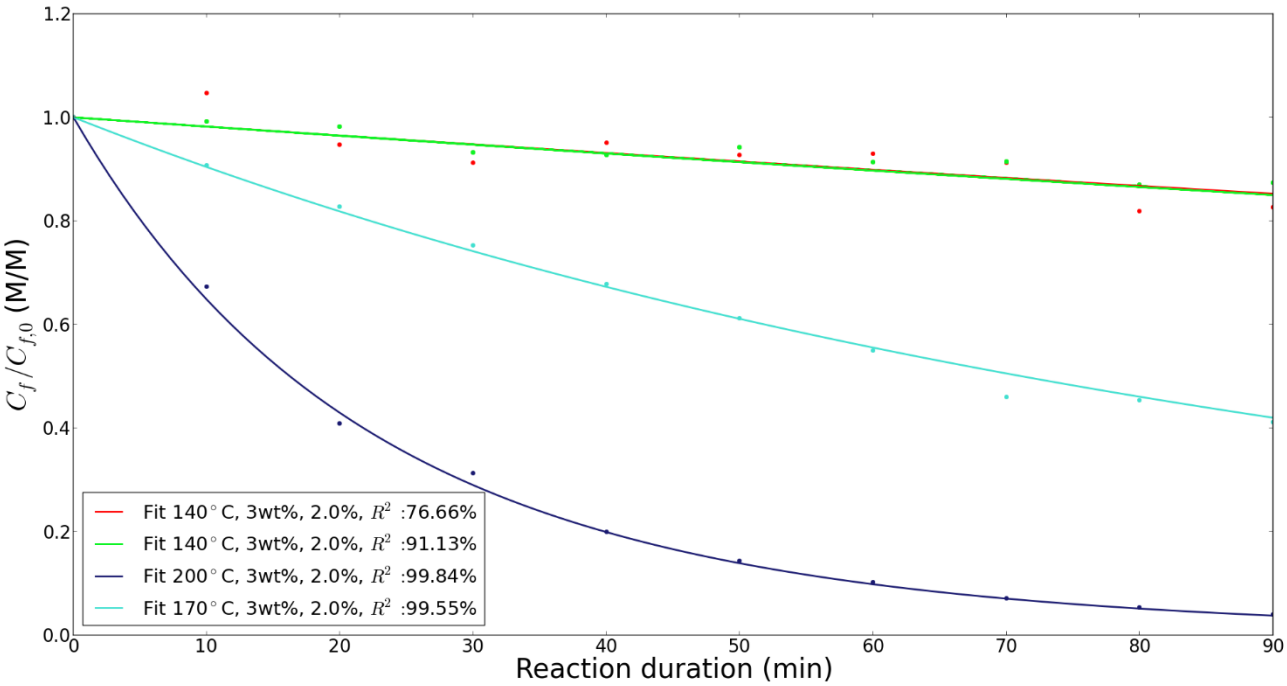

Figure 26: FF degradation experimental data and fitted model values with 3.0 wt% FF and 2 wt% H_2SO_4

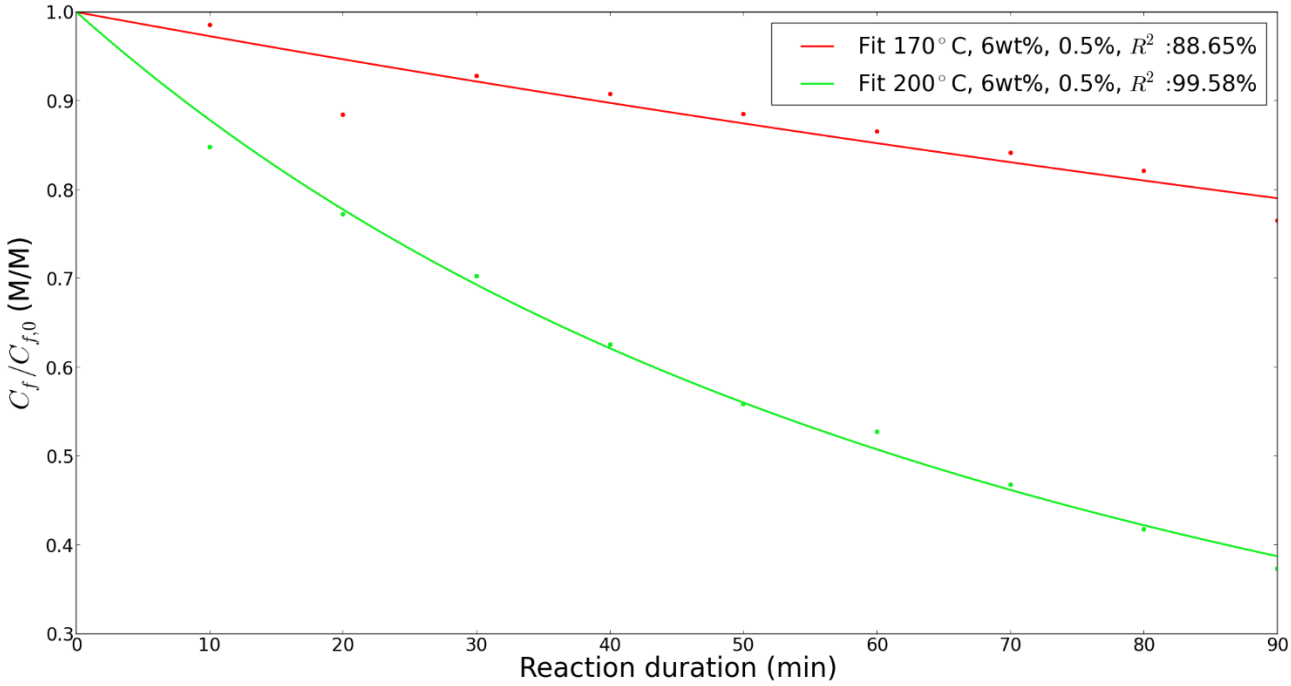

Figure 27: FF degradation experimental data and fitted model values with 6.0 wt% FF and 0.5 wt% H_2SO_4

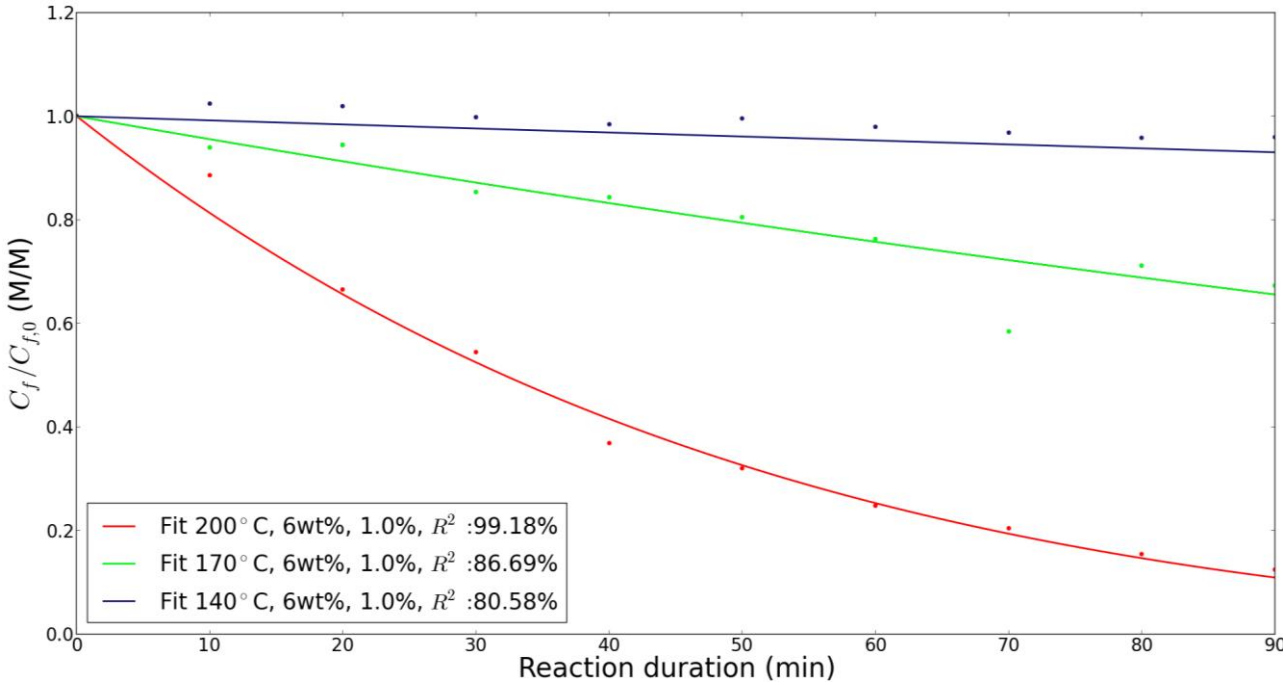

Figure 28: FF degradation experimental data and fitted model values with 6.0 wt% FF and 1 wt% H_2SO_4

Stellenbosch University https://scholar.sun.ac.za

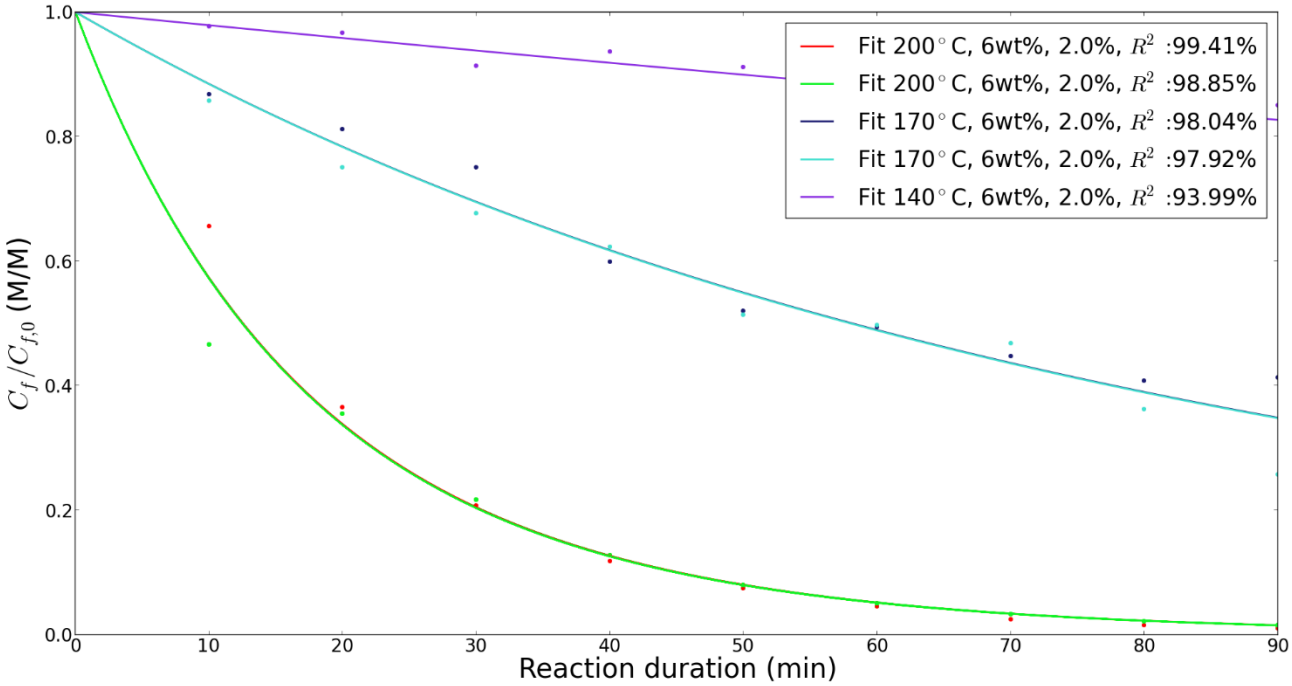

Figure 29: FF degradation experimental data and fitted model values with 6.0 wt% FF and 2 wt% H_2SO_4

Stellenbosch University https://scholar.sun.ac.za

5.2.2 Repeatability

The following figures show the concentration profiles of duplicate runs for the same set of reaction conditions. These duplicates demonstrate that the data exhibits good repeatability. In some of the previous datasets (e.g. Figure 26 & Figure 28), data was recorded where $\frac{C_f}{C_{f,0}} > 1$which is not possible because FF degradation isn't reversible, i.e. FF can't be generated and so $C_{f,0}$ is the maximum FF concentration and the data points recorded above this concentration are erroneous. This error arose, most probably, in HPLC analysis of the samples or in sample preparation (dilution) of samples for HPLC analysis. It would have been ideal to repeat these runs, but unfortunately unforeseen circumstances did not allow for this.

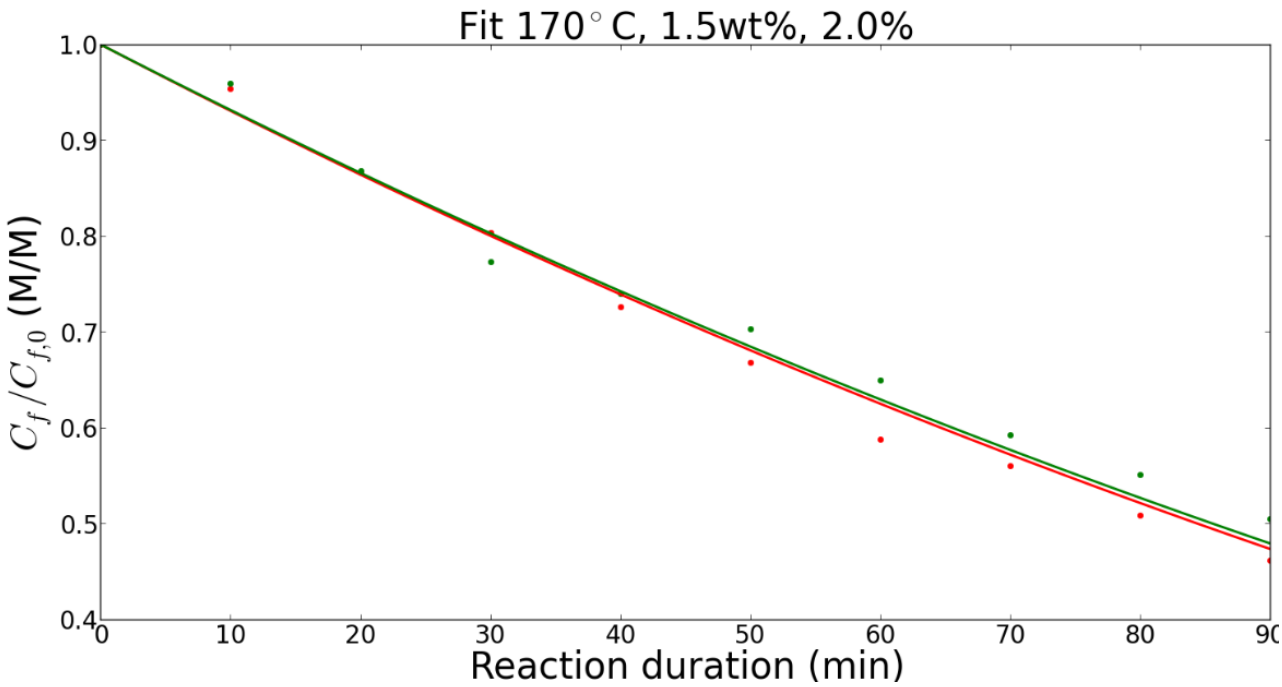

Figure 30: Experimental data from duplicate runs at 170 °C, 1.5 wt% FF & 2 % sulfuric acid

Stellenbosch University https://scholar.sun.ac.za

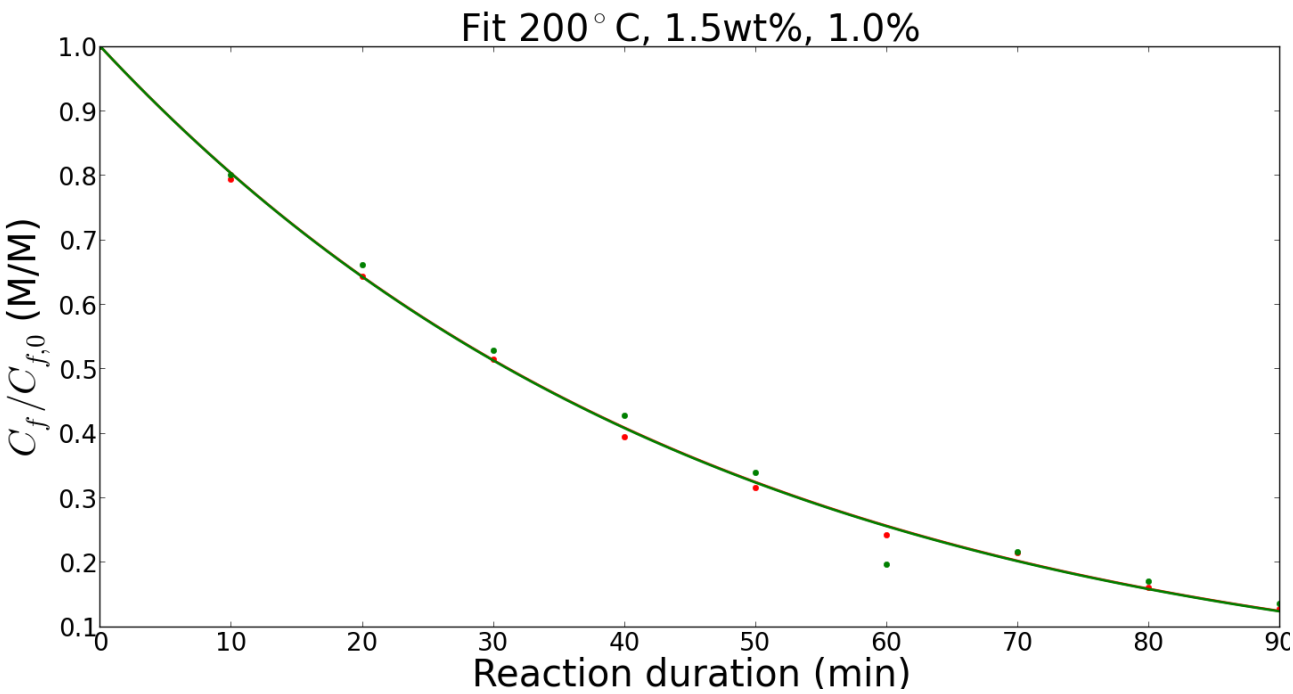

Figure 31: Experimental data from duplicate runs at 200 °C, 1.5 wt% FF & 1 % sulfuric acid

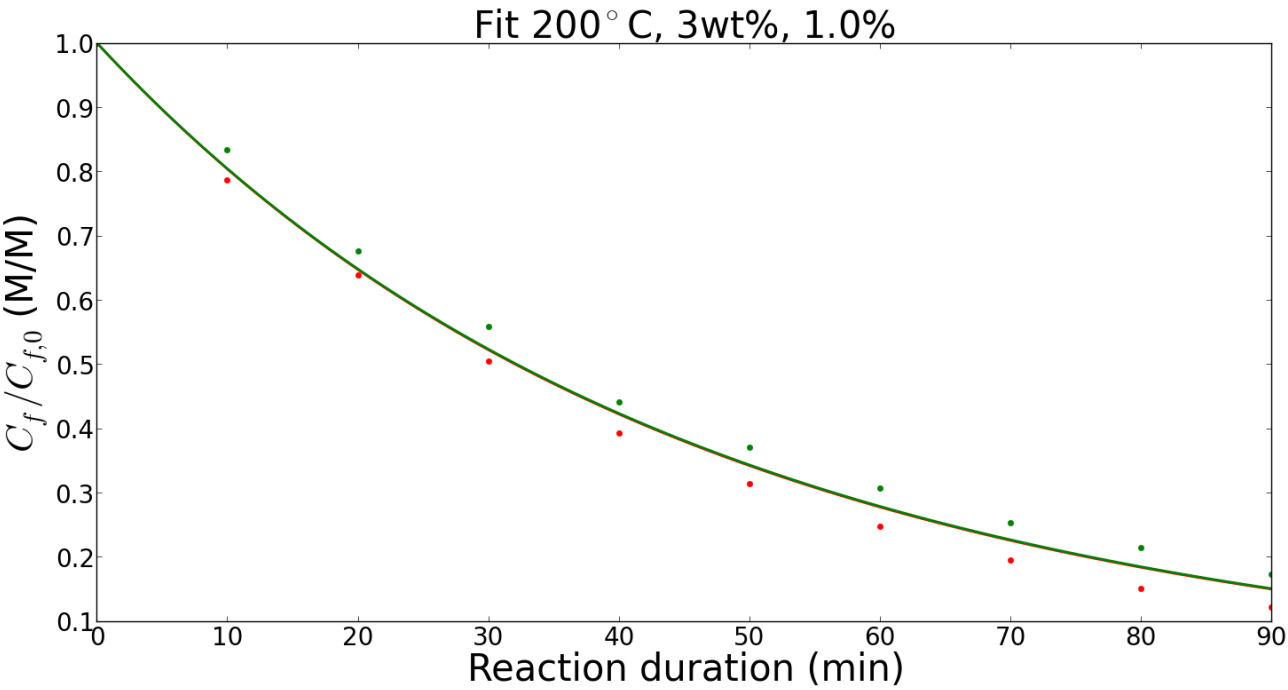

Figure 32: Experimental data from duplicate runs at 200 °C, 3 wt% FF & 1 % sulfuric acid

Stellenbosch University https://scholar.sun.ac.za

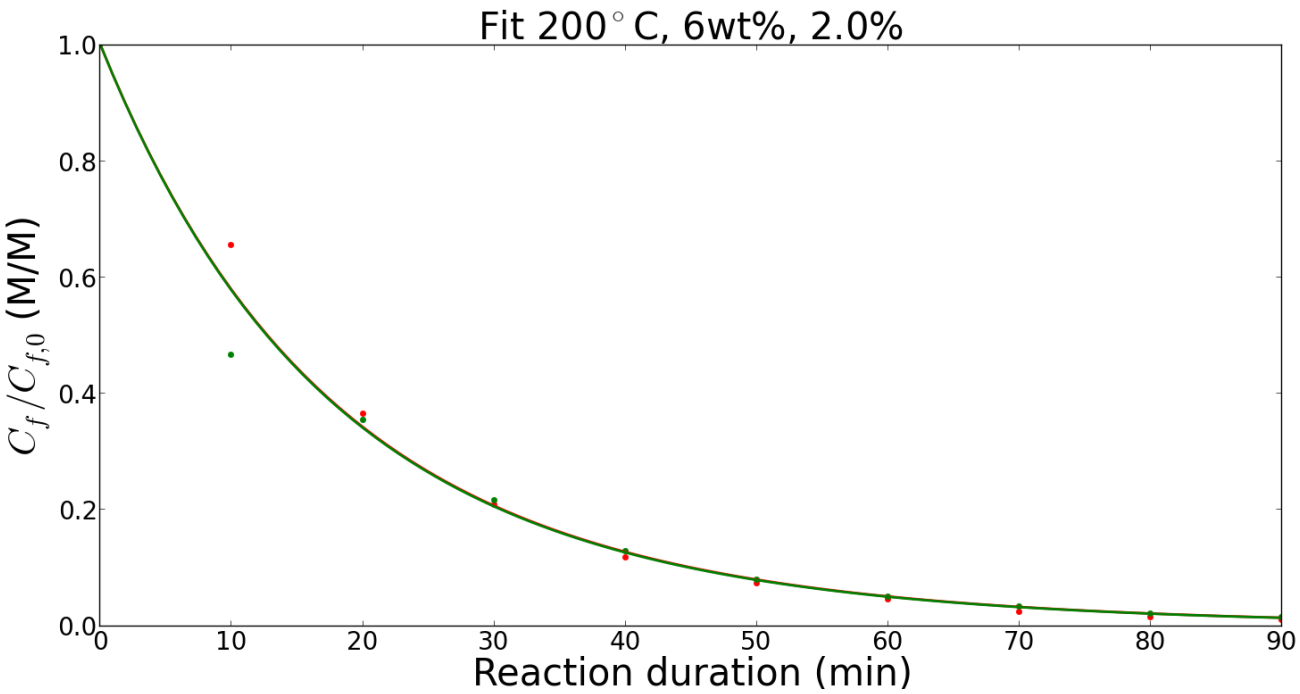

Figure 33: Experimental data from duplicate runs at 200 °C, 6 wt% FF & 3 % sulfuric acid

Stellenbosch University https://scholar.sun.ac.za

5.3. Rate of furfural degradation

The statistical analysis of the experimental data, via p-value (presented in Table 9) demonstrated that FF degradation rate was a function of temperature and initial FF concentration. Temperature and initial FF concentration significantly affect the rate of FF degradation ($p<0.05$). This relationship is shown in Figure 34 and as can be seen the degradation rate increased more with temperature at higher initial FF concentration.

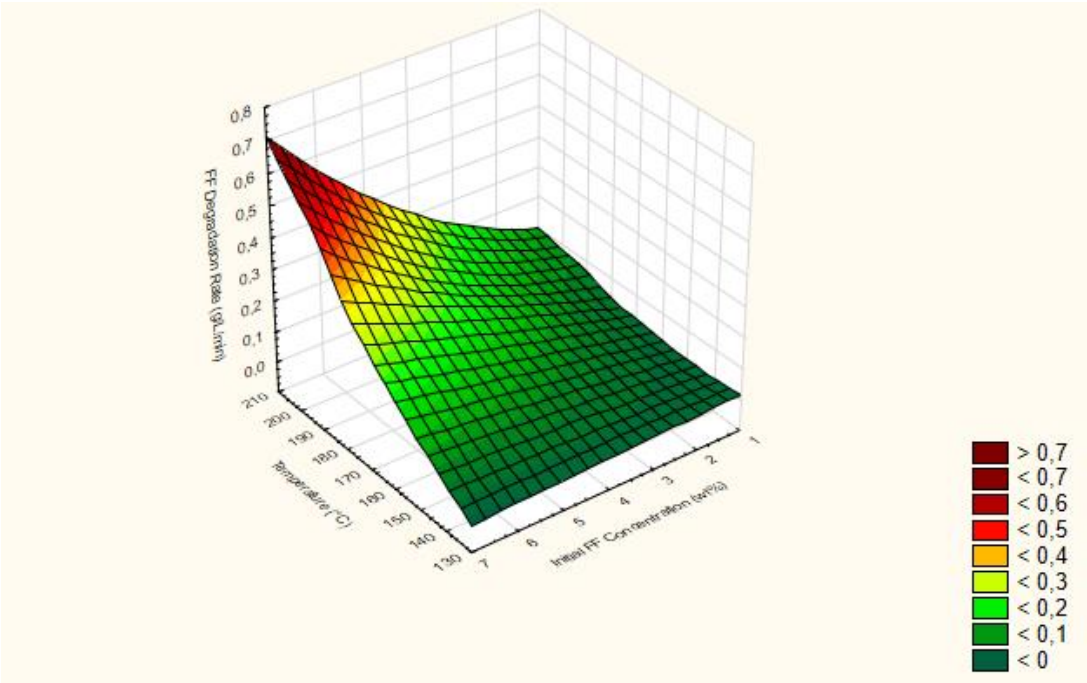

Figure 34: 3D Surface Plot of FF Degradation Rate ($g \cdot L^{-1} \cdot min^{-1}$) against Temperature (°C) and Initial FF Concentration (wt%)

Table 9: Asymptotic significance of experimental factors with respect to FF degradation rate

Factor	p-value
Temperature	0,000038
Initial FF Concentration	0,000111
Sulfuric Acid Concentration	0,074267

The relationship between FF degradation rate and sulfuric acid concentration/ initial FF concentration is shown in Figure 35. From this surface plot, it can be seen that sulfuric acid concentration has a far less significant effect on FF degradation rate

Stellenbosch University https://scholar.sun.ac.za

than initial FF concentration which agrees with the p-value of 0.074 (>0.05). However, the effects of sulfuric acid concentration on FF degradation rate should not be ignored. Williams & Dunlop (1948) found that “the rate of destruction of FF, at fixed initial acid concentration and temperature, was found to be directly proportional to the concentration of FF”(Williams & Dunlop, 1948). Dunlop (1948) established that the rate of FF degradation was proportional to the concentration of FF and to the hydrogen ion concentration (Dunlop, 1948). Chen et al. (2015) observed that higher FF concentration in their reaction system accelerated the degradation reaction rate of FF (Chen *et al.*, 2015). Danon, Marcotullio & De Jong (2013) state that the rate of FF degradation showed dependency not only on the hydrogen ion concentration and the temperature, but also on the FF concentration (Danon, Marcotullio & De Jong, 2013). Some researchers investiagted the effects of acid concentration in terms of pH. Lamminpaa, Ahola & Tanskanen (2012) found that for FA catalysed xylose dehydration into FF and FF decomposition, the pH of the reactant solutions has more effect on reaction rate of FF decomposition when temperature rises (Lamminpaa *et al.*, 2012). Sener *et al.* (2018) found that the rate of FF disappearance was proportional to the hydrogen ion concentration in aqueous media using mineral acids as catalysts. (Sener *et al.*, 2018). These sources, whether gaging the acidity of the degradation reaction by pH, hydrogen ion concentration or mineral acid concentration, all support the notion that the rate of FF degradation is a function of all 3 experimental factors (initial FF concentration, sulfuric acid concentration and reaction temperature).

Stellenbosch University https://scholar.sun.ac.za

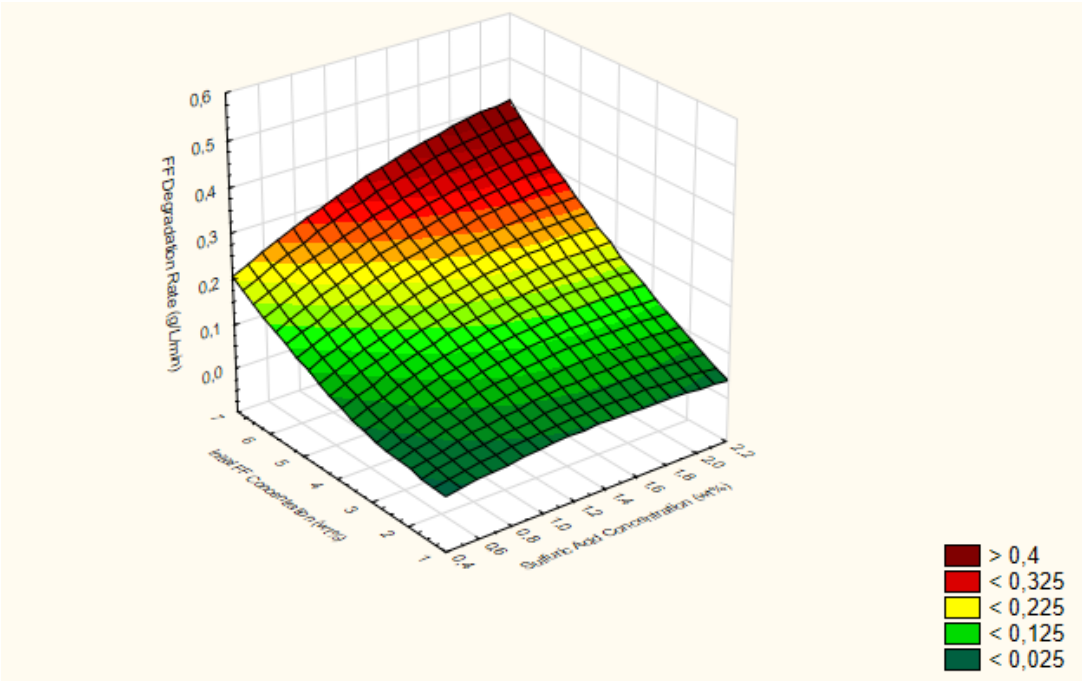

Figure 35: 3D Surface Plot of FF Degradation Rate ($g \cdot L^{-1} \cdot min^{-1}$) against Initial FF Concentration (wt%) and Sulfuric acid concentration (wt%)

5.4. Humins

5.4.1 Humins composition

The average C:H:O values for all the humins generated in this study was determined as 63.75:4.07:32.17. This value is very similar to C:H:O ratio of FF (62.5:4.2:33.3), which is logical since FF is the precursor to humins. This also agrees well with literature as the C:H:O content for humins formed from many sources was reported to be approximately 66:5:29 (See Table 2).

The composition of humins formed in this study was fairly uniform and the composition was independent of processing conditions (temperature, acid and FF concentration). The mean composition of the humins is presented in Table 10 (percentage C, H & O) as well as the variance and standard deviation for the percentages of C, H & O.

The standard deviation (maximum 2.36 for O) and variance (maximum 5.68 for O) of the results shows that the experimental results do not vary much from the average values (See Table 10).

Stellenbosch University https://scholar.sun.ac.za

Table 10: Standard deviation, variance and mean for C, H & O elemental composition of humins formed in this study

	C	H	O
Mean	63.75	4.07	32.17
Variance	5.20	0.02	5.68
Standard Deviation	2.25	0.14	2.36

5.4.2 Humins formation mechanism

Based on the results, from the 5 potential mechanisms for humin formation (Table 11), the Sanchez mechanism describes the humin formation over the operating conditions examined in this study because the average C:H:O composition of the humins in this study (63.75:4.07:32.17) on the Van Krevelen diagram (demonstrated in Figure 36) was located very close to a propagation (± 10 FF molecules) of the molecule formed through the Sanchez mechanism (64.74:4.00:31.26). This molecule is illustrated in Figure 2.

Stellenbosch University https://scholar.sun.ac.za

Table 11: Summary of possible FF degradation mechanisms which produce humins

Qualifying/disqualifying factor	Key molecule	Mechanism name	Ref.
This molecule (trifurylic dialdehyde) is cited often in literature as the molecule that is repeated in the humins structure. The propagation of the molecule (±10 FF molecules) formed by the Sanchez mechanism is plotted in Figure 36 (green circles) and it can be seen that it is very similar to the average composition of the humins formed in this study.	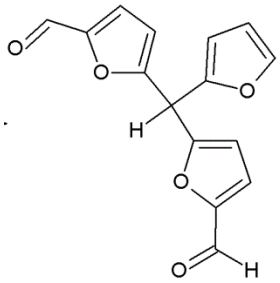	Sanchez mechanism	(Gandini & Belgacem, 1997; Mariscal *et al.*, 2016; Sánchez, Hernández and Keresztury, 1994; Sumerskii *et al.*, 2010; Van Zandvoort *et al.*, 2013)
The composition of the humin structure moves away from the C:H:O average composition of the humins in this study on the Van Krevelen diagram as it grows (becomes more conjugated) (See Figure 36 : yellow circles).	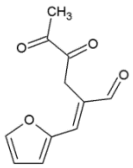	O'Neil mechanism	(O'Neil *et al.*, 2009)
The Diels-alder molecule formed from multiple FF molecules is plotted on the Van Krevelen diagram (Figure 36 : blue stars) and as the molecule becomes more conjugated, the composition moves away from the humins on the Van Krevelen diagram.	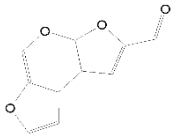	Danon mechanism	(Danon *et al.*, 2013)

Stellenbosch University https://scholar.sun.ac.za

3,8-dihydroxy-2-methylchromone (DMC) was found to be a major product in the acid degradation of xylose and xylose is not involved in resinification so it seems unlikely that DMC forms part of the humin structure.	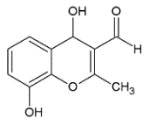	Rasmussen mechanism	(Rasmussen *et al.*, 2014)
1,2,5-tripentanon (TP) has eno and keto forms and can (potentially) react with FF in aldol addition/condensation reactions. One molecule of TP is plotted on the Van Krevelen diagram as well as TP bonded to 1 FF molecule and the direction of the growth is away from the position of the average composition of humins in this study.	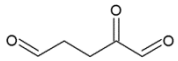	Lamminpaa mechanism	(Lamminpaa *et al.*, 2014)

Stellenbosch University https://scholar.sun.ac.za

A Van Krevelen diagram of FF, all the humins that were generated during degradation and the molecules formed by the potential humins formation mechanisms is plotted in Figure 36. A Van Krevelen diagram is a plot of the molar ratio O/C vs the molar ratio H/C (Wang *et al.*, 2016). The solid line is the dehydration line ($y = \frac{1}{2}x$) and components on the line are products of dehydration of components which are higher up on the line (i.e. loss of H_2O which has $\frac{O}{H} = \frac{\frac{16}{16}}{\frac{2}{1}} = \frac{1}{2}$ hence the gradient of the dehydration line). FF has the molecular formula $C_5H_4O_2$ and thus has an O/C ratio of $\frac{\frac{32}{16}}{\frac{60}{12}} = \frac{2}{5}$ and H/C ratio of $\frac{\frac{4}{1}}{\frac{60}{12}} = \frac{4}{5}$ and $\frac{2}{5} = \frac{1}{2} \cdot \frac{4}{5}$ hence FF falls on the dehydration line.

As demonstrated in Figure 36, FF undergoes dehydration in the formation of humins because the humins fall on the dehydration line below and to the left of FF which indicates that this molecule is a product of dehydration of FF. Since the Sanchez mechanism involves a dehydration step (See Figure 2), it is further confirmed that the Sanchez mechanism is responsible for the formation of humins in this study. The composition of the molecules generated by the Sanchez mechanism, illustrated in Figure 36 (green circles), are very near the point which represents the average composition of humins in the present study (red triangle).

Previous studies have also used a Van Krevelen diagram to determine the reactions leading to humin formation. Wang *et al.*(2016) explained that formation of humins was a result of severe dehydration and condensation reactions catalysed by strong acid, because humins in their study were located near the dehydration reaction line of the Van Krevelen diagram, below and to the left of FF (Wang *et al.*, 2016). Rasrendra et al. (2013) found that the samples prepared in their study as well as literature data are near to the dehydration line, suggesting that dehydration reactions dominate in the course of the reactions (Rasrendra *et al.* 2013).

In Figure 36(Van Krevelen diagram.), the compositions of the humins formed by the various mechanisms are plotted and where a solid line is plotted, the arrow points in the direction of the humin molecule as it becomes more conjugated (grows).

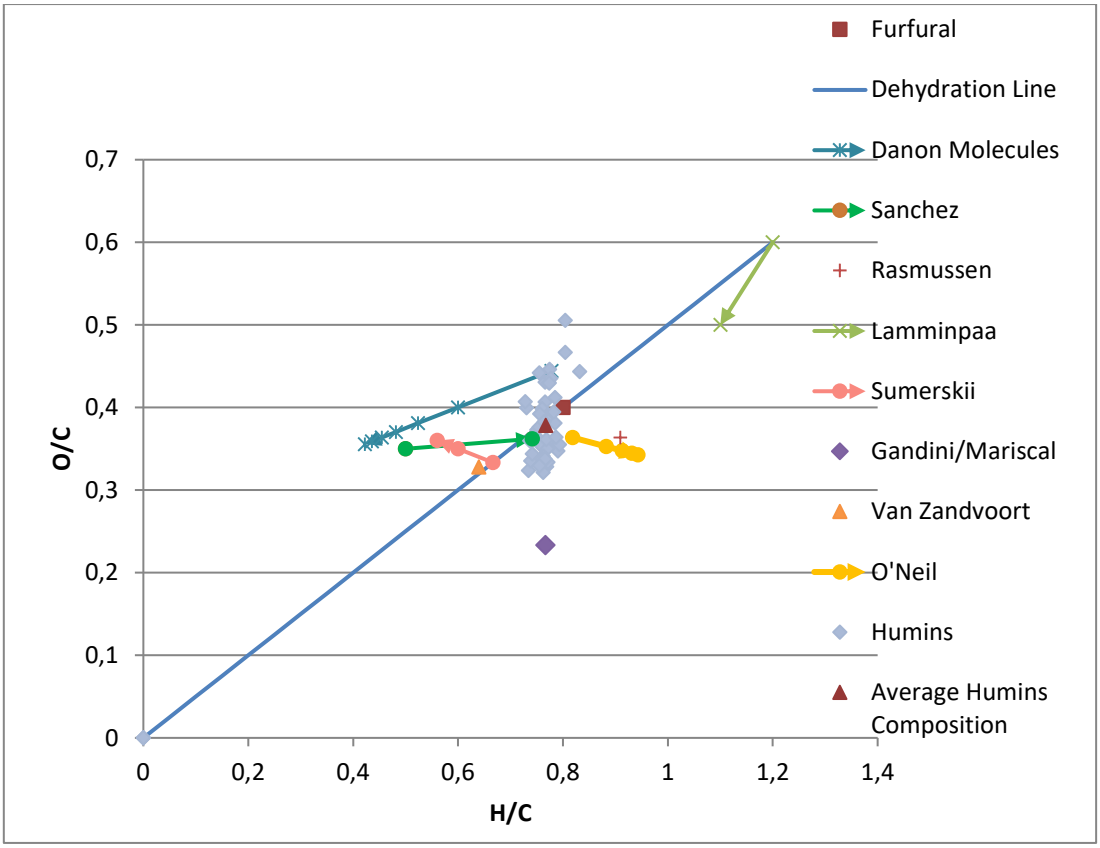

Figure 36: Van Krevelen diagram for humins formed during FF degradation

The predicted conjugated molecule for the O'Neil mechanism is plotted in Figure 36, showing that this structure is not responsible for the humins formed in this study. The Danon mechanism involves a Diels-Alder reaction and the furan ring of FF is not susceptible to Diels–Alder reactions (See section 2.3.3). The composition of the molecule produced by the Danon mechanism moves away from the average composition of humins in this study (on the Van Krevelen diagram) as it becomes more conjugated (See Figure 36). The composition of the molecule formed in the Lamminpaa mechanism is far away from the average composition of the humins in this study on the Van Krevelen diagram so it is unlikely that it is the molecule involved in humin formation. The Rasmussen mechanism involves DMC as an intermediate in the humin formation reaction and it has been demonstrated that this molecule is an unlikely participant in the humin formation reaction (See section 2.2.3)

In summary, the Sanchez mechanism was found to be responsible for the formation of the humins formed in this study by two criteria:

- The humins formation reaction involves a dehydration reaction, this is clear because the humins on average are found below FF to the left on the

Stellenbosch University https://scholar.sun.ac.za

dehydration line (see Figure 36). The Sanchez mechanism involves a dehydration step.

- The Sanchez mechanism is the only mechanism that moves closer to the humins composition of humins in the present study as the humin molecule becomes more conjugated, i.e. this conjugated humins molecule represents my humins.

5.4.3 Humins soxhlet washing

Humins were washed in a glass soxhlet extractor with water to determine the mass loss due to washing with water and to determine whether washing with water has any effect on humins composition. Washing with water had no major effect on the composition of the humins. The C:H:O values for humins, recorded every 8 hours are presented in Figure 37 and they are all very similar. The mass loss for the washing procedure is recorded in Table 12:

Table 12: Mass loss due to soxhlet washing of humins for 24 hours

Repetition	Mass Loss (%)
Triplicate 1	1.19
Triplicate 2	1.21
Triplicate 3	1.17

In Table 12, it can be seen that there are no functional groups trapped in the humin structure because washing with water produces no significant mass loss. There was almost no change to the humins after each 8-hour washing period so one can conclude that there are no water-soluble components in the humins. Hoang *et al.* (2015) prepared humins from 1 M glucose in 0.01 M H_2SO_4 at 180 °C for 6 h. They also purified the humins via soxhlet extraction with water for 24 h to remove the sugar derivatives entrapped in the humins(Hoang *et al.*, 2015). In the present study, sugars are not used so therefore no molecules are trapped in the humin structure.

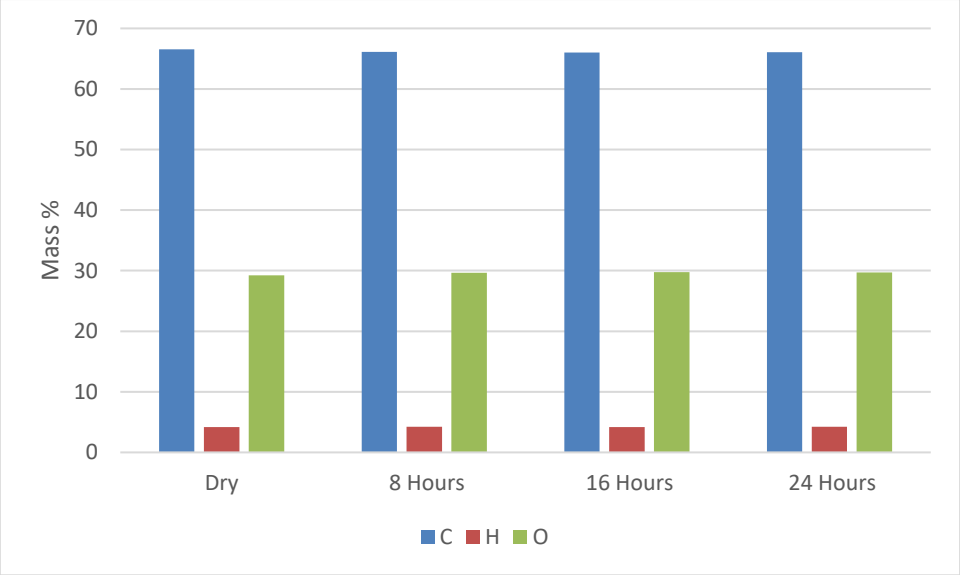

Figure 37: C:H:O data for soxhlet washes

5.4.4 Humins concentration

The asymptotic significance (p-value) of each experimental factor on humin concentration which resulted from statistical analysis is given in In Table 13, which shows that temperature and initial FF concentration significantly affect the humins concentration (See Figure 38 & Figure 39). The effect of sulfuric acid is also important as demonstrated in Figure 38 even though the calculated ANOVA p-value is slightly larger than 0.05.

Karinen, Vilonen & Niemelä (2011) found that the yields of humins in xylose to FF dehydration reactions was low at low temperatures, while it increased as a function of temperature. (Karinen *et al.*, 2011). Atilio De Frias & Feng (2014) found that humins production increased by 30 % when increasing the reaction temperature from 170 °C to 180 °C for their reactions where sugarcane bagasse was converted in a batch reactor to FF via dilute sulfuric acid catalysis (Atilio De Frias & Feng, 2014). Wang, Balsara & Bell (2016) found that the formation of humins can be minimized by removal of FF, either by steam stripping or by liquid–liquid extraction, i.e. humins concentration is a function of initial FF concentration (Wang, Balsara & Bell, 2016).

Stellenbosch University https://scholar.sun.ac.za

Table 13: Asymptotic significance of experimental factors with respect to humins concentration

Factor	p-value
Temperature	0,000430
Initial FF Concentration	0,001887
Sulfuric Acid Concentration	0,076333

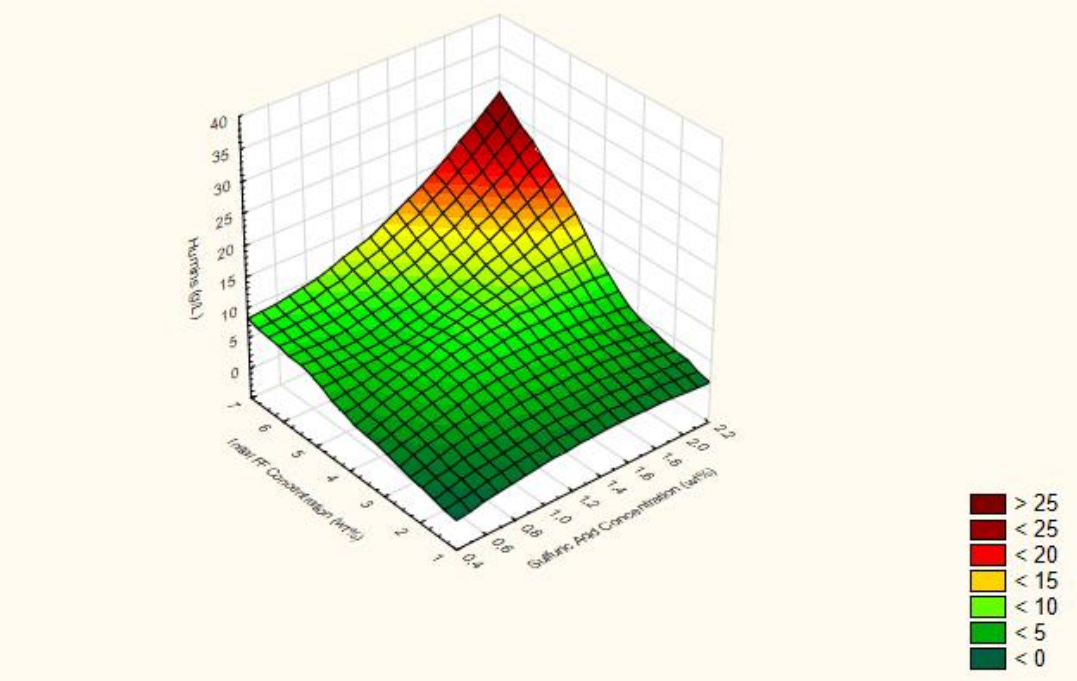

Figure 38: 3D Surface Plot of Humins Concentration (g/L) against Sulfuric Acid Concentration (wt%) and Initial FF Concentration (wt%)

Stellenbosch University https://scholar.sun.ac.za

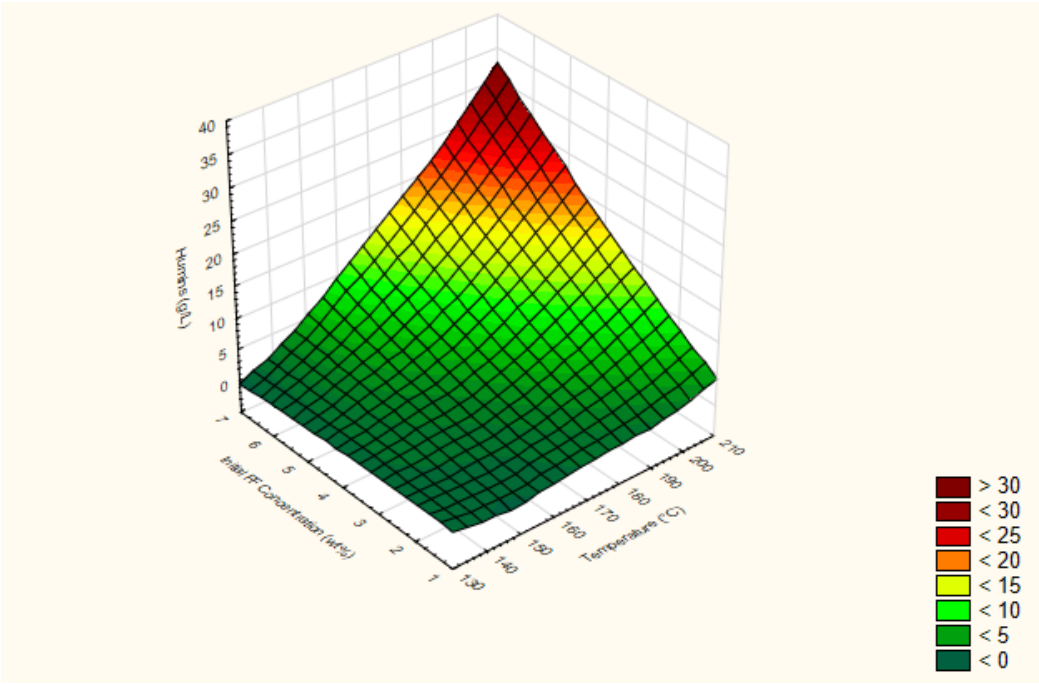

Figure 39: 3D Surface Plot of Humins Concentration (g/L) against Temperature (°C) and Initial FF Concentration (wt%)

5.5. Formic acid

5.5.1 Overall quantity of formic acid produced

The quantity of FA formed as a product of fragmentation was proportional to initial FF concentration and as demonstrated in Figure 40, FA concentration increases with an increase in the initial FF concentration. The p-values (ANOVA) for the experimental factors with respect to FA concentration reported in Table 14, prove the significant effect of initial FF concentration on FA concentration. The insignificant effect of temperature on FA formation has previously been reported by Rahubadda, Montoya & Haynes (2010)

They found that for their study of the decomposition of C_5 sugars under hot compressed water conditions (T=220-320 °C, P=200 bar), between 240°C and 260°C, the FA yield increased up to 40 seconds and then started to decrease, i.e. FA formation is not directly related to temperature (Rahubadda, Montoya & Haynes, 2010). The effect of initial FF concentration was not investigated previously.

Table 14: Asymptotic significance of experimental factors with respect to the mass of formic acid produced through fragmentation

Factor	p-value
Temperature	0,645753
Initial FF Concentration	0,000001
Sulfuric Acid Concentration	0,174864

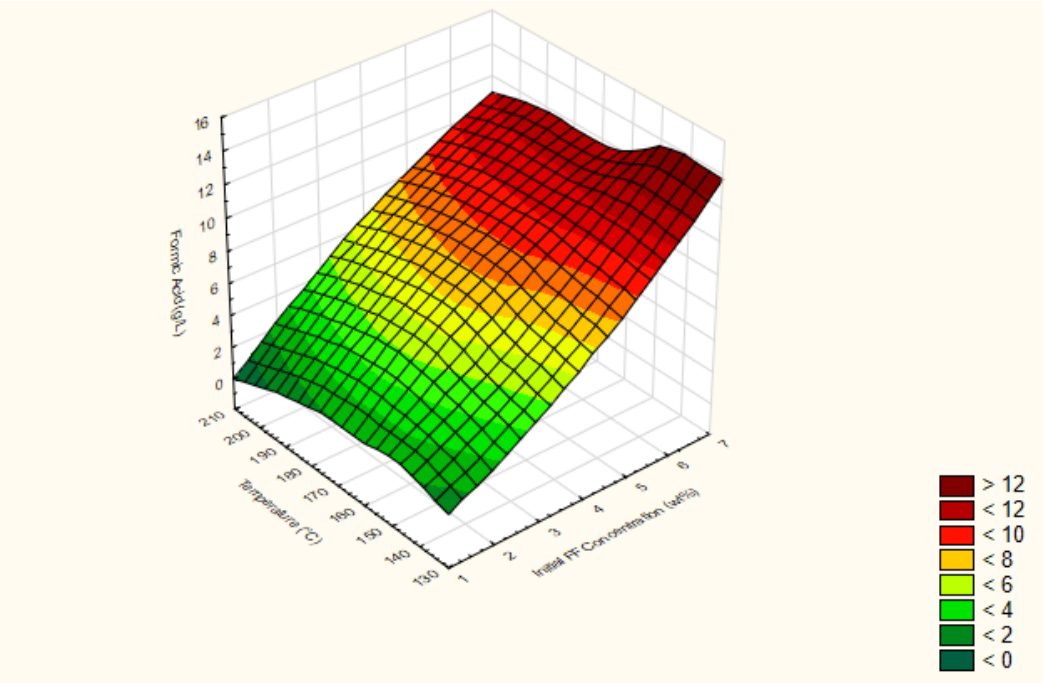

Figure 40: 3D Surface Plot of Formic Acid Concentration (g/L) against Initial FF Concentration (wt%) and Temperature (°C)

5.5.2 Extent of fragmentation reaction under studied conditions

The results indicated that FA accounts for 1.7-56 % of the reacted FF which shows the significance of fragmentation in the FF degradation process under these (industrially relevant) reaction conditions. However, Marcotullio et al. (2009) stated that fragmentation played a small part in FF degradation (Marcotullio *et al.*, 2009). It should be mentioned that the initial FF concentrations used by Marcotullio et al. (2009) was 0.0604 M & 0.0725 M compared to

Stellenbosch University https://scholar.sun.ac.za

0.157 M, 0.314 M & 0.631 M, applied in this study. The fact that their initial FF concentration was dilute was the reason that they found fragmentation to be less significant.

As calculated in Equation 13, for each mol of FF degraded, 0.86 mol FA forms on average, which is slightly higher than the value reported in literature. Williams & Dunlop (1948) reported that the total formed FA never exceeded two thirds of a mole per mole of FF lost (Williams & Dunlop, 1948). It is worth mentioning that their experiments were conducted on FF only and xylose wasn't present in the reaction mixture (like the present study). Their study was conducted with a FF loading of 10 g/L and the present study was conducted with a FF loading of 15, 30 & 60 g/L hence more FA is formed via fragmentation.

$$\frac{\%_{\mathrm{FF(reacted)}}}{\mathrm{mm_{FF}}} \times \mathrm{x} = \frac{\%_{\mathrm{FA}}}{\mathrm{mm_{FA}}}$$
$$\frac{1-0.5312}{96.08} \times \mathrm{x} = \frac{0.1931}{46.03} \qquad 13$$
$$x = 0.86$$

where 0.5312 is the average 53.12 % unreacted FF from mass balances

5.5.3 Formic acid yield as a function of acid catalyst type

Comparison of the results of this study and previous literature demonstrated that FA yield is a function of acid catalyst type (not just pH). In this study, the average FA yield for 51 mM H_2SO_4 (0.5 wt%), 156 mM FF (1.5 wt%) and 200 °C was 32.9 %. Hongsiri, Danon & De Jong (2014) determined the kinetics of FF (50 mM) degradation in an acidic medium (50 mM HCl) and they observed FA formation with a yield of almost 20 % after 60 minutes at 200 °C (Hongsiri *et al.*, 2014). The initial FF concentration used in the present study was 3 times that of Hongsiri, Danon & De Jong (2014) and the reaction duration was 50 % (30 minutes) longer. Despite this, the FF yield under the same conditions of temperature and acid concentration was only 50 % higher than Hongsiri, Danon & De Jong (2014). Hongsiri, Danon & De Jong (2014) used HCl as acid catalyst which is a stronger acid than H_2SO_4 ($\mathrm{pKa_{HCl}} = -8, \mathrm{pka_{H_2SO_{4,1}}} = -3, \mathrm{pKa_{H_2SO_{4,2(25°\,C)}}} = 1.99$ (Van Der Hagen & Järnberg, 2009)). This result highlights the effect that different acid catalysts have on FA production.

Stellenbosch University https://scholar.sun.ac.za

Acid activity has not been discussed in this study, but it may be an important factor in determining the extent of FF degradation. The lack of a trend for FA formed in the studies listed in Table 3 might have to do with the fact that the studies all make use of different acid catalysts (The other studies made use of H_2SO_4, FA, hot water (no acid), ZSM-5 zeolite and AA).

Aqueous acid catalysts behave differently from each other (due to differing acid activity) and so the conclusions made in this study are specific to H_2SO_4 catalysed systems only.

Stellenbosch University https://scholar.sun.ac.za

6. Conclusions & Recommendations

6.1 Conclusions

FA mass percentage varied in the range of 1.7-56%. Humins mass percentage varied in the range of 2.6-33%. Unreacted FF varied in the range of 14-88%. A range of 3-30 % of mass was unaccounted for (due to analytical error or smaller components that were not detected by the HPLC).

The mechanism that is responsible for the humins formed in this study is the Sanchez mechanism. This mechanism involves bifurylic and trifurylic structures. The C:H:O composition of a molecule of this mechanism is 64.74:4.00:31.26 and the average C:H:O composition of the humins formed in this study is 63.75:4.07:32.17, i.e. they are very similar, and humins in this study form via the Sanchez mechanism. The humins in this study are found lower down on the dehydration line than the FF molecule which indicates that there is a dehydration reaction in the formation of humins from FF and the Sanchez mechanism does involve a dehydration reaction.

The reaction order discovered in this study is n = 1.15. For all runs, the average natural log of the pre-exponential factor has been established to be lnA = 20.22 s^{-1}, and the average activation energy is Ea = 93.63 $kJ \cdot mol^{-1}$, like previous values. Therefore, FF degradation is pseudo-unimolecular. The overall order is just greater than unity which supports the proposition that for degradation, a polymerisation reaction is potentially initiated with two FF molecules (second order) and polymer growth occurs one FF molecule at a time (first order). Growth is dominant because the reaction order is close to unity. Alternatively, this slight deviation from unity may simply be a result of experimental error.

In a conventional FF production plant, humins are generated amongst the (pentosan containing) biomass fibres and combusting these humins alone (instead of coal) produces 1.3 % of the energy required to generate steam for the FF production process. When humins are generated in biorefinery pre-treatment stages or from processing pulp mill pre-hydrolysis liquor. A valorisation method should be explored so that humins do not remain in the system, blocking up pipes & adhering to reactor walls. Humins can be combined with PFA to give a lower cost resin composite with decreased brittleness and higher tensile strength compared to pure PFA resins. This

Stellenbosch University https://scholar.sun.ac.za

is the most promising valorisation route for humins that will be generated in pre-hydrolysis units.

There is very little mass loss for humins that are washed with water in a glass soxhlet extractor (1.2 %) which means that these humins are not water soluble. It also means that no functional groups are trapped in the humins structure. i.e. the elemental composition that is reported is only for the humin structure.

The composition of humins formed in this study is fairly uniform and the composition is independent of processing conditions. The maximum standard deviation is 2.36 % for composition and the maximum variance is 5.68 %.

Stellenbosch University https://scholar.sun.ac.za

6.1.1 Summary of reaction conditions

A summary of the influential factors in this study is presented in Table 15.

Table 15: Summary of influential factors in this study

Factor	Condition causing an increase
FA concentration	Increased initial FF concentration
Humins concentration	Increased temperature & increased initial FF concentration
Rate of FF degradation	Increased temperature, increased sulfuric acid concentration & increased initial FF concentration

In this study, it was found that initial FF concentration was the most influential factor towards FF degradation. Increasing the initial FF concentration caused an increase in the rate of degradation, more humins were formed and more FA was formed. Increasing reaction temperature caused an increase in the amount of humins formed and an increase in the rate of degradation. Increasing the concentration of sulfuric acid caused an increase in the rate of FF degradation.

6.2. Recommendations

It is recommended that FF production is conducted at the lowest possible temperature and sulfuric acid concentration (to minimise degradation). To produce the least amount of degradation products (FA & humins), the lowest initial concentration of FF should be exposed to degradation conditions. To decrease the initial FF concentration exposed to degradation conditions, either less FF should be produced by processing less biomass or more FF should be stripped. Decreasing FF production and increasing stripping are both uneconomical avenues to minimise degradation. Therefore, optimisation must include the managing of the extent of FF degradation, because FF degradation and the amount of FF that is produced are both dependent on the same reaction conditions (temperature, sulfuric acid concentration & reaction duration). The data presented in this study can be used in a FF production model to determine the extent of the degradation reaction under a given set of reaction conditions.

Stellenbosch University https://scholar.sun.ac.za

For acid catalysed hydrolysis of hemicellulosic pentose fractions of biomass and consecutive dehydration of the pentose monomers, it was found that the optimal reaction temperatures were 155, 160, and 180 °C for sulfuric acid, phosphoric acid, and FA, respectively (Yang *et al.*, 2012). This confirms that an optimization of FF production by minimising degradation and maximising FF output would also be specific to the (mineral) acid selected as catalyst (as found in section 5.5.4).

As discussed in 2.6, elevated temperature causes more resinification (as demonstrated in this study) but condensation is minimised at elevated temperatures (Sener *et al.*, 2018). In order to optimize the production of humins, it is necessary to study condensation reactions over a range of temperatures (170 °C-230 °C). Note that FF formation temperature is 175 °C and Sener *et al.* (2018) found that condensation is minimised at high temperatures (>200 °C). Once an understanding exists of the conditions that facilitate condensation, an optimization can be conducted to determine the reaction conditions that produce the most FF at the lowest cost by minimising the humins formed through condensation or resinification.

The aim of this study was to create understanding of the degradation reactions using pure FF. Using the same experimental conditions, it is now recommended to broaden the understanding of FF degradation obtained in this study by the inclusion of the other molecules present during FF production. For example:

1. To included xylose in the reaction mixture so that condensation can occur. This will permit a comparison of the FF degradation kinetics with and without xylose so that the impact of the condensation reaction can be measured.
2. A further study should then be conducted, extending the experimental setup to include lignocellulosic biomass. The aim of that study would be to observe additional FF degradation caused by e.g. the presence of lignins and or fibre.

In both proposed studies, special focus should be given to comparing the elemental composition of humins to the composition of humins formed in the present study. Although it was discovered that the composition was independent of processing conditions, it is not known whether generating humins from xylose and/or biomass (not pure FF) would result in different humins compositions.

Reaction duration is an important factor that affects the extent of FF degradation in combination with the experimental factors tested in the present study (initial FF concentration, sulfuric acid concentration and reaction temperature). O'Neil *et al.* (2009) highlights the significance of the reaction duration for the degradation reaction

Stellenbosch University https://scholar.sun.ac.za

(during aqueous phase dehydration of xylose to FF) and recommends that the reaction duration is optimised to minimise FA & humin formation, thus maximising FF production (O'Neil *et al.*, 2009). Karinen, Vilonen & Niemelä (2011) found that the selectivity of FF in xylose dehydration was a function of the reaction duration (Karinen *et al.*, 2011). In the present study, a constant reaction duration was used (90 minutes). Reaction duration is factor that should be optimised with the target of maximising FF production and minimising FF degradation. For future degradation studies, it is recommended to vary the reaction duration.

Stellenbosch University https://scholar.sun.ac.za

7. References

Antal, M.J., Leesomboon, T., Mok, W.S. & Richards, G.N. 1991. Mechanism of formation of 2-furaldehyde from d-xylose. *Carbohydrate Research*. 217(C):71–85.

Atilio De Frias, J. & Feng, H. 2014. Pretreatment of furfural residues with switchable butadiene sulfone in the sugarcane bagasse biorefinery. *Green Chemistry*. 16(5):2779–2787.

Buzzard, J. 2003. *The conventional furfural production technology using spherical rotating reactors as practiced in the Omaha and Cedar Rapids Plants*.

Cai, C.M., Zhang, T., Kumar, R. & Wyman, C.E. 2014. Integrated furfural production as a renewable fuel and chemical platform from lignocellulosic biomass. *Journal of Chemical Technology and Biotechnology*. 89(1):2–10.

Chen, Z., Zhang, W., Xu, J. & Li, P. 2015. Kinetics of xylose dehydration into furfural in acetic acid. *Chinese Journal of Chemical Engineering*. 23(4):659–666.

Cherubini, F. 2010. The biorefinery concept: Using biomass instead of oil for producing energy and chemicals. *Energy Conversion and Management*. 51(7):1412–1421.

Choudhary, V., Pinar, A.B., Sandler, S.I., Vlachos, D.G. & Lobo, R.F. 2011. Xylose isomerization to xylulose and its dehydration to furfural in aqueous media. *ACS Catalysis*. 1(12):1724–1728.

Cooper, J. & Le Fevre, E. 1969. *Thermophysical Properties of Water Substance*. 1st ed. Elsevier.

Council, N.R. 2014. *Review of the Formaldehyde Assessment in the National Toxicology Program 12th Report on Carcinogens*. Washington, DC: The National Academies Press.

Dalinyebo. 2018. *Furfural: How is it made?* [Online], Available: http://dalinyebo.com/furfural#how-is-it-made.

Danon, B., Van Der Aa, L. & De Jong, W. 2013. Furfural degradation in a dilute acidic and saline solution in the presence of glucose. *Carbohydrate Research*. 375:145–152.

Danon, B., Marcotullio, G. & De Jong, W. 2013. Mechanistic and kinetic aspects of pentose dehydration towards furfural in aqueous media employing homogeneous catalysis. *Green Chemistry*. 1–16.

Dewick, P.M. 2006. *Essentials of Organic Chemistry: For Students of Pharmacy, Medicinal Chemistry and Biological Chemistry*. Wiley.

Dunlop, A.P. 1948. Furfural formation and behaviour. *INDUSTRIAL AND ENGINEERING CHEMISTRY*. 40(2):204–209.

Dussan, K., Girisuta, B., Lopes, M., Leahy, J.J. & Hayes, M.H.B. 2015. Conversion

Stellenbosch University https://scholar.sun.ac.za

of hemicellulose sugars catalysed by formic acid: Kinetics of the dehydration of D-xylose, L-arabinose and Dglucose. *ChemSusChem*. 8(8):1411–1428.

Feather, M.S. 1969. Reductic acid-14C derived from D-xylose-1-14C and 2-furaldehyde-. alpha.-14C. *The Journal of Organic Chemistry*. 34(6):1998–1999.

Gandini, A. & Belgacem, M.N. 1997. Furans In Polymer Chemistry. *Progress in Polymer Science*. 22(97):1203–1379.

Girisuta, B., Dussan, K., Haverty, D., Leahy, J.J. & Hayes, M.H.B. 2013. A kinetic study of acid catalysed hydrolysis of sugar cane bagasse to levulinic acid. *Chemical Engineering Journal*. 217:61–70.

Van Der Hagen, M. & Järnberg, J. 2009. *Sulphuric, hydrochloric, nitric and phosphoric acids*. Vol. 43.

Hoang, T., van Eck, E., Bula, W., Gardeniers, J., Lefferts, L. & Seshan, K. 2015. Humin based by-products from biomass processing as a potential carbonaceous source for synthesis gas production. *Green Chemistry*. 17(2):959–972.

Hongsiri, W., Danon, B. & De Jong, W. 2014. Kinetic study on the dilute acidic dehydration of pentoses toward furfural in seawater. *Industrial and Engineering Chemistry Research*. 53(13):5455–5463.

Hongsiri, W., Danon, B. & de Jong, W. 2015. The effects of combined catalysis of oxalic acid and seawater on the kinetics of xylose and arabinose dehydration to furfural. *International Journal of Energy and Environmental Engineering*. 6(1):21–30.

Hu, F. & Ragauskas, A. 2014. Suppression of pseudo-lignin formation under dilute acid pretreatment conditions. *RSC Advances*. 4(9):4317.

IndexMundi. 2018. *Coal, South African export price Monthly Price - US Dollars per Metric Ton*. [Online], Available: https://www.indexmundi.com/commodities/?commodity=coal-south-african&months=12 [2018, August 01].

Jing, Q. & Lü, X. 2007. Kinetics of Non-catalyzed Decomposition of D-xylose in High Temperature Liquid Water. *Chinese Journal of Chemical Engineering*. 15(5):666–669.

de Jong, W. & Marcotullio, G. 2010. Overview of Biorefineries based on Co-Production of Furfural, Existing Concepts and Novel Developments. *International Journal of Chemical Reactor Engineering*. 8(A69):1–24.

Karinen, R., Vilonen, K. & Niemelä, M. 2011. Biorefining: Heterogeneously catalyzed reactions of carbohydrates for the production of furfural and hydroxymethylfurfural. *ChemSusChem*. 4(8):1002–1016.

Kiesselbach, T.A. & Lyness, W.E. 1993. The Effects of Stinking Smut (Bunt) and Seed Treatment upon the Yield of Winter Wheat. (1939).

Lamminpaa, K., Ahola, J. & Tanskanen, J. 2012. Kinetics of Xylose Dehydration into Furfural in Formic Acid. 6297–6303.

Stellenbosch University https://scholar.sun.ac.za

Lamminpaa, K., Ahola, J. & Tanskanen, J. 2014. Kinetics of furfural destruction in a formic acid medium. *Rsc Advances*. 4(104):60243–60248.

Lamminpää, K. 2015. Formic acid catalysed xylose dehydration into furfural. University of Oulu.

Lange, J.P., Van Der Heide, E., Van Buijtenen, J. & Price, R. 2012. Furfural-A promising platform for lignocellulosic biofuels. *ChemSusChem*. 5(1):150–166.

Lau, C.-S., Thoma, G.J., Clausen, E.C. & Carrier, D.J. 2015. Kinetic Modeling of Switchgrass-Derived Xylose Oligomers Degradation during Pretreatment in Dilute Acid or in Water. *ACS Sustainable Chemistry and Engineering*. 3(9):2030–2035.

Liu, H., Hu, H., Jahan, M.S. & Ni, Y. 2013. Furfural formation from the pre-hydrolysis liquor of a hardwood kraft-based dissolving pulp production process. *Bioresource technology*. 131:315–320.

Mandalika, A. & Runge, T. 2012. Enabling integrated biorefineries through high-yield conversion of fractionated pentosans into furfural. *Green Chemistry*. 14:3175–3184.

Marcotullio, G. 2011. The Chemistry and Technology of Furfural Production in Modern Lignocellulose-Feedstock Biorefineries. Delft University of Technology.

Marcotullio, G., Cardoso, M. a. T., De Jong, W. & Verkooijen, A.H.M. 2009. Bioenergy II: Furfural Destruction Kinetics during Sulphuric Acid-Catalyzed Production from Biomass. *International Journal of Chemical Reactor Engineering*. 7(1).

Mariscal, R., Maireles-Torres, P., Ojeda, M., Sádaba, I. & López Granados, M. 2016. Furfural: A renewable and versatile platform molecule for the synthesis of chemicals and fuels. *Energy and Environmental Science*. 9(4):1144–1189.

Naude, D.P., McIntyre, P.J. & Field, S.L.J. 1993. The Design and Operation of Boiler Plant Utilising Furfural Residue as a Fuel. *Carbon*. 8:0.

O'Neil, R., Ahmad, M.N., Vanoye, L. & Aiouache, F. 2009. Kinetics of aqueous phase dehydration of xylose into furfural catalyzed by ZSM-5 zeolite. *Industrial and Engineering Chemistry Research*. 48(9):4300–4306.

Oefner, P.J., Lanziner, A.H., Bonn, G. & Bobleter, O. 1992. Quantitative Studies on Furfural and Organic-Acid Formation during Hydrothermal, Acidic and Alkaline-Degradation of Deuterium-Xylose. *Monatshefte Fur Chemie*. 123(6–7):547–556.

Patil, S., Heltzel, J. & Lund, C. 2012. Comparison of structural features of humins formed catalytically from glucose, fructose, and 5-hydroxymethylfurfuraldehyde. *Energy and Fuels*. 26(8):5281–5293.

Peleteiro, S., Rivas, S., Alonso, J.L., Santos, V. & Parajó, J.C. 2015. Furfural production using ionic liquids: A review. *Bioresource Technology*. 202:181–191.

Pin, J.M., Guigo, N., Mija, A., Vincent, L., Sbirrazzuoli, N., Van Der Waal, J.C. & De Jong, E. 2014. Valorization of biorefinery side-stream products: Combination of

Stellenbosch University https://scholar.sun.ac.za

humins with polyfurfuryl alcohol for composite elaboration. *ACS Sustainable Chemistry and Engineering*. 2(9):2182–2190.

Popoff, T. & Theander, O. 1970. Formation of aromatic compounds from D-glucuronic acid and D-xylose under slightly acidic conditions. *Journal of the Chemical Society D: Chemical Communications*. (22):1970.

Rahubadda, A., Montoya, A. & Haynes, B.S. 2010. C5 Sugar Decomposition Products Under Hot.

Rasmussen, H., Sørensen, H.R. & Meyer, A.S. 2014. Formation of degradation compounds from lignocellulosic biomass in the biorefinery: Sugar reaction mechanisms. *Carbohydrate Research*. 385:45–57.

Rasrendra, C.B., Windt, M., Wang, Y., Adisasmito, S., Makertihartha, I.G.B.N., Van Eck, E.R.H., Meier, D. & Heeres, H.J. 2013. Experimental studies on the pyrolysis of humins from the acid-catalysed dehydration of C6-sugars. *Journal of Analytical and Applied Pyrolysis*. 104:299–307.

Rice, F.A.H. & Fishbein, L. 1956. Spectrophotometric Studies on the Action of Sulfuric Acid on. Reducing Sugars and the Isolation and identification of the Ether-soluble Substances Produced from Pentoses under Acid Conditions. *Journal of the American Chemical Society*. 78(5):1005–1009.

Rivas, S., González-Muñoz, M.J., Santos, V. & Parajó, J.C. 2014. Acidic processing of hemicellulosic saccharides from pine wood: Product distribution and kinetic modeling. *Bioresource Technology*. 162:192–199.

Root, D.F., Saeman, J.F., Harris, J.F. & Neil, W.K. 1959. Kinetics of the Acid Catalyzed Conversion of Xylose to Furfural. *Forest Products Journal*. 9:158–165.

Rose, I.C., Epstein, N. & Watkinson, A.P. 2000. Acid-Catalyzed 2-Furaldehyde (Furfural) Decomposition Kinetics. 843–845.

Rushin, M.S. 1992.

Sanchez, R., Hernandez, C. & Keresztury, G. 1994. Structural analysis of acid catalysed furfuraldehyde resins by thermal degradation techniques. 30(1):43–50.

Sánchez, R., Hernández, C., Jalsovszky, G. & Czira, G. 1994. Thermal degradation of furfuraldehyde resins. Pyrolysis-gas chromatography-mass spectrometry and fourier transform infrared. *European Polymer Journal*. 30(1):37–42.

Sannigrahi, P., Kim, D.H., Jung, S. & Ragauskas, A. 2011. Pseudo-lignin and pretreatment chemistry. *Energy & Environmental Science*. 4(4):1306.

Sappi. 2017. *Sappi invests in sugar separations and clean-up technology to strengthen its renewable bio-chemicals offering*. [Online], Available: https://www.sappi.com/sappi-invests-sugar-separations-and-clean-technology-strengthen-its-renewable-bio-chemicals-offering [2018, August 31].

Sener, C., Motagamwala, A.H., Alonso, D.M. & Dumesic, J. 2018. Enhanced Furfural

Stellenbosch University https://scholar.sun.ac.za

Yields from Xylose Dehydration in the gamma-Valerolactone/Water Solvent System at Elevated Temperatures. *Sustainable chemistry*.

Shinde, S.D., Meng, X., Kumar, R. & Ragauskas, A.J. 2018. Recent advances in understanding the pseudo-lignin formation in a lignocellulosic biorefinery. *Green Chemistry*. 20(10):2192–2205.

Sokhansanj, S. 2011. The Effect of Moisture on Heating Values. *Biomass Energy Data Book*. (C):1–5. [Online], Available: http://cta.ornl.gov/bedb.

Sumerskii, I. V, Krutov, S.M. & Zarubin, M.Y. 2010. Humin-like substances formed under the conditions of industrial hydrolysis of wood. *Russian Journal of Applied Chemistry*. 83(2):320–327.

Tsilomelekis, G., Orella, M.J., Lin, Z., Cheng, Z., Zheng, W., Nikolakis, V. & Vlachos, D.G. 2016. Molecular structure, morphology and growth mechanisms and rates of 5-hydroxymethyl furfural (HMF) derived humins. *Green Chem.*

Wang, A., Balsara, N.P. & Bell, A.T. 2016. Pervaporation-assisted catalytic conversion of xylose to furfural. *Green Chemistry*. 18(14):4073–4085.

Wang, C.-H., Wu, B.-S., Tung, G.-Y., Lin, H.-C., Chen, W.-H. & Wan, B.-Z. 2018. Kinetics of xylose conversion to furfural in sulfuric acid solution with chromium(III) ions. *Industrial & Engineering Chemistry Research*.

Wang, S., Lin, H., Chen, J., Zhao, Y., Ru, B., Qiu, K. & Zhou, J. 2015. Conversion of carbohydrates into 5-hydroxymethylfurfural in an advanced single-phase reaction system consisting of water and 1,2-dimethoxyethane. *RSC Adv.* 5(102):84014–84021.

Wang, S., Lin, H., Zhao, Y., Chen, J. & Zhou, J. 2016. Structural characterization and pyrolysis behavior of humin by-products from the acid-catalyzed conversion of C6 and C5 carbohydrates. *Journal of Analytical and Applied Pyrolysis*.

Weingarten, R., Cho, J., Conner, Jr., W.C. & Huber, G.W. 2010. Kinetics of furfural production by dehydration of xylose in a biphasic reactor with microwave heating. *Green Chemistry*. 12(8):1423.

Weingarten, R., Tompsett, G.A., Conner, W.C. & Huber, G.W. 2011. Design of solid acid catalysts for aqueous-phase dehydration of carbohydrates: The role of Lewis and Brønsted acid sites. *Journal of Catalysis*. 279(1):174–182.

Williams, D.L. & Dunlop, A.P. 1948. Kinetics of Furfural Destruction in Acidic Aqueous Media. *Ind. Eng. Chem.* 40:239–241.

Wu, Y., Xu, G. & Shao, H.B. 2014. Furfural and its biochar improve the general properties of a saline soil. *Solid Earth*. 5(2):665–671.

Xing, R., Qi, W. & Huber, G.W. 2011. Production of furfural and carboxylic acids from waste aqueous hemicellulose solutions from the pulp and paper and cellulosic ethanol industries. *Energy & Environmental Science*. 4(6):2193.

Xu, W., Zhang, S., Lu, J. & Cai, Q. 2017. Furfural production from corncobs using thiourea as additive. *Environmental Progress & Sustainable Energy*. 36(3):690–

Stellenbosch University https://scholar.sun.ac.za

695.

Yang, W., Li, P., Bo, D. & Chang, H. 2012. The optimization of formic acid hydrolysis of xylose in furfural production. *Carbohydrate Research*. 357:53–61.

van Zandvoort, I. 2015. *Towards the Valorization of Humin By-products : Characterization , Solubilization and Catalysis*.

Van Zandvoort, I., Wang, Y., Rasrendra, C.B., Van Eck, E.R.H., Bruijnincx, P.C.A., Heeres, H.J. & Weckhuysen, B.M. 2013. Formation, molecular structure, and morphology of humins in biomass conversion: Influence of feedstock and processing conditions. *ChemSusChem*. 6(9):1745–1758.

Zeitsch, K.J. 2000. *The Chemistry and Technology of Furfural and its Many By-products*. Vol. 13.

Stellenbosch University https://scholar.sun.ac.za

Appendix I

Python code

```
from __future__ import division
from scipy.integrate import odeint
from scipy.optimize import minimize
from numpy import linspace, genfromtxt, interp, mean,zeros
from math import exp, log, sqrt
import matplotlib.pyplot as plt

fn = 'thesis'
data_file_name = 'Run Data\\'+fn+'.dat'
d = genfromtxt(data_file_name,skip_header=(3))
conditions = genfromtxt(data_file_name, skip_footer=10)
T_arr = conditions[0] #C
CF_arr = conditions[1] #M
CA_arr = conditions[2] #%
CA_arr = CA_arr*100/98.079 #% to M
t = d[:,0] #min
d = d[:,1:]/96.09 #M
n=len(d[0])
#Filter Data
Filter_arr = [0,0,0]
i=0
while i<n and Filter_arr[0] !=0:
    if T_arr[i] != Filter_arr[0]:
        for j in range(i,n-1):
            d[:,j] = d[:,j+1]
            T_arr[j] = T_arr[j+1]
            CA_arr[j] = CA_arr[j+1]
            CF_arr[j] = CF_arr[j+1]
        n -= 1
    else:
        i += 1
i=0
while i<n and Filter_arr[1] !=0:
    if CF_arr[i] != Filter_arr[1]:
        for j in range(i,n-1):
            d[:,j] = d[:,j+1]
            T_arr[j] = T_arr[j+1]
            CA_arr[j] = CA_arr[j+1]
            CF_arr[j] = CF_arr[j+1]
        n -= 1
    else:
        i += 1
i=0
while i<n and Filter_arr[2] !=0:
    if CA_arr[i] != Filter_arr[2]:
```

Stellenbosch University https://scholar.sun.ac.za

```
        for j in range(i,n-1):
            d[:,j] = d[:,j+1]
            T_arr[j] = T_arr[j+1]
            CA_arr[j] = CA_arr[j+1]
            CF_arr[j] = CF_arr[j+1]
        n -= 1
    else:
        i += 1



Fspan = zeros((100,1))
tspan = linspace(t[0],t[len(t)-1],100)

A_1 = 1.55e-3 #min^-1
Ea_1 = 1.021e5 #J/mol
R = 8.314 #J/mol/K
T_0 = 453.15 #K (180 C)

Ka2_arr = [2.8e-4,1.1e-4,4.12e-5] #Zeitsch Approx
Ka2_T_arr = [413.15,443.15,473.15]
def H_func(T,CA):#CA is [H2SO4] in %
    Ka1 = 1000
    for i in range(3):
        if T == Ka2_T_arr[i]:
            Ka2 = Ka2_arr[i]
    H_conc = sqrt(CA*Ka1)+sqrt(CA*Ka2)
    return H_conc

def Arr(T,A,Ea):
    return A*exp(-Ea/R*(1/T-1/T_0))

def dCFdt(CF,t,T,A,Ea,CA,o,m): #CF in mM
    return -Arr(T,A,Ea)*CF**o*H_func(T,CA)**m #mmol/L/min

def SSNE(CF_0,T,A,Ea,CA,dd,o,m):
    CFspan = odeint(dCFdt,CF_0,tspan,(T,A,Ea,CA,o,m),)[:,0]
    CFspanInterp = interp(t,tspan,CFspan)
    out = 0
    for i in range(len(t)):
        out += (dd[i]/CF_0-CFspanInterp[i]/CF_0)**2
    return out

def minfun(X):
    A,Ea,o,m = X
    SSNE_sum = 0
    for i in range(n):
        SSNE_sum += SSNE(d[0,i],T_arr[i]+273.15,A,Ea,CA_arr[i],d[:,i],o,m)
    return SSNE_sum
```

Stellenbosch University https://scholar.sun.ac.za

```
def R_squared(X):
    A,Ea,o,m = X
    R_arr = []
    for i in range(n):
        CFspan =
odeint(dCFdt,d[0,i],tspan,args=(T_arr[i]+273.15,A,Ea,CA_arr[i],o,m))[:,0]
        CFspanInterp = interp(t,tspan,CFspan)
        mn = mean(d[:,i])
        CFmn = mean(CFspanInterp)
        x_squared = []
        y_squared = []
        xy = []
        mod_dif = 0
        mean_dif = 0
        for j in range(len(t)):
            if abs(CFspanInterp[j]-d[j,i])>mod_dif:
                mod_dif = abs(CFspanInterp[j]-d[j,i])
            if abs(d[j,i]-mn)>mean_dif:
                mean_dif = abs(d[j,i]-mn)
            x_squared.append((d[j,i]-mn)**2)
            y_squared.append((CFspanInterp[j]-CFmn)**2)
            xy.append((d[j,i]-mn)*(CFspanInterp[j]-CFmn))
        R_arr.append(100*(sum(xy)/sqrt(sum(x_squared)*sum(y_squared)))**2)
    return R_arr

# callback function
eval_track = 0
Nfeval = 1
X_arr = []
Y_arr = []
YY_arr = []
YYY_arr = []
def callbackfunc(x):
    global Nfeval
    #print("%s, %.2f, %e" % (Nfeval, x[1], minfun(x)))
    Nfeval += 1
    if eval_track:
        X_arr.append(Nfeval)
        Y_arr.append(x[0])
        YY_arr.append(x[1])
        YYY_arr.append(x[2])

tryVals = [1e-02, 1.5e5, 1.08, 1]


res = minimize(minfun, tryVals,
               method='Nelder-Mead',
               options={'maxiter':1e2,'maxfev':1e3,
               'ftol':1e-4,'xtol':1e-4},
               callback=callbackfunc)
```

Stellenbosch University https://scholar.sun.ac.za

```
lnA = log(res.x[0]/60*res.x[1]/(T_0*R))
print(res.x)

R_squared_ave = 0
for i in range(n):
    R_squared_ave+=R_squared(res.x)[i]
R_squared_ave=R_squared_ave/n

#Plot Data
if eval_track:
    fig, ax1 = plt.subplots()
    ax1.plot(X_arr, Y_arr, 'b')
    ax1.set_xlabel('Iterations')
    ax1.set_ylabel('A', color='b')
    for tl in ax1.get_yticklabels():
        tl.set_color('b')
    ax2 = ax1.twinx()
    ax2.plot(X_arr, YYY_arr, 'r')
    ax2.set_ylabel('n', color='r')
    for tl in ax2.get_yticklabels():
        tl.set_color('r')

normalized_plot = 1
'''
import matplotlib
c_list = []
for name, hex in matplotlib.colors.cnames.items():
    c_list.append(name)
#print(c_list)
'''
plt.figure(2)
c_list = [ 'red', 'gold', 'midnightblue', 'turquoise', 'blueviolet', 'darkslategrey',
'darkslateblue', 'darkred', 'slategrey', 'cyan', 'darkkhaki', 'royalblue', 'olive',
'mediumturquoise', 'green', 'slateblue', 'maroon', 'cornflowerblue', 'palegreen',
'gainsboro', 'darkolivegreen', 'darkgrey', 'whitesmoke', 'palevioletred', 'aliceblue',
'bisque', 'darkturquoise', 'snow', 'darkviolet', 'mintcream', 'gold', 'fuchsia', 'mistyrose',
'palegoldenrod', 'plum', 'beige', 'rosybrown', 'olivedrab', 'honeydew', 'white',
'darkgreen', 'indianred', 'antiquewhite', 'teal', 'mediumslateblue', 'orangered',
'floralwhite', 'darkgoldenrod', 'darkgray', 'darkblue', 'lavender', 'darkcyan',
'aquamarine', 'slategray', 'darksalmon', 'papayawhip', 'black', 'darksage', 'cadetblue',
'violet', 'greenyellow', 'saddlebrown', 'orange', 'mediumorchid', 'lime', 'darkmagenta',
'mediumblue', 'seagreen', 'blue', 'thistle', 'magenta', 'linen', 'purple', 'mediumvioletred',
'peru', 'pink', 'wheat', 'limegreen', 'tomato', 'aqua', 'peachpuff', 'powderblue',
'mediumpurple', 'khaki', 'darkslategray', 'skyblue', 'darkseagreen', 'brown',
'yellowgreen', 'mediumspringgreen', 'orchid', 'azure', 'yellow', 'lavenderblush',
'chartreuse', 'dodgerblue', 'lemonchiffon', 'darkorchid', 'burlywood',
'mediumseagreen', 'darkorange', 'springgreen', 'forestgreen', 'cornsilk', 'indigo',
'hotpink', 'ivory', 'sandybrown', 'salmon', 'moccasin', 'deeppink', 'red',
'mediumaquamarine', 'dimgrey', 'sienna', 'oldlace', 'seashell', 'gray', 'sage', 'steelblue',
```

Stellenbosch University https://scholar.sun.ac.za

```
'lawngreen', 'blanchedalmond', 'dimgray', 'navajowhite', 'deepskyblue', 'goldenrod',
'chocolate', 'firebrick', 'coral', 'paleturquoise', 'crimson']

for i in range(n):
    #labstr = str(round(T_arr[i])).rstrip('0').rstrip('.')+'$^\circ$C, '+str(CA_arr[i])+'%,
'+str(round(CF_arr[i])).rstrip('0').rstrip('.')+' wt%'
    if normalized_plot:
        plt.plot(t,d[:,i]/d[0,i],c=c_list[i],ls='',marker='.',markersize=10)#,label=labstr)
    else:
        plt.plot(t,d[:,i],c=c_list[i],ls='',marker='.',markersize=10)#,label=labstr)
#Fit
for i in range(n):
      if normalized_plot:
          plt.ylabel(r'$C_f/C_{f, 0}$ (M/M)', fontsize = 30)
          Fspan =
odeint(dCFdt,d[0,i],tspan,(T_arr[i]+273.15,res.x[0],res.x[1],CA_arr[i],res.x[2],res.x[3]))
/d[0,i]
      else:
          plt.ylabel('Furfural concentration (M)', fontsize = 10)
          Fspan =
odeint(dCFdt,d[0,i],tspan,(T_arr[i]+273.15,res.x[0],res.x[1],CA_arr[i],res.x[2],res.x[3]))
      labstr = 'Fit '+str(round(T_arr[i])).rstrip('0').rstrip('.')+'$^\circ$C,
'+str(CF_arr[i]).rstrip('0').rstrip('.')+'wt%, '+str(CA_arr[i])+'%, '+'$R^2:
$'+str(round(R_squared(res.x)[i],2))+'%'
      plt.plot(tspan,Fspan,c=c_list[i],linewidth=2,label=labstr)
#plt.legend(loc=0, prop ={'size':25})
titleStr = r'$ln(A) = $'+ str(round(lnA,3)) + r' $ s^{-1}$' +'\t' +'Ea = '+
str(round(res.x[1]/1000,2)) +r' $ kJ \cdot mol^{-1}$'+'\t Order: '+
str(round(res.x[2],2))+'\t R'+r'$^2$'+r'$_{ave}=$'+str(round(R_squared_ave,2))
##r'$R^2: $'+str(round(100*(1-minfun(res.x)),2))+'\n' +
plt.title(titleStr, fontsize = 30)
plt.xlabel('Reaction duration (min)', fontsize = 30)
plt.tick_params(axis='both', labelsize=20)
mng = plt.get_current_fig_manager()
mng.window.showMaximized()
plt.show()
```

Stellenbosch University https://scholar.sun.ac.za

Appendix II

Sketch of ice bath and sampling system

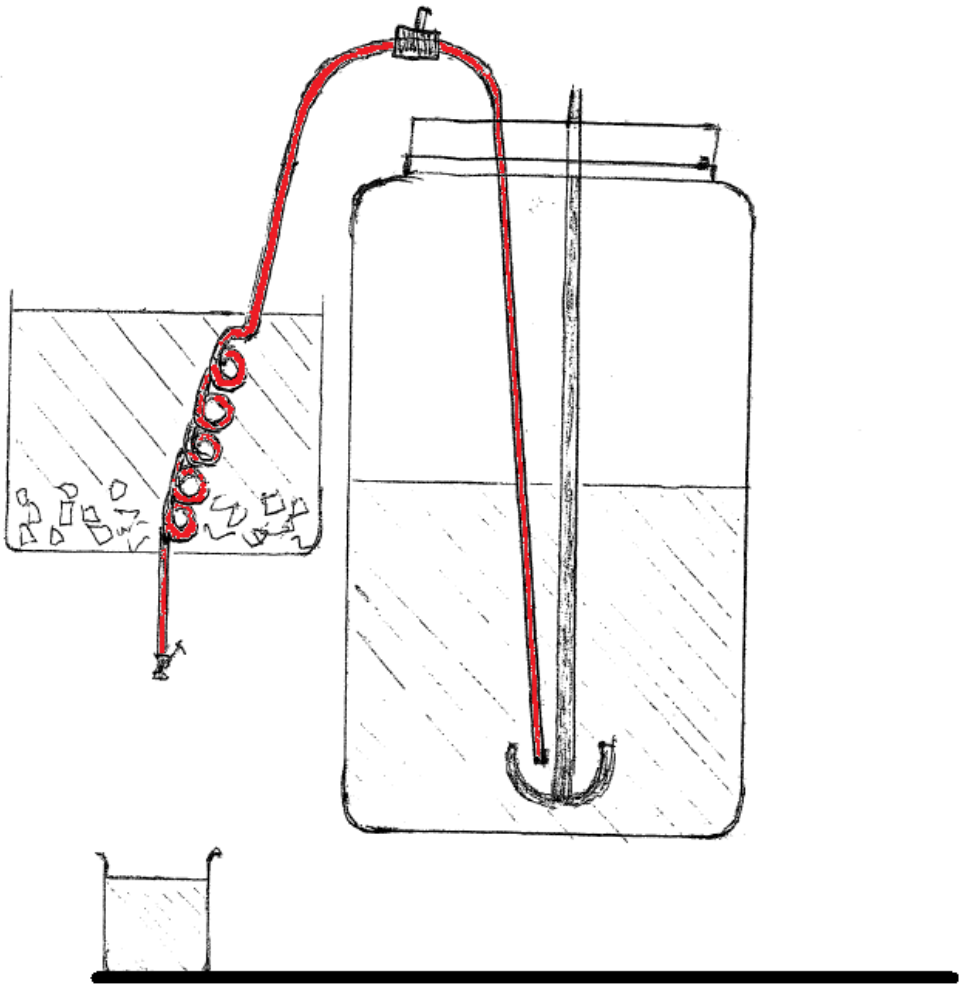

Stellenbosch University https://scholar.sun.ac.za

Appendix III

Calorific value of humins

Humins were collected with each experimental run, filtered with a Büchner funnel, dried overnight in a kiln at 70 °C and stored for elemental analysis. Once all the runs were completed, the humins were analysed using a CHNS elemental analyser. The remaining composition was assumed to consist entirely of oxygen as FF is made up of only carbon, hydrogen and oxygen so the oxygen constituent could be calculated in the following manner:

$$\%_{\mathrm{O}} = 100 - \%_{\mathrm{C}} - \%_{\mathrm{H}} \qquad 14$$

where $\%_{\mathrm{C}}$ was, for example, the elemental percentage of the sample which was carbon.

To reach the LCV of $9\,688.64\ \mathrm{kJ \cdot kg^{-1}}$, the following calculations were executed:

The average C:H:O composition for these humins is 63.75:4.07: 32.17, so 100 kg humins contains 4.07 kg H which can form 36.63 kg H_2O (See Equation 15)

$$\frac{\mathrm{mm_{H_2O}}}{\mathrm{mm_{H_2}}} \times \%_{\mathrm{H}} = \frac{18}{2} \times 4.07 = 36.63\ \mathrm{kg} \qquad 15$$

where $\frac{\mathrm{mm_{H_2O}}}{\mathrm{mm_{H_2}}}$ is the ratio of the molar mass of water to the molar mass of hydrogen in the water molecule

The LCV is calculated from the HHV which is 23.9 $\mathrm{MJ \cdot kg^{-1}}$ (See Literature Review Equation 1 for the equation used to calculate HHV)

$$\mathrm{HHV_{wet}} = 23\,900\ \mathrm{kJ \cdot kg^{-1}} - 50\ \% \times 23\,900\ \mathrm{kJ} = 11\,950\ \mathrm{kJ \cdot kg^{-1}}$$

$$\mathrm{LCV} = \mathrm{HHV} - \frac{1}{100} \times \frac{\mathrm{mm_{H_2O}}}{\mathrm{mm_{H_2}}} \times \%_{\mathrm{H}} \times \mathrm{h_{20°C}} - 50\ \% \times \mathrm{h_{20°C}}$$

$$\mathrm{LCV} = 11\,950 - 0.01 \times \frac{18}{2} \times 4.7 \times 2450 - 50\ \% \times 2450 \qquad 16$$

$$\mathrm{LCV} = 11\,950 - 1\,036.36 - 1\,225 = 9\,688.64\ \mathrm{kJ \cdot kg^{-1}}$$

where 2450 $\mathrm{kJ \cdot kg^{-1}}$ is the ASTM International Heat of Vaporization @T=20 °C

From the steam tables, the enthalpy of 300 °C steam at a pressure of 40 bar is 2961 $\mathrm{kJ \cdot kg^{-1}}$ (Cooper & Le Fevre, 1969). This is the specification for steam

Stellenbosch University https://scholar.sun.ac.za

produced by a boiler on a modern FF plant (Wilson, 2018) and working with a boiler efficiency of 70 %, the enthalpy required is 4230 $\mathrm{kJ \cdot kg^{-1}}$:

$$\mathrm{h} = \frac{2961}{0.7} = 4230\ \mathrm{kJ \cdot kg^{-1}}$$

The lower calorific value (LCV) of the humins formed in this study (at 50 % moisture content) is 9 688.64 $\mathrm{kJ \cdot kg^{-1}}$. To produce 1 tonne FF, approximately 30 tonnes of steam is required (Lange *et al.*, 2012). Therefore, for every tonne of humins burnt, 76.35 kg FF can be produced:

$$1000\ \mathrm{kg_{humins}} \times \frac{9\ 688.64\ \mathrm{kJ \cdot kg^{-1}_{humins}}}{4\ 230\ \mathrm{kJ \cdot kg^{-1}_{steam}}} = 2\ 290.46\ \mathrm{kg_{steam}}$$

$$\frac{2\ 290.46\ \mathrm{kg_{steam}}}{30\ \mathrm{kg_{steam} \cdot kg^{-1}_{FF}}} = 76.35\ \mathrm{kg_{FF}}$$

Under the studied conditions, 16.82 % of FF is converted to humins and therefore 12.84 kg humins are also produced for 1 tonne of humins burnt $(76.35\ \mathrm{kg} \times 16.82\ \%)$. i.e. the net contribution energy is 1.3 % if humins are burnt (See Equation 17)

$$1\ \text{tonne humins}: 76.35\ \mathrm{kg\ FF}: 12.84\ \mathrm{kg\ humins}\ \&\ \frac{12.84}{1000} = 1.3\ \% \qquad 17$$

For a FF plant, operating with a throughput of 10 000 $\mathrm{t \cdot yr^{-1}}$

(The throughput of an average FF plant (Wilson, 2018)), 300 000 $\mathrm{t_{steam} \cdot yr^{-1}}$is required (To produce 1 tonne FF, approximately 30 tonnes of steam is required for a modern FF plant (Wilson, 2018)) which is

$$300\ 000\ \mathrm{t_{steam} \cdot yr^{-1}} \times 4230\ \mathrm{MJ \cdot t^{-1}_{steam}} = 1.269 \times 10^{9}\ \mathrm{MJ \cdot yr^{-1}}.$$

$$1.296 \times 10^{9}\ \mathrm{MJ \cdot yr^{-1}} \div 25\ 120.8\ \mathrm{MJ \cdot t^{-1}_{coal}} = 50\ 515.91\ \mathrm{t_{coal} \cdot yr^{-1}}$$

where 25 120.8 MJ/t coal is the calorific value of coal exported via Richard's Bay harbour (South Africa) (IndexMundi, 2018) and it costs $\pm 100\ \$/t$.

$$50\ 515.91\ \mathrm{t_{coal} \cdot yr^{-1}} \times 100\$ \cdot t^{-1}_{coal} = 5.0516 \times 10^{6}\ \$ \cdot \mathrm{yr^{-1}}$$

$$5.0516 \times 10^{6}\ \$ \cdot \mathrm{yr^{-1}} \times 1.3\ \% = 6.567 \times 10^{4}\ \$ \cdot \mathrm{yr^{-1}}$$

Burning humins will save $\pm 65\ 670\ \$ \cdot \mathrm{yr^{-1}}$ on an average FF plant.

It should also be pointed out that, currently, burning humins is the only established humins valorisation route that is plausible on a conventional FF plant because

Stellenbosch University https://scholar.sun.ac.za

humins are formed amongst the fibres of the biomass (biomass is referred to as FF residue after FF has been extracted from it). It is impossible to separate the humins from the fibres to produce products from the humins. However, it is possible to make products from humins when working with hydrolysates (newer technologies) It is then possible to separate the humins from the hydrolysate solution using conventional separation techniques (Sappi, 2017).

FF residue (and humins) is combusted in the boilers on FF plants attached to sugar mills already so the question is "What contribution do humins make to the calorific value of this residue+humins fuel?" The LCV of FF residue (and humins) is 7.254 $\mathrm{MJ \cdot kg^{-1}}$ for residue with a moisture content of 51.6 % and 4 % ash (Wilson, 2018). This value is reasonable because Naude, McIntyre & Field (1993) found that the HHV of FF residue is 9.8 $\mathrm{MJ \cdot kg^{-1}}$ for a residue that contains 54.9 % moisture and 2.9 % ash(Naude, McIntyre & Field, 1993).

Approximately 183 949 $\mathrm{t_{residue+humins} \cdot yr^{-1}}$ is generated in the production of 10 000 $\mathrm{t_{FF} \cdot yr^{-1}}$ (Wilson, 2018). The energy that can be generated by combusting the FF residue (and humins) is calculated as follows:

$$183\ 949\ \mathrm{t_{residue+humins} \cdot yr^{-1}} \times 7\ 254\ \mathrm{MJ \cdot t^{-1}_{residue+humins}} = 1.334 \times 10^{9}\ \mathrm{MJ \cdot yr^{-1}}$$

The steam required to produce 10 000 $\mathrm{t_{FF} \cdot yr^{-1}}$ (for stripping FF and heating) is 300 000 $\mathrm{t_{steam} \cdot yr^{-1}}$ and the thermal energy of the steam is:

$$300\ 000\ \mathrm{t_{steam} \cdot yr^{-1}} \times 4\ 230\ \mathrm{MJ \cdot t^{-1}_{steam}} = 1.269 \times 10^{9}\ \mathrm{MJ \cdot yr^{-1}}$$

i.e. $1.269 \times 10^{9}\ \mathrm{MJ \cdot yr^{-1}}$ must be generated in the boiler to operate a FF plant that produces $10\ 000\ \mathrm{t_{FF} \cdot yr^{-1}}$. $1.334 \times 10^{9}\ \mathrm{MJ \cdot yr^{-1}}$ can be generated by combusting all of the FF residue+humins (1.05 times the required amount of energy). It is possible to operate a FF plant (attached to a sugar mill) without combusting additional coal/gas. The calorific value of the FF residue (and humins) is sufficient to run the boilers for the FF production process. Now to answer the question "What contribution do humins make to the calorific value of this residue+humins fuel?":

For a plant that produces $10\ 000\ \mathrm{t_{FF} \cdot yr^{-1}}$, the contribution of the humins to the residue+humins fuel is calculated as follows (for a 45 % FF yield):

$$0.55 \times \frac{10\ 000}{0.45} \times 0.1682 = 2.056\ \mathrm{t_{humins} \cdot yr^{-1}}$$

Stellenbosch University https://scholar.sun.ac.za

The LCV of humins is 9 688.64 $\mathrm{kJ \cdot kg^{-1}}$ so the contribution of humins to the overall calorific value of the residue+humins fuel can be calculated as follows:

$$9\,688.64\ \mathrm{kJ \cdot kg^{-1}} \times 2\,056\ \mathrm{kg_{humins} \cdot yr^{-1}} = 19\,919.8\ \mathrm{MJ \cdot yr^{-1}}$$

The energy generated by combusting the humins+residue to produce $300\,000\ \mathrm{t_{steam}}$ is $1269 \times 10^9\ \mathrm{MJ \cdot yr^{-1}}$

$$\therefore \text{the humins contribution} = \frac{19\,919.8}{1.269 \times 10^9} = 1.54 \times 10^{-5} = 0.00154\ \%$$

In conclusion, humins make an insignificant contribution to the calorific value of the residue+humins fuel.

It should be noted that this calculation is based on a 45 % FF yield as observed at the Illovo sugar mill/FF plant by Klusener (2018). The 45 % FF is collected by stripping and the 55 % yield loss is the FF that forms the basis for the present study. Although 53.12 % of this 55 % is unreacted FF, i.e. $6\,398.33\ \mathrm{t \cdot yr^{-1}}$, it is unsalvageable because it is found amongst the fibres of the FF residue.